Responses to Referee #1:

This manuscript discussed chemical composition and source apportionment of $PM_{2.5}$ in three northern Chinese cities based on high-time-resolution monitoring equipment. Furthermore, the authors qualitatively explored the mechanisms of secondary aerosols formation. And the authors also compared the changes in the chemical composition and sources of $PM_{2.5}$ in the three pilot cities over past decades. At the end of the article, the authors provided policy recommendations for sustained air quality improvement in the future. In general, this article provides valuable data for local governments to develop scientific pollution control strategies. I recommend this article for publication on Atmospheric Chemistry and Physics. However, some issues should be addressed before the publication.

Response: We kindly appreciate the reviewer to providing those valuable comments and suggestions to our paper. We have carefully revised the relevant contents. We do believe that the revised manuscript has been significantly improved after the revision. The point-to-point responses to each comment are provided in blue, and the revised content is underlined in italics. Attached please also find the marked-up manuscript with tracked changes in the revised manuscript.

Major comments:

Comments (1): In Text S1 from supplement, the error fraction of all chemical species was used to 10% for calculation of uncertainty dataset inputted receptor model. Is it reasonable to choose the same error fraction for different instruments?

Response: Thank you for pointing out this problem. The error fraction value was normally calculated by parallel sample analysis, which can be achieved from off-line experiments. However, our campaigns were conducted by online instruments, the parallel test cannot be conducted due to limitation of instruments. For high time- resolution source apportionment, the value of error fraction was set from 0.05-0.5 (Yang et al., 2022). And the 10% for all species was been widely used to calculate the uncertainty dataset for source apportionment by receptor model in previous serval studies (Liu et al., 2016; Ji et al., 2018; Rai et al., 2020; Wu et al., 2020; Liu et al., 2021; Tian et al., 2022), and those all did not impact the interpretability of the source identification. Therefore, the 10% for error fraction was chosen to calculate the uncertainty data set in this study.

References:

Ji, D., Cui, Y., Li, L., He, J., Wang, L., Zhang, H., Wang, W., Zhou, L., Maenhaut, W., Wen, T., and Wang, Y.: Characterization and source identification of fine particulate matter in urban Beijing during the 2015 Spring Festival, Sci. Total Environ., 430–440, 628–629, https://doi.org/10.1016/j.scitotenv.2018.01.304, 2018.

Liu, B., Liang, D., Yang, J., Dai, Q., Bi, X., Feng, Y., Yuan, J., Xiao, Z., Zhang, Y., Xu, H.: Characterization and source apportionment of volatile organic compounds based on 1-year of observational data in Tianjin, China. Environ. Pollut. 218, 757–769, https://doi.org/10.1016/j.envpol.2016.07.072, 2016

Liu, H., Wang, Q., Ye, J., Su, X., Zhang, T., Zhang, Y., Tian, J., Dong, Y., Chen, Y., Zhu, C., Han, Y., Cao, J. J.: Changes in Source-Specific Black Carbon Aerosol and the Induced Radiative Effects Due to the COVID-19 Lockdown. Geophys. Res. Lett., 48: e2021GL092987, 2021.

Rai, P., Furger, M., Slowik, J., Canonaco, F., Prévt, A.: Source apportionment of highly time-resolved elements during a firework episode from a rural freeway site in Switzerland. Atmospheric Chemistry and Physics, 20(3), 1657–1674. https://doi.org/10.5194/acp-20-1657-2020, 2020

Tian, J., Wang, Q., Liu, H., Ma, Y., Liu, S., Zhang, Y., Ran, W., Han, Y., and Cao, J.: Measurement report: The importance of biomass burning in light extinction and direct radiative effect of urban aerosol during the COVID-19 lockdown in Xi'an, China, Atmos. Chem. Phys., 22, 8369–8384, https://doi.org/10.5194/acp-22-8369-2022, 2022.

Wu, R., Zhao, Y., Zhang, J., Zhang, L.: Variability and Sources of Ambient Volatile Organic Compounds Based on Online Measurements in a Suburban Region of Nanjing, Eastern China. Aerosol Air Qual. Res. 20, 606-619, https://doi.org/10.4209/AAQR.2019.10.0517, 2020.

Yang Y., Liu B., Hua J., Yang T., Dai Q., Wu J., Feng Y., Hopke P.: Global review of source apportionment of volatile organic compounds based on highly time-resolved data from 2015 to 2021, Sci. Total Environ., 165, 107330, https://doi.org/10.1016/j.envint.2022.107330, 2022.

Comments (2): In Sect3.2, the secondary sources from three cities were resolved by HERM model. And one factor named secondary nitrate plus sulfate was identified in Xi'an and Shijiazhuang (Fig. S6 and S7), but two factors named secondary nitrate and secondary sulfate were identified in Beijing (Fig. S8). What causes such differences in sources identification among cities? Moreover, the secondary sources were characterized by high EV values for SO42- , NO3-, NH4+, and those three species are inorganic aerosols. Secondary organic aerosols (SOA) were not identified in this study, dose SOA was ignored in this study?

Response: (a) Thank you for pointing out this out. The factor number for optimal solution of receptor model was depended on characteristics of data set inputted model (Chen et al., 2010). So, it is not unusual for the number of factors to vary in different cities. Although two factors about secondary source were identified in Beijing, the source characteristics reflected by these two factors together are equivalent those reflected by one factor in Xi'an and Shijiazhuang. And we also point out this in manuscript (see section 3.2).

(b) Due to lack of critical tracers of SOA in this study, the sources of SOA cannot be individually resolved by receptor model. In this study, the secondary sources were mainly characterized by high EV values for inorganic aerosols such as SO_4^{2-} , NO_3^-, NH_4^+, but the medium EV values for OA (16~29%) were also presented on secondary sources in three pilot cities. This means that the SOA maybe mixed in with the factors of secondary sources. To

verify this, we estimated the SOA concentrations using a BC-tracer method (Wang et al., 2019) and then compared the results with those based on source apportionment. The formula of SOA calculation based on BC-tracer method was shown as follow:

$$[SOA]_{BC\text{-}tracer} = [OA] - (OA/BC)_{pri} \times [BC] \quad (R\text{-}1)$$

where [ ] means mass concentration, $(OA/BC)_{pri}$ is the ratio of [OA] to [BC] in primary emission. The $(OA/BC)_{pri}$ ratios vary among sources, therefore, a minimum R squired (MRS) method was used to derive appropriate $(OA/BC)_{pri}$ values for three pilot cities. In previous studies (Srivastava et al., 2018; Wang et al., 2019), MRS method has been used to calculated the concertation of secondary organic carbon and brown carbon. Detailed information on the method and a validation of this approach can be found in Wang et al. (2019).

In addition, according source apportionment results, SOA concentration can also be estimated as follow based on EV values of OA from secondary source factors

$$[SOA]_{source\ apportionment} = [OA] \times EV_{OA} \quad (R\text{-}2)$$

where EV_{OA} represents the EV values of OA in secondary sources factors resolved by HERM model.

As shown in Fig. R1, the $(OA/BC)_{pri}$ ratios were determined as 4.73 for Xi'an, 3.12 for Shijiazhuang and 7.6 for Beijing, respectively. Furthermore, the concentrations of SOA from three pilot cities were shown in Table R1 based two different methods. As we can see, the SOA concentrations estimated by EV values of OA are close to that by BC-tracer method for three pilot cities. This indicated SOA was mixed in secondary sources factors.

To avoid unnecessary misunderstanding to the readers, we re-named the source of secondary nitrate plus sulfate as secondary formation source, secondary nitrate as secondary nitrate plus OA, and secondary sulfate as secondary sulfate plus OA, respectively in revised manuscript.

The main changes about identification of secondary source were revised as follows:

> "The secondary sources resolved by HERM are different among the three cities. In Xi'an and Shijiazhuang, this factor are characterized by high EV values for SO_4^{2-} (62–75%), NO_3^- (55–53%), NH_4^+ (60–56%) and a medium EV value for OA (23–29%), which showed good correlations with SO_4^{2-} ($R^2 = 0.85$–0.90) and NO_3^- ($R^2 = 0.85$–0.92) (Dai et al., 2020; Tian et al., 2022). In addition, The OA concentration in this factor was calculated by EV value of OA, which was close to the secondary OA (SOA) concentration estimated by BC-trace method (see Text S3 and Table S6). This means that SOA was mixed in this factor, therefore, this factor was identified as secondary formation source. In Beijing, two secondary sources were resolved. The first one was characterized by high EV value for NO_3^-(58%), NH_4^+ (42%) and medium
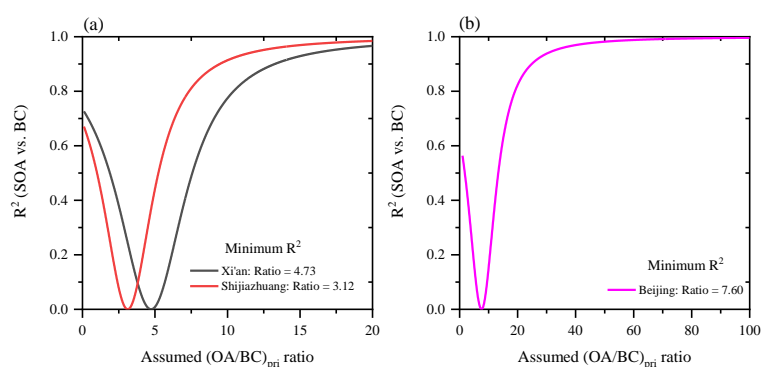
Figure R1. Coefficients of determination (R_2) for SOA versus BC mass concentration plotted against assumed ratios for OA to BC in primary emissions ((OA/BC)$_{pri}$).

Table R1 Average concentrations of SOA in Xi'an, Shijiazhuang, and Beijing during sampling periods estimated by BC-tracer method and source apportionment results ($\mu g\ m^{-3}$)

SOA	Xi'an	Shijiazhuang	Beijing
SOA_BC-tracer	5.1 ± 5.8	4.2 ± 4.4	8.0 ± 9.0
SOA_ source apportionment	6.0 ± 4.1	4.6 ± 2.8	8.2 ± 6.7

References:

Chen, L., Lowenthal, D., Watson, J., Koracin, D., Kumar, N., Knipping, E., Wheeler, N., Craig, K., Reid, S.: Toward effective source apportionment using positive matrix factorization: experiments with simulated PM2.5 data. J. Air Waste Manage., 60(1), 43–54, https://doi.org/10.3155/1047-3289.60.1.43, 2010.

Wang, Q.; Han, Y.; Ye, J.; Liu, S.; Pongpiachan, S.; Zhang, N.; Han, Y.; Tian, J.; Wu, C.; Long, X.; Zhang, Q.; Zhang, W.; Zhao, Z.; Cao, J.: High Contribution of secondary brown carbon to aerosol light absorption in the southeastern margin of Tibetan Plateau. Geophys. Res. Lett. 46, 4962−4970, https://doi.org/10.1029/2019GL082731, 2019.

Shrivastava, M., Cappa, C., Fan, J., Goldstein, A., Guenther, A., Jimenez, J., Kuang, C., Laskin, A., Martin S., Ng, N., Petaja, T., Pierce, J., Rasch, P., Roldin, P., Senfeld, J., Shiling, J., Smith, J., Thornton, J., Volkamer, R., Wang, J., Worsnop, D., Zaveri, R., Zelenyuk, A., Zhang, Q.: secondary organic aerosol: Implications for global climate forcing. Rev. Geophys., 55, 509–559. https://doi.org/10.1002/2016RG000540, 2017.

Comments (3): In Sect3.3, the authors explored the potential function of aqueous-phase reaction to secondary aerosol formation based on data during nighttime. It should be noted that aqueous-phase reaction may also promote secondary aerosol formation during daytime. I suggest that the authors take the data from daytime hours into account when discussing the role

of the aqueous-phase reaction.

Response: Thanks for reviewer's wonderful suggestion. We investigated the correlations of secondary formation source/ΔCO ration and ALWC based on data during daytime (08:00–17:00 LST). As shown in Fig. R2a-c, the secondary formation source/ΔCO also showed a significant linear correlation to ALWC ($R^2 = 0.84$–0.98) when RH < 80%, this indicated that the aqueous-phase reaction on the secondary aerosol formation also occurred during the daytime. Therefore, the functions of aqueous-phase reaction to the secondary aerosol formation in three pilot cities were re-evaluated by all data during sampling periods in revised manuscript.
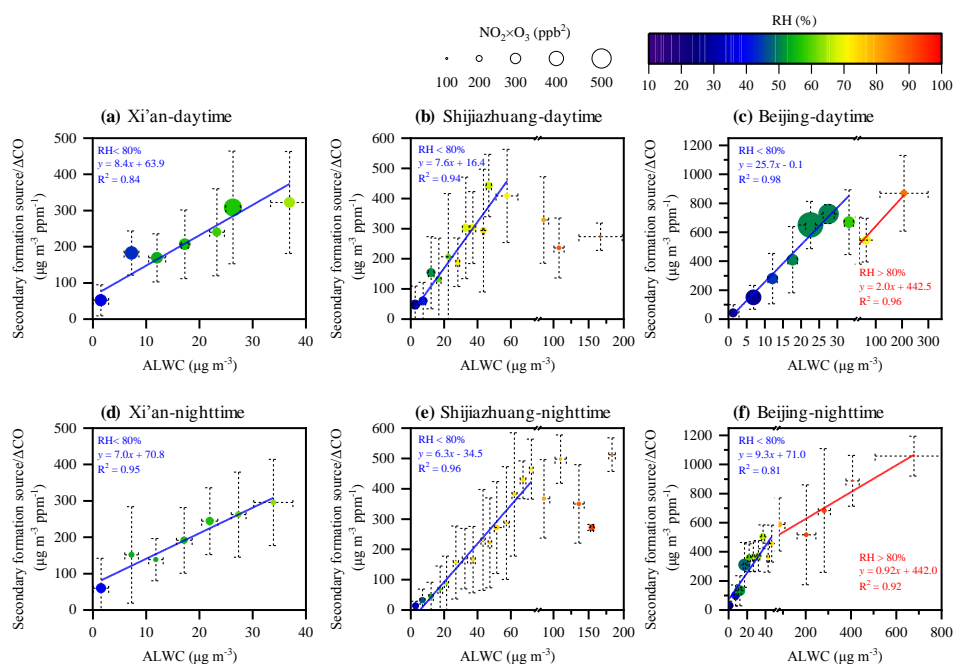

Figure R2. Correlation of secondary formation source/ΔCO and ALWC during daytime (08:00–17:00 LST, a–c) and nighttime (18:00–7:00 the next day LST, d–f) in Xi'an, Shijiazhuang, and Beijing, respectively. The points and error bar represent the mean values and standard deviation values of secondary formation source /ΔCO and ALWC in each bin. In Xi'an, each bin is 5 μg m^{-3} (ΔALWC = 5 μg m^{-3}). In Shijiazhuang, each bin is 5 μg m^{-3} (ΔALWC = 5 μg m^{-3}) when ALWC ranged from 0 to 75μg m^{-3}, but 25 μg m^{-3} (ΔALWC = 25 μg m^{-3}) for ALWC ranged from 75 to 200 μg m^{-3} due to limitations in data. In Beijing, during daytime, each bin is 5 μg m^{-3} (ΔALWC = 5 μg m^{-3}) when ALWC ranged from 0 to 40 μg m^{-3}, but 100 μg m^{-3} (ΔALWC = 100 μg m^{-3}) for ALWC ranged from 40 to 450 μg m^{-3} due to limitations in data. During nighttime, each bin is 5 μg m^{-3} (ΔALWC = 5 μg m^{-3}) when ALWC ranged from 0 to 50 μg m^{-3}, but 100 μg m^{-3} (ΔALWC = 100 μg m^{-3}) for ALWC ranged from 50 to 900 μg m^{-3} due to limitations in data.

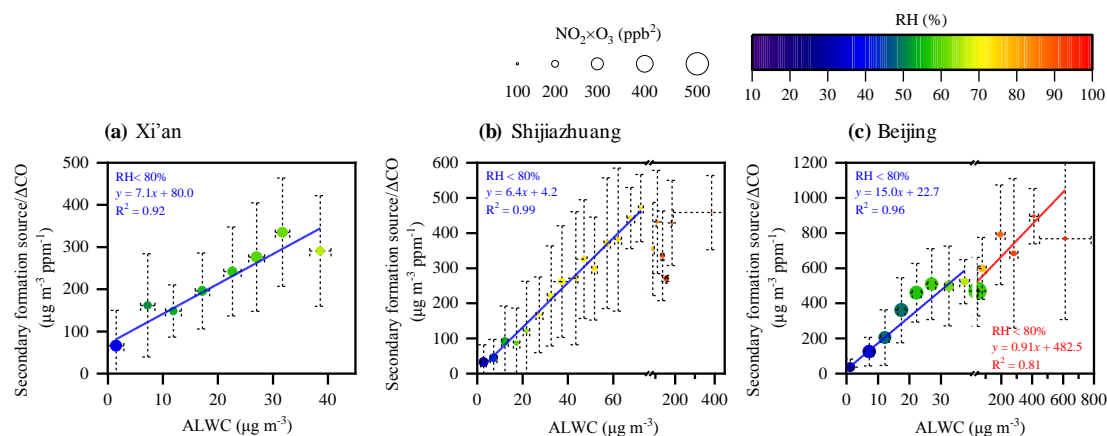In the revised manuscript, Figure 4 was replaced by Figure R3.

Figure R3. Correlation of secondary formation source/ΔCO and ALWC during sampling periods in (a) Xi'an, (b) Shijiazhuang, and (c) Beijing, respectively. The points and error bar represent the mean values and standard deviation values of secondary formation source /ΔCO and ALWC in each bin. In Xi'an, each bin is 5 μg m^{-3} (ΔALWC = 5 μg m^{-3}). In Shijiazhuang, each bin is 5 μg m^{-3} (ΔALWC = 5 μg m^{-3}) when ALWC ranged from 0 to 75μg m^{-3}, but 25 μg m^{-3} (ΔALWC = 25 μg m^{-3}) for ALWC ranged from 75 to 200 μg m^{-3} due to limitations in data. In Beijing, each bin is 5 μg m^{-3} (ΔALWC = 5 μg m^{-3}) when ALWC ranged from 0 to 50 μg m^{-3}, but 100 μg m^{-3} (ΔALWC = 100 μg m^{-3}) for ALWC ranged from 50 to 900 μg m^{-3} due to limitations in data.

The relevant contents in section 3.3 were revised as follows:

"The aqueous-phase reaction is another important pathway for secondary aerosol formation in the atmosphere (Wang et al., 2018; Xue et al., 2014). ALWC is considered an indicator of an aqueous-phase reaction (Ervens et al., 2011). Considering that the aqueous-phase reaction occurs both during the daytime and nighttime characterized by good correlations between secondary formation source/ΔCO and ALWC (R^2 = 0.81–0.98, Fig. S14). The correlations of secondary formation source/ΔCO ratio and ALWC during all sampling periods were re-established in three pilot cities to assess the implications of aqueous-phase chemistry for secondary aerosol production. As shown in Fig. 4, the secondary formation source/ΔCO showed a significant linear correlation to ALWC (R^2 = 0.92–0.99) when RH < 80%, indicating an obvious effect of aqueous-phase reaction on the secondary aerosol formation during the sampling periods. However, when RH >80%, the secondary formation source/ΔCO showed no notable increase with ALWC in Shijiazhuang (Fig. 4b), whereas a tiny increase with ALWC in Beijing (Fig. 4c). The higher ALWC at RH > 80% probably inhibits secondary aerosol formation due to the decrease in aerosol acidity (Huang et al., 2019; Meng et al., 2014). Khan et al. (2008) found that NO$_3$ radicals can rapidly generate from the reaction between NO$_2$ and O$_3$ with unsaturated organic species during nighttime. The value of O$_3$×NO$_2$ can thus represent its production reaction rate or be used as a proxy for the NO$_3$ radical. The highest NO$_3$ radical production rate was found in Beijing, followed by Xi'an and Shijiazhuang, when RH<80%. This could be used to explain the highest contribution of secondary formation source to PM$_{2.5}$

in Beijing during the daytime and nighttime (Fig. S13). Moreover, the results showed that both photochemical oxidation and aqueous-phase reaction play more important roles in Beijing, where the primary sources have been better controlled. This reflects that pollution control policies need to be focused on the suppression of secondary formations" *(Page 11,12 Line 334–353)*

Specific Comments:

Comments (4): line18 & 352： change "progress of" to "process of"

Response: We have corrected the relevant sentences as follows:

"In this study, intensive real-time measurement campaigns were conducted in Xi'an, Shijiazhuang, and Beijing to investigate the chemical characteristics and source contributions of $PM_{2.5}$ and explored the formation of heavy pollution for policy implications." *(Page 1 Line 16–18)*

"To gain insights into the process of pollution episodes, three typical pollution events were chosen for detailed discussion (i.e., EP2 in Xi'an, EP4 in Shijiazhuang, and EP7 in Beijing) based on the validity and integrity of the data and the representativeness of the selected pollution events." *(Page 14 Line 369–371)*

Comments (5): line 22-23: change "but is no longer important contributor...." to "but is no longer an important contributor...."

Response: We have added an indefinite article of to this sentence as follows:

"The contribution of coal combustion to $PM_{2.5}$ is non-negligible in Xi'an and Shijiazhuang but is no longer an important contributor in the capital city of Beijing due to the execution of a strict coal-banning policy." *(Page 1 Line 22–24)*

Comments (6): line 27： change "According to source variations, to "According to sources variations,"

Response: We have corrected the relevant sentence as follows:

"According to sources variations, air pollution events that occurred in campaigns were classified into three types: biomass combustion dominated, secondary formation source dominated, and a combination of primary and secondary sources." *(Page 1 Line 27–30)*

Comments (7): line 49： change "In perspective of PM2.5 sources" to "In terms of PM2.5 sources"

Response: We have changed "In perspective of PM$_{2.5}$ sources" to "In terms of PM$_{2.5}$ sources" as follows:

> "In <u>terms</u> of PM$_{2.5}$ sources, contribution of secondary source increased obviously while contribution of industrial emission and coal combustion decreased due to elimination of industries and enterprises with high pollutant emissions, promotion of desulfurization in industrial facilities, replacement of clean energy, and optimization of industrial and energy structures (Lu et al., 2021; Ma et al., 2022;Tao et al., 2017; Wang et al., 2019)." *(Page 2 Line 50–54)*

Comments (8): line 67：change "Liu et. al (2019)" to "Liu et al. (2019)"

Response: Corrected. *(Page 2 Line 68)*

Comments (9): line 73：change "should be pointed out previous researches" to "should be pointed out that previous studies"

Response: We have corrected the relevant sentence as follows:

> "It should be pointed out <u>that</u> previous researches were mainly focused on individual cities, and those results have some limitations in guiding the improvement of air quality in the entire northern region of China." *(Page 3 Line 73–75)*

Comments (10): line 78 & 85-86：change "are located to" to "are located in"

Response: We have corrected the relevant sentence as follows:

> "The cities of Beijing and Shijiazhuang are located <u>in</u> the North China Plain, which is one of the most polluted regions in China (Chan and Yao, 2008)." *(Page 3 Line 79–80)*
>
> "Xi'an is located <u>in</u> the Fenwei Plain, which is a region that suffered from heavy pollution and was designated as a key region for TAPFAP in 2018 (Cao and Cui, 2021)." *(Page 3 Line 87–88)*

Comments (11): line 237：change "With increasing of the PM$_{2.5}$ mass concentration" to "With increases of the PM$_{2.5}$ mass concentration"

Response: We have corrected the relevant sentence as follows:

> "With <u>increases</u> of the PM$_{2.5}$ mass concentration, the fractions of chemical components in Xi'an and Shijiazhuang changed notably." *(Page 9 Line 238–239)*

Comments (12): line 431&454：change "atmosphere oxidation capacity" to "atmospheric oxidation capacity"

Response: We have corrected the relevant sentences as follows:

"Therefore, more control measures should focus on weakening the atmospheric oxidation capacity, such as reduction of O_3 formation, to reduce the formation of secondary pollutants which are now identified as the most critical drivers of pollution." *(Page 16,17 Line 453–456)*

"Furthermore, to weaken the atmospheric oxidation capacity for reducing the contribution of secondary formation source, it is necessary to promote the collaborative control on ozone and particulate matter." (*Page 17 Line 477–479*)

1 **High-time-resolution chemical composition and source apportionment of PM$_{2.5}$ in northern**

2 **Chinese cities: implications for policy**

3 Yong Zhang[1,2,3], Jie Tian[1,2,4], Qiyuan Wang[1,2,3,4*], Lu Qi[5], Manousos Ioannis Manousakas[5], Yuemei Han[1,4], Weikang

4 Ran[1,2], Yele Sun[6], Huikun Liu[1,2,4], Renjian Zhang[6], Yunfei Wu[6], Tianqu Cui[5], Kaspar Rudolf Daellenbach[5], Jay

5 Gates Slowik[5], André S. H. Prévôt[5], Junji Cao[6*]

6 [1] State Key Laboratory of Loess and Quaternary Geology, Institute of Earth Environment, Chinese Academy of

7 Sciences, Xi'an 710061, China

8 [2] National Observation and Research Station of Regional Ecological Environment Change and Comprehensive

9 Management in the Guanzhong Plain, Shaanxi, Xi'an 710061, China

10 [3] University of Chinese Academy of Sciences, Beijing 100049, China

11 [4] Center for Excellence in Quaternary Science and Global Change, Xi'an 710061, China

12 [5] Laboratory of Atmospheric Chemistry, Paul Scherrer Institute (PSI), Villigen 5232, Switzerland

13 [6] Institute of Atmospheric Physics, Chinese Academy of Sciences, Beijing 100029, China

14 *Correspondence:* wangqy@ieecas.cn (Qiyuan Wang), jjcao@mail.iap.ac.cn (Junji Cao).

15 **Abstract:** Fine particulate matter (PM$_{2.5}$) pollution is still one of China's most important environmental issues,

16 especially in northern cities during wintertime. In this study, intensive real-time measurement campaigns were

17 conducted in Xi'an, Shijiazhuang, and Beijing to investigate the chemical characteristics and source contributions of

18 PM$_{2.5}$ and explored the formation ~~progress~~ of heavy pollution for policy implications. The chemical compositions of

19 PM$_{2.5}$ in three cities were all dominated by organic aerosol (OA) and nitrate (NO$_3^-$). Results of source apportionment

20 analyzed by hybrid environmental receptor model (HERM) showed that the ~~secondary nitrate plus sulfate~~secondary

21 formation source contributed higher to PM$_{2.5}$ compared to other primary sources. Biomass burning was the dominant

22 primary source in three pilot cities. The contribution of coal combustion to PM$_{2.5}$ is non-negligible in Xi'an and

23 Shijiazhuang but is no longer an important contributor in the capital city of Beijing due to the execution of a strict

24 coal-banning policy. The potential formation mechanisms of secondary aerosol in three cities were further explored

25 by establishing the correlations between the ~~secondary nitrate plus sulfate~~secondary formation source and aerosol

26 liquid water content (ALWC), and O$_x$ (O$_3$ + NO$_2$), respectively. The results showed that photochemical oxidation and

27 aqueous-phase reaction were two important pathways of secondary aerosol formation. According to sources

28 variations, air pollution events that occurred in campaigns were classified into three types: biomass combustion

29 dominated, ~~secondary nitrate plus sulfate~~secondary formation source dominated, and a combination of primary and

30 secondary sources. Additionally, this study compared the changes in chemical composition and source contributions

31 of PM$_{2.5}$ in past decades. The results suggested that the clean energy replacements for rural household should be

urgently encouraged to reduce the primary source emissions in northern China, and collaborative control on ozone and particulate matter need to be continuously promoted to weaken the atmosphere oxidation capacity for the sake of reducing secondary aerosol formation.

1. Introduction

Fine particulate matter ($PM_{2.5}$, aerodynamic diameter <= 2.5 μm) is of large concern because of its adverse effects on both natural environment (Kuniyal and Guleria, 2019; Kuo et al., 2013) and human health (Pöschl, 2005; Shen et al., 2021; Zeng and He, 2019). With the soaring economic growth and urbanization in China, $PM_{2.5}$ pollution has been a most serious environmental issue in recent decades (Chan and Yao, 2008; He et al., 2002; Pui et al., 2014; Zhang et al., 2013). The most impressive case is that an extremely severe haze pollution episode occurred in eastern and central China in January 2013 with peak value of $PM_{2.5}$ concentration over 500 μg m^{-3}. This month had been reported as the haziest month in the past 60 years in Beijing, China (Wang et al., 2014; Huang et al., 2014). Thereafter, aiming to improve air quality, the China central government ~~implemented~~ issued the Air Pollution Prevention and Control Action Plan (APCAP) in September 2013 (http://www.gov.cn/zwgk/2013-09/12/content_2486773.htm, in Chinese), and the Three-year Action Plan to Fight Air Pollution (TAPFAP) in June 2018 (http://www.gov.cn/zhengce/content/2018-07/03/content_5303158.htm, in Chinese). With the implementation of strict pollution controls, air quality in northern China has improved significantly over the past decade (Wang et al., 2020a, 2017; Li et al., 2020). Previous studies show that $PM_{2.5}$ concentration decreased notably in past two decades, and the composition of organic aerosol (OA), black carbon (BC) and sulfate (SO_4^{2-}) decreased as well, while the ammonium (NH_4^+) slightly increased and nitrate (NO_3^-) increased obviously. In ~~perspective~~ terms of $PM_{2.5}$ sources, contribution of secondary source increased obviously while contribution of industrial emission and coal combustion decreased due to elimination of industries and enterprises with high pollutant emissions, promotion of desulfurization in industrial facilities, replacement of clean energy, and optimization of industrial and energy structures (Lu et al., 2021; Ma et al., 2022;Tao et al., 2017; Wang et al., 2019). However, there is still a significant gap between the $PM_{2.5}$ concentration in northern China and its latest recommendations on air quality guideline (5 μg m^{-3}) by the World Health Organization (https://apps.who.int/iris/bitstream/handle/10665/345329/9789240034228-eng.pdf, page 78). In addition, severe $PM_{2.5}$ pollutions still frequently occurred in northern China during wintertime (Guo et al., 2021; Li et al., 2017a, 2021b). To figure out the causes behind the pollutions and further improve ~~furtherly~~ air quality in northern China, it is essential to use online high-time-resolution source apportionment technology to understand the chemical composition and source contribution of $PM_{2.5}$ in those pollution events.

Recently, more research on measurements of $PM_{2.5}$ and its source apportionments were conducted using online high-time-resolution technologies (Li et al., 2017c; Wang et al., 2021a; Elser et al., 2015). Compared to traditional offline filter-based approach, online methods characterize the short-time variation of $PM_{2.5}$. It allows for distinguishing the rapid changes and evolutions of chemical components, and is particularly profitable to gain knowledge on the formations of heavy air pollution or episode events (Liu et al., 2016; Ouyang et al., 2019; Zheng et al., 2016; Elser et al., 2015). For instance, Lv et al. (2021) employed a Positive matrix factorization (PMF) model with high-time-resolution online $PM_{2.5}$ data to accurately quantify and distinguish the source distributions in Beijing during two haze episodes in January 2019. Liu et al. (2019) recognized the main drivers of haze event occurred in winter Beijing in 2016 according to high-time-resolution source apportionment of $PM_{2.5}$ with multiple models. Furthermore, Wang et al. (2021b) found that vehicle emission contributed most to $PM_{2.5}$ during pollution episodes in downtown Lanzhou based on high-resolution online data source apportionment. Currently, to fully understand and solve heavy pollution events in winter that troubles local governments in northern cities of China (Wang et al., 2022b; Xu et al., 2022; Zhou et al., 2022), more advanced online measurement, and source apportionment is a better choice (Tao et al., 2015). It should be pointed out that previous researches were mainly focused on individual cities, and those results have some limitations in guiding the improvement of air quality in the entire northern region of China. Therefore, it is necessary to conduct comparative research among multiple cities.

Considering the differences in geographical location, population, economy, industrial/energy structure, air quality, and depth of air pollution control measures among different cities, three cities in northern China including Beijing, Shijiazhuang and Xi'an were chosen as pilot research subjects. The cities of Beijing and Shijiazhuang are located in the North China Plain, which is one of the most polluted regions in China (Chan and Yao, 2008). Beijing is the capital of China and its air quality has significantly improved under the implementation of the strictest clean air policy since 2013 (Li et al., 2021a; Pang et al., 2021; Vu et al., 2019; Zhang et al., 2020). However, the city was still plagued by pollution events in wintertime (Wang et al., 2020b; Yang et al., 2022c; Zhou et al., 2022). Shijiazhuang was recognized as one of the most serious air pollution cities worldwide (Liu et al., 2018b; Huang et al., 2019). Its air quality had also improved under the implementation of the Clean Air Plan, whereas its annual $PM_{2.5}$ concentration was still unable to meet the China's National Ambient Air Quality Standards (NAAQS-II) of 35 μg m^{-3} until 2021 (Fig. S1). Xi'an is located in the Fenwei Plain, which is a region that suffered from heavy pollution and was designated as a key region for TAPFAP in 2018 (Cao and Cui, 2021). Compared with Beijing and Shijiazhuang, high-intensity air pollution controls in Xi'an started late due to a lack of financial support. And the annual $PM_{2.5}$

90   concentration in Xi'an could not meet the NAAQS-II until 2021 as well (Fig. S1). Meanwhile, it is still unclear ~~to~~

91   about the actual causes of the pollution, either topography, meteorological conditions, or local emissions (Chen et al.,

92   2021; Tian et al., 2022; Wang et al., 2015, 2022b). In this study, we conducted intensive real-time observation of

93   PM$_{2.5}$ chemical components in Xi'an, Shijiazhuang, and Beijing during wintertime. The objectives are 1) to determine

94   the characteristics of PM$_{2.5}$ and its chemical components in the three typical northern China cities during wintertime;

95   2) to quantify the source contribution and explore the potential formation mechanism of secondary aerosols; 3) to

96   explore the unique causes of heavy pollution events in different cities; and 4) to provide suggestions on establishment

97   of efficient policies for air quality continuous improvement. This study provides scientific guidance for developing

98   policy on air quality improvement for northern China cities.

2.   Methods

2.1   Sampling sites and periods

101   In this study, intensive online measurements of PM$_{2.5}$ were conducted at three pilot cities of Xi'an, Shijiazhuang, and

102   Beijing during wintertime (Fig. 1). The sampling sites in Xi'an and Beijing are located at two Chinese Academy of

103   Sciences (CAS) stations. The one in Xi'an is the Guanzhong Plain Ecological Environment Change and

104   Comprehensive Treatment National Observation and Research Station, Institute of Earth Environment (IEE)

105   (34.24°N, 108.87°E), and another one in Beijing is Tower Branch of the Institute of Atmospheric Physics (IAP)

106   (39.98°N, 116.39°E). Both two sites are surrounded by commercial and residential buildings without intense

107   industrial emissions nearby. Previous studies indicated that these two sites were influenced by biomass and coal

108   burning for heating and cooking during wintertime as well as usual local traffic emissions (Tian et al., 2021; Xu et

109   al., 2021). The sampling site in Shijiazhuang is situated in the courtyard of Hebei Sailhero Environmental Protection

110   High-tech Co., Ltd. (38.04°N, 114.65°E), which is surrounded by pharmaceutical and machine-building industries

111   and close to the streets. The intensive campaigns were continuously conducted for ~1 month in each city (i.e., 12

112   December 12th 2020 to January 7th 2021 in Xi'an, December 20th 2021 to January 24th 2022 in Shijiazhuang, and

113   January 17th 2021 to February 20th 2021 in Beijing).

2.2   Online measurements of PM$_{2.5}$ chemical components

2.2.1 Organic aerosol and inorganic ions

116   Concentrations of OA, NO$_3^-$, SO$_4^{2-}$, ammonium (NH$_4^+$), and chloride (Cl$^-$) in PM$_{2.5}$ at a 15-minute time resolution

117   were monitored by a quadrupole aerosol chemical speciation monitor (Q-ACSM, Aerodyne Research Inc., Billerica,

118   Massachusetts, USA) equipped with a $PM_{2.5}$ lens. The detailed operational principles and calibration method of the

119   Q-ACSM are described elsewhere (Ng et al., 2011; Hu et al., 2017). First, the sampled ambient air stream passed

120   through a PM_{10} impactor inlet and a Nafion® dryer (MD-700-24F-3; Perma Pure, Inc., Lakewood, NJ, USA) with a

121   flowrate of 5 L min^{-1} before entering the Q-ACSM chamber. Then, the pre-treatment particles passed through a 100

122   μm critical orifice at 0.1 L min^{-1} and were focused into a narrow beam by an aerodynamic intermediate pressure lens.

123   The focused particle beam was flash vaporized by a capture vaporizer (CV) at ~600 C°. The vaporized compounds

124   were then ionized by an electron impactor (EI) ionization source at 70 eV and subsequently analyzed by the

125   quadrupole mass spectrometer.

126   Based on calibration system consists of an atomizer (Model 9302, TSI Inc., Shoreview, MN, USA), a differential

127   mobility analyzer (DMA, TSI model 3080, TSI Inc.), and a condensation particle counter (CPC, TSI model 3772,

128   TSI Inc.), ammonium nitrate (NH_4NO_3) and ammonium sulfate (($NH_4)_2SO_4$) aerosol were used for calibration. The

129   raw data of Q-ACSM were analyzed by the ACSM local tool (V1.5.3.5, Aerodyne Research Inc., Billerica,

130   Massachusetts, USA) compiled with Igor Pro 6.37 (Wavemetrics, Lake Oswego, OR, USA). The response factors

131   (RFs) for NO_3^- in Xi'an, Shijiazhuang, and Beijing were set as 2.03×10^{-11}, and 5.9×10^{-11}, 2.20×10^{-11}, respectively,

132   and the relative ionization efficiencies (RIEs) for NH_4^+ and SO_4^{2-} were set as 8.06 and 0.83 in Xi'an, 5.82 and 0.30

133   in Shijiazhuang, 6.31 and 0.38 in Beijing, respectively. Other RIEs for NO_3^-, OA, and Cl^- were set as default values

134   of 1.4, 1.1, and 1.3, respectively (Ng et al., 2011). In addition, the collection efficiency (CE) value of Q-ACSM

135   equipped with a $PM_{2.5}$ lens was recommended as 1 based on laboratory simulation experiments by Xu et al. (2017).

136   Finally, the chemical components monitored by Q-ACSM was corrected by the results of offline filter sampling

137   experiments during the same periods (Fig. S2).

138   **2.2.2 Black carbon**

139   BC concentration in $PM_{2.5}$ was obtained by an Aethalometer (Model AE33, Magee Scientific Inc., Berkeley, CA,

140   USA) with a 1-minute time resolution. The AE33 monitors the light attenuation of seven wavelengths (λ = 370, 470,

141   525, 590, 660, 880, and 940 nm), and the light attenuation at λ = 880 nm was used to calculate BC concentration

142   (Wang et al., 2019; Drinovec et al., 2015). Briefly, the ambient air was first sampled on a filter tape inside the

143   instrument through a $PM_{2.5}$ cyclone (SCC-1.829, BGI Inc., USA) at a flowrate of 5 L min^{-1}. The entering particles

144   were divided into two sample spots on the filter through two channels with different follows. Then the light

145   attenuation transmitted through two parallel spots was detected. For quality accuracies of monitoring, the sampled

146   particles were desiccated with a Nafion® dryer (MD-700-24F-3; Perma Pure, Inc., Lakewood, NJ, USA) before

147   entering the AE33. Furthermore, a real-time loading effect compensation algorithm based on two spots measurement

148   was used to eliminate the nonlinear loading effects of the Aethalometer. A detailed description of the Model AE33

149   principle can be found in Drinovec et al. (2015).

150   **2.2.3 Elements**

151   Twenty-four elements, including Si, K, Ca, V, Cr, Mn, Fe, Co, Ni, Cu, Zn, Ga, As, Se, Ag, Cd, Sn, Ba, Au, Hg, Th,

152   Pb, and Pd in $PM_{2.5}$, were analyzed by a Xact625 Ambient Metals Monitor (Cooper Environmental Services, Tigard,

153   Oregon, USA) with a 1-hour time resolution. Si, K, Ca, Cr, Mn, Fe, Ni, Cu, Zn, As, Se, Ba, and Pb were selected for

154   further analysis in Xi'an and Beijing, while other elements were excluded due to most of their concentration below

155   the method detection limit. In Shijiazhuang, S, Cl, and Ti were analyzed by replacement of Ga, Ag and Au,

156   respectively. Finally, Si, K, Ca, Ti, Cr, Mn, Fe, Ni, Cu, Zn, As, Se, Ba, and Pb were selected for further analysis. The

157   description and detection principles of Xact625 were introduced by Furger et al. (2020) and Rai et al. (2020). In brief,

158   the ambient air stream was firstly sampled on a Teflon filter tape inside the instrument through a $PM_{2.5}$ cyclone inlet

159   at a constant flow rate of 16.7 L min^{-1}, and then the sample was automatically analyzed by nondestructive energy-

160   dispersive X-ray fluorescence (XRF) to determine the mass of the species. For quality control and assurance, the

161   Xact625 performed automatic internal quality control by testing the Pd rod every hour to ensure the stability of the

162   instrument. Energy calibration was performed daily from 00:00 to 00:15 and a range calibration from 00:15 to 00:30

163   local standard time (LST) to monitor any possible shift and instability of the XRF (Liu et al., 2019). During our

164   sampling periods, the concentration of Pd varies within 3 standard deviations (Fig. S3), illustrating the reliable and

165   stable performance of the Xact625.

166   **2.2.4 Complementary data**

167   Online hourly concentrations of $PM_{2.5}$ and gas pollutants (i.e., NO_x, NO_2, CO, SO_2, and O_3) were acquired from the

168   National Air Quality Monitoring Station (https://air.cnemc.cn:18007/). Meteorological parameters, including wind

169   speed (WS), wind direction (WD), relative humidity (RH), and temperature (T) were obtained from National

170   Meteorological Station (http://data.cma.cn/). The detailed information for complementary data was listed in Table S1.

171   **2.3 Data analysis**

6

172 **2.3.1 PM$_{2.5}$ mass reconstruction**

173 Chemical closure was utilized to assess whether chemical compositions can be representative of PM$_{2.5}$. The sum of

174 OA, NO$_3^-$, SO$_4^{2-}$, NH$_4^+$, Cl$^-$, BC, mineral dust (MD), and trace elements (TE) was considered as the reconstructed

175 PM$_{2.5}$, where MD and TE were calculated as follows (Chow et al., 2015).

176 [MD] = 2.20×[Al] + 2.49×[Si] + 1.63×[Ca] + 2.42×[Fe] + 1.94×[Ti] (1)

177 [TE] = [K] + [Cr] + [Mn] + [Ni] + [Cu] + [Zn] + [As] + [Se] + [Ba] + [Pb] (2)

178 where [ ] represents the chemical species concentration; [Al] and [Ti] were calculated by the concentration of Ca

179 ([Al] = 4.3×[Ca] and [Ti] = 0.25×[Ca]) (Wei et al., 1991). Good correlations between online and reconstructed PM$_{2.5}$

180 mass (slope = 0.87–1.10, R^2 = 0.82–0.93) in three pilot cities (Fig. S4) indicated that our measurements could detect

181 major components of PM$_{2.5}$. The PM$_{2.5}$ concentration used in the following discussion referred to the reconstructed

182 PM$_{2.5}$ concentration.

183 **2.3.2 Hybrid environment receptor model**

184 Source apportionment of PM$_{2.5}$ was analyzed with a bilinear model named the hybrid environment receptor model

185 (HERM). HERM is developed by the IEECAS and the University of Nevada, Las Vegas (Chen and Cao, 2018). Like

186 other receptor models, the speciation of pollutants at a receptor site can be separated into emission sources and the

187 chemical compositions of the sources. To solve the mass balance of PM$_{2.5}$, the bilinear HERM in matrix notation is

188 defined as follows

189 $$C_{mn} = \sum_{i=1}^{I} F_{mi} G_{in} + Q_{mn} \qquad (3)$$

190 where C_{mn} is the measured concentration of chemical species m during time n; F_{mi} is the source profile, that is the

191 fractional quantity of species m in source i emission; G_{in} represents the contribution of source i during time n; and

192 Q_{mn} is the model residual for species m concentration measured during time n. Based on an iterative conjugate

193 gradient algorithm, the HERM solves G_{in} and unknown F_{mi} by minimizing the Q_{mn}, which is defined as follows.

194 $$Q_{mn} = \sum_{m=1}^{M} \sum_{n=1}^{N} \frac{(C_{mn} - \sum_{i=1}^{I} F_{mi} G_{in})^2}{\sigma_{C_{mn}}^2 + \sum_{i=1}^{I}(\sigma_{F_{mi}}^2 G_{in}^2 + \delta_{mi}\sigma_{C_{mn}}^2)} \qquad (4)$$

195 where M, N, and I are the number of samples, chemical species, and sources, respectively; $\sigma_{F_{mi}}$ represents the error

196 in the variability in the constrained factor profile. δ_{mi} was set to 0 or 1 depending on whether the ith factor profile

197 is constrained or unconstrained, respectively.

198 The HERM input data included the concentration and uncertainty data of chemical species. 19 chemical species in

199 Xi'an and Shijiazhuang and 20 chemical species in Beijing were selected for source apportionment, respectively.

200 Details of selected chemical species and its uncertainty calculation was described in Text S1 in the Supplement. A

201 range from two to ten factors solutions was investigated by HERM with completely unconstrained factor profiles to

202 search for optimal solutions. The detailed diagnostics can be seen in Text S2 in the Supplement. A six-factor solution

203 for Xi'an and Shijiazhuang and an eight-factor solution for Beijing were found to be the optimal solution based on

204 multiple criteria including 1) variations in Q/Q_{exp} which can be used to choose the optimal number of resolved factors,

205 2) physical meaningfulness of distinct factor profiles and explained variation (EV) values of variables, 3) good

206 correlations between sources contribution and external and internal tracers, and 4) agreement between the measured

207 and modeled $PM_{2.5}$ mass. More detailed information on the final selected factor profiles and contributions is presented

208 in Sect. 3.2.

209 2.3.3 Aerosol liquid water content

210 Aerosol liquid water content (ALWC) was calculated by ISORROPIA-II thermodynamic equilibrium model

211 (http://isorropia.eas.gatech.edu/) based on data of $PM_{2.5}$ chemical species (including NO_3^-, SO_4^{2-}, NH_4^+, and Cl^-) and

212 meteorological parameters including relative humidity (RH) and temperature (T), more model information can be

213 found in Fountoukis and Nenes (2007). It should be noted that the ISORROPIA-II model does not consider the

214 contribution of the organic, as inorganic aerosols are the most hygroscopic species and dominant contributor to

215 ALWC (Huang et al., 2020).

216 3. Results and discussion

217 3.1 –Characteristics of $PM_{2.5}$ and its chemical components

218 Figure 1 illustrates the mass composition of $PM_{2.5}$ in three pilot cities during the sampling periods, and their

219 concentrations levels are summarized in Table S4. The average $PM_{2.5}$ concentrations in Xi'an, Beijing, and

220 Shijiazhuang were 77±47 μg m^{-3}, 64±57 μg m^{-3}, and 60±39 μg m^{-3}, respectively. It is noted that the average $PM_{2.5}$

221 concentrations in Xi'an, Beijing, and Shijiazhuang did not meet the second level of the NAAQS, indicating that it is

222 necessary to establish more particular and efficient pollution reduction measures. As shown in Fig. 1, the chemical

223 compositions of $PM_{2.5}$ were similar in Beijing and Shijiazhuang (Fig. 1b and c) which was mainly composed of OA

224 (26.9–34.2%), followed by NO_3^- (23.6–26.5%), SO_4^{2-} (11.8–15.0%), NH_4^+ (11.8–14.8%), MD (7.4–10.1%), BC (2.9–

225 6.5%), and Cl^- (1.1–4.8%). However, in Xi'an, MD contributed in comparison more to $PM_{2.5}$ (17.3%), while SO_4^{2-}

had a smaller contribution (6.8%). This could be explained by more construction activities and MD transport from the Loess Plateau to Xi'an (Long et al., 2016; Yan et al., 2015). Meanwhile, the lowest sulfur oxidation ratio (SOR) was observed in Xi'an (0.18 ± 0.08, see Table S5), indicating weak efficiency of the second generation of SO_4^{2-}. The sum of SO_4^{2-}, NO_3^- and NH_4^+ accounted for 39.0–53.0% of $PM_{2.5}$ in three pilot cities, highlighting the importance of the secondary inorganic components in northern China. In addition, the fractions of BC, Cl^-, and TE in $PM_{2.5}$ were lower in Beijing than those in the other two cities, which can be explained by the stricter local control policies on solid fuels combustion and tightening the industrial emission standards in and near the capital city of China (Li et al., 2021a; Pang et al., 2021).

To ~~have a~~ better understanding ~~of~~ the impact of the chemical components, the mass fraction of each component was plotted as a function of the $PM_{2.5}$ mass concentration (Fig. 2a–c). The two dominant components of $PM_{2.5}$ were OA (25.7–38.0%) and MD (19.9–37.1%) while the $PM_{2.5}$ concentrations were below 40 μg m^{-3}. The faction of OA in $PM_{2.5}$ was the highest in Shijiazhuang and Beijing, while MD contributed most to $PM_{2.5}$ in Xi'an. This is potentially related to more emissions and higher backgrounds of local dust. With ~~increasing~~ increases of the $PM_{2.5}$ mass concentration, the fractions of chemical components in Xi'an and Shijiazhuang changed notably. The factions of OA and NO_3^- increased the most and reached the peaks of 40.1% and 28.7%, respectively, when the $PM_{2.5}$ concentration reached ~196 μg m^{-3} in Xi'an. On the contrary, NO_3^- and SO_4^{2-} were two dominant drivers of increasing $PM_{2.5}$ concentrations in Shijiazhuang, showing peak contributions of 32.5% and 18.7%, respectively, when the $PM_{2.5}$ concentration was over 100 μg m^{-3}. Compared to Xi'an and Shijiazhuang, Beijing had relatively stable fractions of each chemical component with increasing $PM_{2.5}$ concentrations. Particularly, the fractions of OA and NO_3^- contributed dominantly with averages of $33.3\pm3.0\%$ and $25.3\pm2.5\%$, respectively, when the $PM_{2.5} > 40$ μg m^{-3}.

3.2 Source apportionment of PM$_{2.5}$

Six potential sources, including biomass burning, fugitive dust, industrial emission, coal combustion, vehicle emission, and ~~secondary nitrate plus sulfate~~secondary formation source, were resolved by the HERM analysis. In Beijing, ~~secondary nitrate plus sulfate~~secondary formation source was furtherly divided into secondary nitrate plus OA and secondary sulfate plus OA. A special pollution source of firework was separated due to the Chinese Spring Festival (from New Year's Eve to January 3rd in the lunar calendar). Figures S6–S8 present the sources profiles and contributions in Xi'an, Shijiazhuang, and Beijing, respectively. Biomass burning features high Explained Variation (EV) for the two tracers Cl^- (33–58%) and K (30–44%) in the three cities (Ni et al., 2017; Zhao et al., 2021). The

9

254 fugitive dust is characterized by high EV values for Si (60–90%) and Ca (34–54%), which are the dominant chemical

255 species in the fugitive dust profiles in northern China (Shen et al., 2016; Zhao et al., 2006). The fractions of industrial

256 emission vary among the cities, showing high EV for Ni (55% and 87%) and Cr (25% and 70%) in Xi'an and

257 Shijiazhuang, and high EV for Cr (26%), Mn (40%), and Pb (27%) in Beijing. Ni is possibly emitted from the

258 semiconductor industry (Simka et al., 2005). Cr, Mn, and Pb could originate from the steel manufacturing and

259 incinerator fly ash (Duan and Tan, 2013; Ledoux et al., 2017). Coal combustion is characterized by high EV values

260 for As (38–75%), Se (40–50%), and Pb (31–57%). These elements are enriched in coals, which are reliable indicators

261 of coal combustion (Tian et al., 2013; Xu et al., 2012). The vehicle non-exhaust emissions could be identified by the

262 elements Ba, Cu, Ca, Fe, and Mn. Cu and Ba can be released from brake and tire wear of vehicles (Adachi and

263 Tainosho, 2004; Thorpe and Harrison, 2008). Moreover, Fe and Mn could be emitted from the combustion of

264 lubricating oil and fuel additives (Ålander et al., 2005; Lewis et al., 2003). Relatively high EV values for Ba (68%),

265 Cu (36%), and Ca (35%) are seen in Xi'an, significantly high EV values of Mn (68%), Fe (65%), Cu (53%), and Ba

266 (80%) are characterized in Shijiazhang and relatively high EV values of Fe (34%) and Cu (39%) are featured in

267 Beijing, respectively. Moreover, moderate EV values for BC (18–27%) and OA (13–22%) are commonly regarded

268 as contributions of vehicles engine exhaust, while the temporal variations of VE are well correlated with gaseous

269 NO_x or NO_2 in three cities ($R^2 = 0.45$–0.78), which is the good tracer of traffic-related emissions (Huang et al., 2017;

270 Li et al., 2017b). The secondary sources resolved by HERM are different among the three cities. In Xi'an and

271 Shijiazhuang, ~~the source of secondary nitrate plus sulfate~~this factor are characterized by high EV values for SO_4^{2-}

272 (62–75%), NO_3^- (55–53%), NH_4^+ (60–56%) and a medium EV value for OA (23–29%), which showed good

273 correlations with SO_4^{2-} ($R^2 = 0.85$–0.90) and NO_3^- ($R^2 = 0.85$–0.92) (Dai et al., 2020; Tian et al., 2022). In addition,

274 The OA concentration in this factor was calculated by EV value of OA, which was close to the secondary OA (SOA)

275 concentration estimated by BC-trace method (see Text S3 and Table S6). This means that SOA was mixed in this

276 factor, therefore, this factor was identified as secondary formation source. In Beijing, two secondary sources were

277 resolved. The first one was characterized by high EV value for NO_3^-(58%), NH_4^+ (42%) and medium values for OA

278 (21%), another one was characterized by high EV value for SO_4^{2-}(58%), and medium values for OA (16%), NH_4^+

279 (30%). The OA concentration in those two factors was also comparable to that estimated by BC-trace method (see

280 Text S3). So, those two sources were identified as secondary nitrate plus OA and secondary sulfate plus OA~~the~~

281 ~~secondary sources of nitrate and sulfate show high EV values of 58% and 65%~~, respectively. The combination of

282 secondary nitrate plus OA and secondary sulfate plus OA~~secondary nitrate and secondary sulfate~~ is equivalent to the

283 ~~secondary nitrate plus sulfate~~secondary formation source for next discussion. Additionally, the source of firework

10

284   emission is characterized by high EV values of Ba (83%), Cu (45%), and K (38%), which are recognized as common

285   indication in fireworks (Rai et al., 2020; Tian et al., 2014).

286   The modeled $PM_{2.5}$ mass was well correlated with the reconstructed $PM_{2.5}$ mass (R^2 = 0.99, slope = 0.90–1.01, Fig.

287   ~~S9~~S10) in three pilot cities, indicating the established models are reasonable. As shown in Fig. 1d and e, the

288   contributions of primary sources (i.e., the sum of biomass burning, fugitive dust, industrial emission, coal combustion,

289   and vehicle emission) in $PM_{2.5}$ were significantly higher than those of the ~~source of secondary nitrate plus~~

290   ~~sulfate~~secondary formation source in Xi'an and Shijiazhuang, indicating the $PM_{2.5}$ in these two cities are mainly

291   influenced by the primary source emissions during wintertime. Particularly, biomass burning and coal combustion

292   were two dominant contributors to $PM_{2.5}$ with contributions of 24.6% and 15.1%, respectively, in Xi'an; and 24.4%

293   and 16.0%, respectively, in Shijiazhuang. These suggest that controls of solid fuel combustion are critical to reducing

294    $PM_{2.5}$ pollution in these cities. In contrast, the contribution of ~~secondary nitrate plus sulfate~~secondary formation

295   source to $PM_{2.5}$ in Beijing was highly dominant (> 50%), potentially attributed to strict control of primary emissions

296   under the execution of a series of pollution control policies (Lv et al., 2016; Pang et al., 2021), and more regional

297   transportation of secondary pollutants (Liu et al., 2019; Wang and Zhao, 2018). Among the primary sources, the

298   contributions of biomass burning and vehicle emission were only 18.4% and 11.3%, respectively, further reflecting

299   the benefits of reductions of all primary emissions. Due to the Chinese Spring Festival, the contribution of firework

300   (7.9%) to $PM_{2.5}$ ranked second in primary sources (Fig. ~~S10~~S11). Which indicates more refined control schemes need

301   to be encouraged to deal with such special event in the future. It should be noted that contribution of fugitive dust

302   was all lower than fraction of mineral dust in the three pilot cities (Fig. 1). This is because fugitive dust defined here

303   mainly refers road and construction dust emission. While mineral dust represents material assumed oxides of mineral

304   elements such as Al, Si, Ca, Ti and Fe (Chow et al., 2015). These mineral elements in $PM_{2.5}$ comes from more

305   emission sectors including industry, crust, and transportation, construction, combustion (Liu et al., 2018a; Lu et al.,

306   2014; Pant and Harrison, 2013; Shen et al., 2016).

307   Figures 2d–f shows variations of source contribution with increases in $PM_{2.5}$ mass concentrations in three pilot cities.

308   The most two dominant sources were ~~secondary nitrate plus sulfate~~secondary formation source (32.1%) and fugitive

309   dust (31.4%) in Xi'an, coal combustion (24.9%) and vehicle emission (21.3%) in Shijiazhuang, and ~~secondary nitrate~~

310   ~~plus sulfate~~secondary formation source (24.3%) and fugitive dust (23.8%) in Beijing, when the $PM_{2.5}$ mass

311   concentration <40 μg m^{-3}. In Xi'an, when the $PM_{2.5}$ mass concentrations exceeded 180 μg m^{-3}, the contribution of

312 biomass burning raised mostly and reached the peak of 38.4%, demonstrating that biomass burning plays an important

313 role in worsening of air quality in Xi'an. On the contrary, the contributions of ~~secondary nitrate plus sulfate~~secondary

314 formation source increased mostly in comparison to other sources in Shijiazhuang and Beijing, indicating the $PM_{2.5}$

315 pollution was mainly dominated by the secondary aerosol formations during the wintertime. And the peak

316 contributions of secondary nitrate and sulfate were 66.5% and 74,7% while the $PM_{2.5}$ mass concentration increased

317 to 113 μg m^{-3} and 223 μg m^{-3} in Shijiazhuang and Beijing, respectively.

318 **3.3 Formation of secondary aerosols**

319 Using the high-time-resolution data, we further explored the possible formation mechanisms of ~~secondary nitrate~~

320 ~~plus sulfate~~secondary formation source. The concentration of ~~secondary nitrate plus sulfate~~secondary formation

321 source is standardized by dividing background corrected CO (ΔCO) to ~~~~weaken impact of planetary boundary layer

322 height (PBLH) (DeCarlo et al., 2010). In this study, ΔCO is defined as the 1.25th percentile of CO concentration

323 during the campaign, which are 0.17, 0.15, and 0.16 ppm in Xi'an, Shijiazhuang, and Beijing, respectively. O_x (NO_2

324 + O_3) is an indicator of the photochemical oxidation degree (Wood et al., 2010). The function between ~~secondary~~

325 ~~nitrate plus sulfate~~secondary formation source/ΔCO ratio and O_x during the daytime (i.e., 08:00–17:00 LST) (Fig.

326 ~~S11~~S12) was plotted to explain the effect of photochemical oxidations in three pilot cities. As shown in Fig. 3, good

327 linear correlations of ~~secondary nitrate plus sulfate~~secondary formation source/ΔCO and O_x (R^2 = 0.83–0.99) suggest

328 that photochemical oxidations play an important role in the formation of secondary aerosol during the daytime.

329 Compared to the low-level O_x, formation of secondary aerosol significantly enhanced at high-level O_x (>50 ppb) in

330 Xi'an and Beijing, characterized by larger slopes of 17.2 and 38.9, respectively (Fig. 3a and c). Furthermore, the

331 highest atmospheric oxidation capacity was found in Beijing, inferring by the highest fraction of O_3 to O_x. This is

332 consistent with the highest contribution of ~~secondary nitrate plus sulfate~~secondary formation source to $PM_{2.5}$ in

333 Beijing during the daytime (Fig. ~~S12a~~S13a–c).

334 The aqueous-phase reaction is another important pathway for secondary aerosol formation in the atmosphere (Wang

335 et al., 2018; Xue et al., 2014). ALWC is considered an indicator of an aqueous-phase reaction (Ervens et al., 2011).

336 Considering that the aqueous-phase reaction occurs both during the daytime and nighttime characterized by good

337 correlations between secondary formation source/ΔCO and ALWC (R^2 = 0.81–0.98, Fig. S14). The correlations of

338 ~~secondary nitrate plus sulfate~~secondary formation source/ΔCO ratio and ALWC during ~~nighttime~~ all sampling

339 periods ~~(18:00–07:00 the next day LST, Fig. S11)~~ were re-established in three pilot cities to assess the implications

12

340 of aqueous-phase chemistry for secondary aerosol production. As shown in Fig. 4, ~~The~~ the secondary formation

341 source~~nitrate plus sulfate~~/ΔCO showed a significant linear correlation to ALWC (R^2 = 0.~~81~~92–0.~~95~~99) when RH <

342 80% ~~(Fig. 4)~~, indicating an obvious effect of aqueous-phase reaction on the secondary aerosol formation during the

343 ~~nighttime~~sampling periods. However, when RH >80%, the secondary formation source~~nitrate plus sulfate~~/ΔCO

344 showed no notable increase with ALWC in Shijiazhuang (Fig. 4b), whereas a tiny increase with ALWC in Beijing

345 (Fig. 4c). The higher ALWC at RH > 80% probably inhibits secondary aerosol formation due to the decrease in

346 aerosol acidity (Huang et al., 2019; Meng et al., 2014). Khan et al. (2008) found that NO_3 radicals can rapidly generate

347 from the reaction between NO_2 and O_3 with unsaturated organic species during nighttime. The value of $O_3 \times NO_2$ can

348 thus represent its production reaction rate or be used as a proxy for the NO_3 radical. The highest NO_3 radical

349 production rate was found in Beijing, followed by Xi'an and Shijiazhuang, when RH<80%. This could be used to

350 explain the highest contribution of secondary formation source~~nitrate plus sulfate~~ to $PM_{2.5}$ in Beijing during the

351 daytime and nighttime (Fig. S1~~23~~d ~~f~~). Moreover, the results showed that both photochemical oxidation and aqueous-

352 phase reaction play more important roles in Beijing, where the primary sources have been better controlled. This

353 reflects that pollution control policies need to be focused on the suppression of secondary formations.

3.4 Elaborations of different episode cases

355 During the sampling periods, the concentration of $PM_{2.5}$ and its chemical components ~~simply~~ accumulated within a

356 short period in a few cases (Fig.~~S13a~~S15a–c). We define such a rapid rise in $PM_{2.5}$ mass concentration as a pollution

357 episode. As shown in Table 1, meteorological conditions, the concentration levels of gas~~eous~~ pollutants, chemical

358 compositions, and source contributions of $PM_{2.5}$ during pollution episodes in three pilot cities are summarized. The

359 episodes were accompanied by low wind speed (< 2 m s^{-1}), leading to weak dispersions of ~~the~~ fresh emissions and

360 accumulated pollutants (Chen et al., 2020b). OA and NO_3^- were ~~The~~ the two dominant chemical components in $PM_{2.5}$

361 during all pollution episode cases ~~were OA and NO_3^-~~, with fractions of 26–40% and 23–32%, respectively. Their high

362 abundances could be explained by the significant reduction of SO_2 emissions ~~by~~ because of the prohibiting of burning

363 bulk coals and executing the "Coal-to-Natural Gas" policy in recent years (Meng et al., 2022). In this study, eight

364 pollution episodes (donated as EP1-EP8) were classified into three types: The first type was dominated by biomass

365 burning (30–40%) (EP1, EP4, and EP8). The second type was dominated by ~~secondary nitrate plus sulfate~~secondary

366 formation source (61–70%) (EP5, EP6, and EP7). The two remaining pollution episodes were mutually contributed

367 by both primary and secondary sources (EP2 and EP3), in which ~~secondary nitrate plus sulfate~~secondary formation

368 source (34–39%) and biomass burning (23–24%) were the two dominant contributors to $PM_{2.5}$.

13

369 To ~~profoundly understand~~gain insights into the ~~progress~~process of pollution episodes, three typical pollution events

370 were chosen for detailed discussion (i.e., EP2 in Xi'an, EP4 in Shijiazhuang, and EP7 in Beijing) based on the validity

371 and integrity of the data and the representativeness of the selected pollution events. The two-stage evolution was

372 distinguished for EP4 as an example of the first type of episode (Fig. S16). ~~For the first type of episode represented~~

373 ~~by EP4 (Fig. S14), a two-stages evolution was distinguished.~~ At Stage 1, the $PM_{2.5}$ mass concentrations rapidly

374 increased from 7 to 82 $\mu g\ m^{-3}$ under stable weather conditions inferring by low wind speed ($1.8\pm0.8\ m\ s^{-1}$, Fig.

375 ~~S14b~~S16b), in which the concentrations (fractions) of biomass burning increased from 0.6 $\mu g\ m^{-3}$ (7%) to 36.7 $\mu g\ m^{-}$

376 ^{3} (55%) due to heating ~~demand~~activities during nighttime. Meanwhile, the chemical composition was relatively

377 stable and dominated by OA ($31\pm5\%$) and NO_3^-($21\pm5\%$). At Stage 2, the $PM_{2.5}$ mass concentration continuously

378 increased to 105 $\mu g\ m^{-3}$ in a few hours along with the most notable abundance of the source of ~~secondary nitrate plus~~

379 ~~sulfate~~secondary formation source, which concentration (contribution) rapidly increased from 2.3 $\mu g\ m^{-3}$ (4%) to

380 54.4 $\mu g\ m^{-3}$ (52%) (Fig. ~~S14g~~S16g and h). This is due to the aqueous-phase reactions effect inferring by the rapid

381 increase in ALWC (from 16 $\mu g\ m^{-3}$ to 78 $\mu g\ m^{-3}$, Fig. ~~S14c~~S16c) and RH (from 51% to 79%, Fig. ~~S14a~~S16a).

382 In contrast, a three-stage~~s~~ evolution was discriminated for the second type of episode, using EP7 as an example (Fig.

383 ~~S15~~S17). At Stage 1, the $PM_{2.5}$ concentration gradually increased from 11 to 30 $\mu g\ m^{-3}$, as well as NO_2 (from 15 to

384 59 $\mu g\ m^{-3}$, Fig. ~~S15d~~S17d) due to the boosts of the predominant contributions of vehicle emission and biomass

385 burning (Fig. ~~S15g~~S17g and h). In the meantime, the contribution of coal combustion also slowly increased along

386 with SO_2 (Fig. ~~S15d~~S17d and h). At Stage 2, under the lowest average wind speed in the study period ($0.7\pm0.4\ m\ s^{-}$

387 ^{1}, Fig. ~~S15b~~S17b), the $PM_{2.5}$ mass concentrations moderately increased from 30 to 91 $\mu g\ m^{-3}$ with relatively stable

388 chemical composition and source contribution (Fig. ~~S15f~~S17f and h). Compared to Stage 1, the fractions of NO_3^-

389 increased mostly from $9\pm3\%$ to $23\pm3\%$, this is probably influenced by photochemical oxidations inferring by relative

390 high O_x and NO_2 concentration (Fig. ~~S15c~~S17c and d). At Stage 3, the $PM_{2.5}$ mass concentration rapidly rose to 142

391 $\mu g\ m^{-3}$ and then remained stable. Furthermore, the ~~In which~~ greatest increase of sources ~~the~~ concentrations

392 (~~fractions~~contribution) ~~of~~ was ~~secondary nitrate plus sulfate~~secondary formation source ~~increased mostly~~ from 18.9

393 $\mu g\ m^{-3}$ (48%) to 120.6 $\mu g\ m^{-3}$ (80%). This might be due to the occurrence of an aqueous-phase reaction, which was

394 indicated by the elevation of RH and ALWC (Fig. ~~S15a~~S17a and c).

395 Figure S16 illustrates the third type of episode using EP2 as an example, ~~while~~in which a four-stages evolution was

396 resolved. At Stage 1, the $PM_{2.5}$ mass concentration ($14\pm3\ \mu g\ m^{-3}$) was relatively low and dominated by the

14

397   contributions of ~~secondary nitrate plus sulfate~~secondary formation source (43±17%) and fugitive dust (24±8%), as

398   well as MD (28±7%) and OA (26±7%). At Stage 2, the $PM_{2.5}$ mass concentrations promptly increased from 21 to 82

399    $\mu g\ m^{-3}$, with the two dominant chemical components of OA (21.7 $\mu g\ m^{-3}$) and NO_3^- (17.1 $\mu g\ m^{-3}$). The $PM_{2.5}$ increases

400   can be also ~~contributed~~ attributed to the raise of ~~secondary nitrate plus sulfate~~secondary formation source (25.3 μg

401   m^{-3}) and biomass burning (14.4 $\mu g\ m^{-3}$). The enhancement of secondary aerosol was probably generated through the

402   aqueous-phase reaction evidenced by the increase of ALWC and NO_2 (Fig. ~~S16c~~S18c and d). At Stage 3, $PM_{2.5}$ mass

403   continuously increased to 139 $\mu g\ m^{-3}$ with a dominant increase of primary sources emission including biomass

404   burning (29.0 $\mu g\ m^{-3}$), vehicle emission (21.5 $\mu g\ m^{-3}$) and coal combustion (16.5 $\mu g\ m^{-3}$) along with the increases of

405   SO_2 and NO_2 as well (Fig. ~~S16~~S18d). The three primary sources contributed >60% of the total resolved sources.

406   Meanwhile, the ~~secondary nitrate plus sulfate~~secondary formation source also increased slowly through aqueous-

407   phase reaction inferring by increase of ALWC (Fig. ~~S16c~~S18c). At the final Stage 4, the $PM_{2.5}$ mass concentration

408   maintained relatively stable with an average of 142±11 $\mu g\ m^{-3}$, dominated by ~~sources of secondary nitrate plus~~

409   ~~sulfate~~secondary formation source (34±6%) and biomass burning (28±6%); and chemical components of OA (36±4%)

410   and NO_3^- (25±1%).

411   In summary, the pollution events occurred in Xi'an was mainly derived by stronger emissions of primary sources

412   under adverse meteorological conditions, even though the aqueous-phase reaction also contribute to secondary

413   aerosol formation. In contrast, pollution events occurred in Shijiazhuang and Beijing were mainly influenced by

414   formation of secondary aerosols through both of aqueous-phase reaction and photochemical oxidation. What's more,

415   ~~in which~~ aqueous-phase reaction plays a more important role than photochemical oxidation. Hence, to further

416   improve the air quality in the north of China, primary source emissions should be prioritized for control in the

417   northwest region, with a focus on biomass burning and coal combustion. In the North China Plain, the priority should

418   be given to reduc~~ing~~e emissions of the precursors from secondary sources, with a focus on NO_x and volatile organic

419   compounds (VOCs).

3.5 Policy implications

421   In past decades, the air quality in China improved notably under the implementation of air pollution control policies

422   including APCAP and TAPFAP. The $PM_{2.5}$ mass in Xi'an, Shijiazhuang and Beijing were the lowest during campaigns

423   compared with those in last decades (Table ~~S6~~S7). The variations of the chemical composition and the source

424   contribution of $PM_{2.5}$ in the three pilot cities are displayed in Fig. 5. As shown, the dominant chemical components

425 of $PM_{2.5}$ changed from OA and SO_4^{2-}, to OA and NO_3^- (Fig. 5a–c). This could be attributed to the reduction in coal

426 consumption due to clean energy replacement and the increase of vehicle ownership, which This lead a decrease of

427 the SO_2 and an increase of NO_2 (Wang et al., 2013). Since the atmospheric oxidation reaction (i.e., aqueous-phase

428 reaction and photochemical oxidation) of the precursors (i.e., NO_2, VOCs) is the primary source for the OA and NO_3^-

429 in the atmosphere (Feng et al., 2018; Li et al., 2022; Tao et al., 2016; Yang et al., 2022b; Ziemann and Atkinson,

430 2012), and it is impossible to avoid, thus, the precursors of OA and NO_3^- should be reduced from the combustion and

431 transportation sectors (Fermo et al., 2021; Liu et al., 2022; Wang et al., 2021c; Zhang et al., 2019). In addition, the

432 fraction of NH_4^+ in $PM_{2.5}$ increased with an alarming rate. This is coincidentally in a similar trend of NH_3. Studies

433 have reported that controls of NH_4^+ is more effective than that of NO_x in the reduction of $PM_{2.5}$ mass concentrations

434 (Gu et al., 2021; Zheng et al., 2022). Therefore, collaborative control measures for the emissions of precursors

435 including NO_x, VOCs, and NH_3 are necessary.

436 As shown Table S7 S8 and Fig. 5d-f, coal combustion decreased remarkably due to the coal-related policies

437 implementation including the strength of emissions standards for coal-fired power plants, the change of energy

438 sources from coal to natural gas in some industrials, and the coal burning was forbidden in the main urban areas

439 (Shen, 2016; Yang and Teng, 2018). The similar trend was also founded in the results of $PM_{2.5}$ source apportionment

440 in Beijing released by Beijing Municipal Ecology and Environment Bureau (Fig. S19). Meanwhile, the

441 contribution of industrial emission and vehicle emission decreased slightly because of the improvement of industrial

442 emission standards (He et al., 2020; Wang et al., 2020a) and the traffic-related policy implementation such as the

443 strength of vehicle emission standards, improvement of fuel quality, and elimination of high-emission-vehicles. This

444 resulted in the reduction of the precursor gases and $PM_{2.5}$ from vehicles (Feng et al., 2021; Fontaras et al., 2012; Jin

445 et al., 2012). However, the emission of biomass burning did not show a significant reduction in recent years, and its

446 contribution increased from 9% in 2014 to 25% in 2020 (Xi'an), from 3% in 2015 to 24% in 2022 (Shijiazhuang),

447 and from 6% in 2013 to 18% in 2021 (Beijing) (Fig. 5d-f). This is likely because biomass burning is an open source,

448 which makes it more difficult to control compare with other primary sources. Biomass used for residential heating in

449 rural areas is still frequently occurred (Ren, 2021; Tian et al., 2022; Yang et al., 2022a; Zhang et al., 2017). Hence,

450 the clean energy revolution should be promoted urgently especially in the entire regions in northwest China. Moreover,

451 the contributions of secondary formation sources increased, it is potentially explained by the high reduction rate of

452 primary emissions and the improvement of atmospheric oxidation capacity (Chen et al., 2020a; Feng et al., 2020).

453 Therefore, more control measures should focus on weakening the atmosphere atmospheric oxidation capacity, such

454 as reduction of O_3 formation, to reduce the formation of secondary pollutants which are now identified as the most

455 critical drivers of pollution. Considering those factors, it is also important to promote the mitigation of *both* $PM_{2.5}$

456 and O_3.

4. Conclusion

458 The intensive real-time measurement campaigns about $PM_{2.5}$ chemical components were conducted in Xi'an,

459 Shijiazhuang, and Beijing during the wintertime respectively. Chemical compositions of $PM_{2.5}$ in the three cities were

460 all dominated by OA (26.9–34.2%) and NO_3^- (23.6–26.5%). Six sources of $PM_{2.5}$ in Xi'an and Shijiazhuang were

461 resolved by HERM and their contributions were similar, with a descending order of ~~secondary nitrate plus~~

462 ~~sulfate~~secondary formation source (32.2–37.6%), biomass burning (24.4–24.6 %), coal combustion (15.1–16.0%),

463 vehicle emission (12.2–12.5 %), industrial emission (5.5–7.7%) and fugitive dust (4.4–7.8%). However, the

464 secondary nitrate (29.0%) and the secondary sulfate (23.0%) were separately resolved and relatively more important

465 in Beijing. In addition, the contribution of firework (7.9%) to $PM_{2.5}$ was found during the Chinese Spring Festival.

466 The possible formation mechanism of ~~secondary nitrate plus sulfate~~secondary formation source in three pilot cities

467 was explored. The results showed that secondary aerosols were generated by both photochemical oxidation and

468 aqueous-phase reaction. Meanwhile, the formation rate of secondary aerosols in Beijing was higher than that in Xi'an

469 and Shijiazhuang. Furthermore, the eight pollution episodes within the sampling periods were categorized three types

470 and characterized respectively. The dominant chemical compositions of $PM_{2.5}$ were OA (26–40%) and NO_3^- (23–

471 32%) during all pollution episodes. Furthermore, ~~secondary nitrate plus sulfate~~secondary formation source and

472 biomass burning were two major derivers of the pollution.

473 The dominant chemical components of $PM_{2.5}$ in pilot cities have changed from OA and SO_4^{2-} to OA and NO_3^- under

474 the implementation of a clean air plan in past decades. This indicates that reduction of precursors including NO_2 and

475 VOCs should be a key task in the future. In addition, the contribution of biomass burning increased, especially in

476 Xi'an. This indicates that clean energy for heating activities in rural areas in northwest China is still insufficient.

477 Furthermore, to weaken the ~~atmosphere~~ atmospheric oxidation capacity for reducing the contribution of ~~secondary~~

478 ~~nitrate plus sulfate~~secondary formation source, it is necessary to promote the collaborative control on ozone and

479 particulate matter.

480 *Data availability*. Data used to support the findings in this study are archived at the Institute of Earth Environment,

481   Chinese Academy of Sciences, and are publicly available at https://doi.org/10.5281/zenodo.~~7336744~~8106655.

494

References:

Adachi, K. and Tainosho, Y.: Characterization of heavy metal particles embedded in tire dust, Environ. Int., 30, 1009–1017, https://doi.org/10.1016/j.envint.2004.04.004, 2004.

Ålander, T., Antikainen, E., Raunemaa, T., Elonen, E., Rautiola, A., and Torkkell, K.: Particle emissions from a small Two-Stroke engine: Effects of fuel, lubricating oil, and exhaust aftertreatment on particle characteristics, Aerosol Sci. Technol., 39, 151–161, https://doi.org/10.1080/027868290910224, 2005.

Cao, J. J. and Cui, L.: Current status, characteristics and causes of particulate air pollution in the Fenwei Plain, China: A Review, J. Geophy. Res-Atmos., 126, https://doi.org/10.1029/2020JD034472, 2021.

Chan, C. K. and Yao, X.: Air pollution in mega cities in China, Atmos. Environ., 42, 1–42, https://doi.org/10.1016/j.atmosenv.2007.09.003, 2008.

Chen, L.-W. A. and Cao, J. J.: PM$_{2.5}$ source apportionment using a hybrid environmental receptor model, Environ. Sci. Technol., 52, 6357–6369, https://doi.org/10.1021/acs.est.8b00131, 2018.

Chen, Q., Hua, X., Li, J. W., Chang, T., and Wang, Y.: Diurnal evolutions and sources of water-soluble chromophoric aerosols over Xi'an during haze event, in Northwest China, Sci. Total Environ., 786, 147412, https://doi.org/10.1016/j.scitotenv.2021.147412, 2021.

Chen, S., Wang, H., Lu, K., Zeng, L., Hu, M., and Zhang, Y.: The trend of surface ozone in Beijing from 2013 to 2019: Indications of the persisting strong atmospheric oxidation capacity, Atmos. Environ., 242, 117801, https://doi.org/10.1016/j.atmosenv.2020.117801, 2020a.

Chen, Z., Chen, D., Zhao, C., Kwan, M., Cai, J., Zhuang, Y., Zhao, B., Wang, X., Chen, B., Yang, J., Li, R., He, B., Gao, B., Wang, K., and Xu, B.: Influence of meteorological conditions on PM$_{2.5}$ concentrations across China: A review of methodology and mechanism, Environ. Int., 139, 105558, https://doi.org/10.1016/j.envint.2020.105558, 2020b.

Chow, J. C., Lowenthal, D. H., Chen, L.-W. A., Wang, X., and Watson, J. G.: Mass reconstruction methods for PM$_{2.5}$: a review, Air Qual. Atmos. Health, 8, 243–263, https://doi.org/10.1007/s11869-015-0338-3, 2015.

Dai, Q., Liu, B., Bi, X., Wu, J., Liang, D., Zhang, Y., Feng, Y., and Hopke, P. K.: Dispersion normalized PMF provides insights into the significant changes in source contributions to PM$_{2.5}$ after the COVID-19 outbreak, Environ. Sci. Technol., 54, 9917–9927, https://doi.org/10.1021/acs.est.0c02776, 2020.

DeCarlo, P. F., Ulbrich, I. M., Crounse, J., de Foy, B., Dunlea, E. J., Aiken, A. C., Knapp, D., Weinheimer, A. J., Campos, T., Wennberg, P. O., and Jimenez, J. L.: Investigation of the sources and processing of organic aerosol over the Central Mexican Plateau from aircraft measurements during MILAGRO, Atmos. Chem. Phys., 10, 5257–5280, https://doi.org/10.5194/acp-10-5257-2010, 2010.

Drinovec, L., Močnik, G., Zotter, P., Prévôt, A. S. H., Ruckstuhl, C., Coz, E., Rupakheti, M., Sciare, J., Müller, T., Wiedensohler, A., and Hansen, A. D. A.: The "dual-spo" Aethalometer: an improved measurement of aerosol black carbon with real-time loading compensation, Atmos. Meas. Tech., 8, 1965–1979, https://doi.org/10.5194/amt-8-1965-2015, 2015.

Duan, J. and Tan, J.: Atmospheric heavy metals and Arsenic in China: Situation, sources and control policies, Atmos. Environ., 74, 93–101, https://doi.org/10.1016/j.atmosenv.2013.03.031, 2013.

Elser, M., Huang, R.-J., Wolf, R., Slowik, J. G., Wang, Q.-Y., Canonaco, F., Li, G. H., Bozzetti, C., Daellenbach, K. R., Huang, Y., Zhang, R.-J., Li, Z.-Q., Cao, J. J., Baltensperger, U., El-Haddad, I., and Prévôt, A. S. H.: New insights into PM$_{2.5}$ chemical composition and sources in two major cities in China during extreme haze events using aerosol mass spectrometry, Aerosols/Field Measurements/Troposphere/Chemistry (chemical composition and reactions), https://doi.org/10.5194/acpd-15-30127-2015, 2015.

Ervens, B., Turpin, B. J., and Weber, R. J.: Secondary organic aerosol formation in cloud droplets and aqueous particles (aqSOA): a review of laboratory, field and model studies, Atmos. Chem. Phys., 11, 11069–11102, https://doi.org/10.5194/acp-11-11069-2011, 2011.

Feng, T., Bei, N., Zhao, S., Wu, J. rui, Li, X., Zhang, T., Cao, J., Zhou, W., and Li, G.: Wintertime nitrate formation during haze days in the Guanzhong basin, China: A case study, Environ. Pollut., 243, 1057–1067, https://doi.org/10.1016/j.envpol.2018.09.069, 2018.

Feng, T., Zhao, S., Zhang, X., Wang, Q., Liu, L., Li, G., and Tie, X.: Increasing wintertime ozone levels and secondary aerosol formation in the Guanzhong basin, central China, Sci. Total Environ., 12, 2020.

Feng, X., Zhang, X., He, C., and Wang, J.: Contributions of traffic and industrial emission reductions to the air quality improvement after the lockdown of Wuhan and neighboring Cities due to COVID-19, Toxics, 9, 358, https://doi.org/10.3390/toxics9120358, 2021.

Fermo, P., Artíñano, B., De Gennaro, G., Pantaleo, A. M., Parente, A., Battaglia, F., Colicino, E., Di Tanna, G., Goncalves da Silva Junior, A., Pereira, I. G., Garcia, G. S., Garcia Goncalves, L. M., Comite, V., and Miani, A.: Improving indoor air quality through an air purifier able to reduce aerosol particulate matter (PM) and volatile organic compounds (VOCs): Experimental results, Environ. Pollut., 197, 111131, https://doi.org/10.1016/j.envres.2021.111131, 2021.

Fontaras, G., Martini, G., Manfredi, U., Marotta, A., Krasenbrink, A., Maffioletti, F., Terenghi, R., and Colombo, M.: Assessment of on-road emissions of four Euro V diesel and CNG waste collection trucks for supporting air-quality improvement initiatives in the city of Milan, Sci. Total Environ., 426, 65–72, https://doi.org/10.1016/j.scitotenv.2012.03.038, 2012.

Fountoukis, C. and Nenes, A.: ISORROPIA II: a computationally efficient thermodynamic equilibrium model for K$^+$–Ca^{2+}–Mg^{2+}–NH$_4^+$–Na$^+$–SO$_4^{2-}$–NO$_3^-$–Cl$^-$–H$_2$O aerosols, Atmos. Chem. Phys., 7, 4639–4659, https://doi.org/10.5194/acp-7-4639-2007, 2007.

Furger, M., Rai, P., Slowik, J. G., Cao, J., Visser, S., Baltensperger, U., and Prévôt, A. S. H.: Automated alternating sampling of PM10 and PM2.5 with an online XRF spectrometer, Atmospheric Environment: X, 5, 100065, https://doi.org/10.1016/j.aeaoa.2020.100065, 2020.

Gu, B., Zhang, L., Van Dingenen, R., Vieno, M., Van Grinsven, H. J., Zhang, X., Zhang, S., Chen, Y., Wang, S., Ren, C., Rao, S., Holland, M., Winiwarter, W., Chen, D., Xu, J., and Sutton, M. A.: Abating ammonia is more cost-effective than nitrogen oxides for mitigating PM$_{2.5}$ air pollution, Science, 374, 758–762,

567   https://doi.org/10.1126/science.abf8623, 2021.

568 Guo, Y., Lin, C., Li, J., Wei, L., Yang, Y., Yang, Q., Li, D., Wang, H., and Shen, J.: Persistent pollution episodes,
569   transport pathways, and potential sources of air pollution during the heating season of 2016–2017 in Lanzhou,
570   China, Environ. Monit. Assess., 193, 852, https://doi.org/10.1007/s10661-021-09597-8, 2021.

571 He, J., Zhao, M., Zhang, B., Wang, P., Zhang, D., Wang, M., Liu, B., Li, N., Yu, K., Zhang, Y., Zhou, T., and Jing, B.:
572   The impact of steel emissions on air quality and pollution control strategy in Caofeidian, North China, Atmos.
573   Pollut. Res., 11, 1238–1247, https://doi.org/10.1016/j.apr.2020.04.012, 2020.

574 He, K., Huo, H., and Zhang, Q.: Urban air pollution in China: Current status, characteristics, and progress, Annu.
575   Rev. Energy. Environ., 27, 397–431, https://doi.org/10.1146/annurev.energy.27.122001.083421, 2002.

576 Hu, W. wei, Campuzano-Jost, P., Day, D. A., Croteau, P., Canagaratna, M. R., Jayne, J. T., Worsnop, D. R., and
577   Jimenez, J. L.: Evaluation of the new capture vapourizer for aerosol mass spectrometers (AMS) through
578   laboratory studies of inorganic species, Atmos. Meas. Tech., 10, 2897–2921, https://doi.org/10.5194/amt-10-
579   2897-2017, 2017.

580 Huang, R.-J., He, Y., Duan, J., Li, Y., Chen, Q., Zheng, Y., Chen, Y., Hu, W., Lin, C., Ni, H., Dai, W., Cao, J., Wu, Y.,
581   Zhang, R., Xu, W., Ovadnevaite, J., Ceburnis, D., Hoffmann, T., and O'Dowd, C. D.: Contrasting sources and
582   processes of particulate species in haze days with low and high relative humidity in wintertime Beijing, Atmos.
583   Chem. Phys., 20, 9101–9114, https://doi.org/10.5194/acp-20-9101-2020, 2020.

584 Huang, R.-J., Zhang, Y., Bozzetti, C., Ho, K.-F., Cao, J.-J., Han, Y., Daellenbach, K. R., Slowik, J. G., Platt, S. M.,
585   Canonaco, F., Zotter, P., Wolf, R., Pieber, S. M., Bruns, E. A., Crippa, M., Ciarelli, G., Piazzalunga, A.,
586   Schwikowski, M., Abbaszade, G., Schnelle-Kreis, J., Zimmermann, R., An, Z., Szidat, S., Baltensperger, U.,
587   Haddad, I. E., and Prévôt, A. S. H.: High secondary aerosol contribution to particulate pollution during haze
588   events in China, Nature, 514, 218–222, https://doi.org/10.1038/nature13774, 2014.

589 Huang, X., Liu, Z., Liu, J., Hu, B., Wen, T., Tang, G., Zhang, J., Wu, F. kun, Ji, D., Wang, L., and Wang, Y.: Chemical
590   characterization and source identification of $PM_{2.5}$ at multiple sites in the Beijing–Tianjin–Hebei region, China,
591   Atmos. Chem. Phys., 17, 12941–12962, https://doi.org/10.5194/acp-17-12941-2017, 2017.

592 Huang, R.-J., Wang, Y., Cao, J., Lin, C., Duan, J., Chen, Q., Li, Y., Gu, Y., Yan, J., Xu, W., Fröhlich, R., Canonaco,
593   F., Bozzetti, C., Ovadnevaite, J., Ceburnis, D., Canagaratna, M. R., Jayne, J., Worsnop, D. R., El-Haddad, I.,
594   Prévôt, A. S. H., and O'Dowd, C. D.: Primary emissions versus secondary formation of fine particulate matter
595   in the most polluted city (Shijiazhuang) in North China, Atmos. Chem. Phys., 19, 2283–2298,
596   https://doi.org/10.5194/acp-19-2283-2019, 2019.

597

598 Huang, X., Zhang, J., Luo, B., Luo, J., Zhang, W., and Rao, Z.: Characterization of oxalic acid-containing particles
599   in summer and winter seasons in Chengdu, China, Atmos. Environ., 198, 133–141,
600   https://doi.org/10.1016/j.atmosenv.2018.10.050, 2019.

601 Jin, T. sheng, Gao, J. jia, Fu, L. xin, Ai, Y., and Xu, X. H.: An evaluation of improvements in the air quality of Beijing
602   arising from the use of new vehicle emission standards, Environ. Monit. Assess., 184, 2151–2159,
603   https://doi.org/10.1007/s10661-011-2106-7, 2012.

Khan, M. A. H., Ashfold, M. J., Nickless, G., Martin, D., Watson, L. A., Hamer, P. D., Wayne, R. P., Canosa-Mas, C. E., and Shallcross, D. E.: Night-time NO_3 and OH radical concentrations in the United Kingdom inferred from hydrocarbon measurements, Atmos. Sci. Lett., 9, 140–146, https://doi.org/10.1002/asl.175, 2008.

Kuniyal, J. C. and Guleria, R. P.: The current state of aerosol-radiation interactions: A mini review, J. Aerosol Sci., 130, 45–54, https://doi.org/10.1016/j.jaerosci.2018.12.010, 2019.

Kuo, C.-Y., Cheng, F.-C., Chang, S.-Y., Lin, C.-Y., Chou, C. C. K., Chou, C.-H., and Lin, Y.-R.: Analysis of the major factors affecting the visibility degradation in two stations, J. Air Waste Manage., 63, 433–441, https://doi.org/10.1080/10962247.2012.762813, 2013.

Ledoux, F., Kfoury, A., Delmaire, G., Roussel, G., El Zein, A., and Courcot, D.: Contributions of local and regional anthropogenic sources of metals in $PM_{2.5}$ at an urban site in northern France, Chemosphere, 181, 713–724, https://doi.org/10.1016/j.chemosphere.2017.04.128, 2017.

Lewis, C. W., Norris, G. A., Conner, T. L., and Henry, R. C.: Source apportionment of Phoenix $PM_{2.5}$ aerosol with the Unmix receptor model, J. Air Waste Manage., 53, 325–338, https://doi.org/10.1080/10473289.2003.10466155, 2003.

Li, J., Du, H., Wang, Z., Sun, Y., Yang, W., He, J., Tang, X., and Fu, P.: Rapid formation of a severe regional winter haze episode over a mega-city cluster on the North China Plain, Environ. Pollut., 223, 605–615, https://doi.org/10.1016/j.envpol.2017.01.063, 2017a.

Li, J., Gao, W., Cao, L., Xiao, Y., Zhang, Y., Zhao, S., Liu, Z., Liu, Z., Tang, G., Ji, D., Hu, B., Song, T., He, L., Hu, M., and Wang, Y.: Significant changes in autumn and winter aerosol composition and sources in Beijing from 2012 to 2018: Effects of clean air actions, Environ. Pollut., 268, 115855, https://doi.org/10.1016/j.envpol.2020.115855, 2021a.

Li, K., Zhang, X., Zhao, B., Bloss, W. J., Lin, C., White, S., Yu, H., Chen, L., Geng, C., Yang, W., Azzi, M., George, C., and Bai, Z.: Suppression of anthropogenic secondary organic aerosol formation by isoprene, npj Clim. Atmos. Sci., 5, 12, https://doi.org/10.1038/s41612-022-00233-x, 2022.

Li, L., Tan, Q., Zhang, Y., Feng, M., Qu, Y., An, J., and Liu, X.: Characteristics and source apportionment of $PM_{2.5}$ during persistent extreme haze events in Chengdu, southwest China, Environ. Pollut., 230, 718–729, https://doi.org/10.1016/j.envpol.2017.07.029, 2017b.

Li, W., Shao, L. yi, Wang, W., Li, H., Wang, X., Li, Y., Li, W., Jones, T., and Zhang, D.: Air quality improvement in response to intensified control strategies in Beijing during 2013–2019, Sci. Total Environ., 744, 140776, https://doi.org/10.1016/j.scitotenv.2020.140776, 2020.

Li, X., Bei, N., Tie, X., Wu, J., Liu, S., Wang, Q., Liu, L., Wang, R., and Li, G.: Local and transboundary transport contributions to the wintertime particulate pollution in the Guanzhong Basin (GZB), China: A case study, Sci. Total Environ., 797, 148876, https://doi.org/10.1016/j.scitotenv.2021.148876, 2021b.

Li, Y., Sun, Y., Zhang, Q., Li, X., Li, M., Zhou, Z., and Chan, C. K.: Real-time chemical characterization of atmospheric particulate matter in China: A review, Atmos. Environ., 158, 270–304,

640 https://doi.org/10.1016/j.atmosenv.2017.02.027, 2017c.

641 Liu, J., Chen, Y., Chao, S., Cao, H., Zhang, A., Yang, Y.: Emission control priority of $PM_{2.5}$-bound heavy metals in
642 different seasons: A comprehensive analysis from health risk perspective, Sci. Total Environ., 644, 20-30.
643 https://doi.org/10.1016/j.scitotenv.2018.06.226, 2018a.

644 Liu, B., Cheng, Y., Zhou, M., Liang, D., Dai, Q., Wang, L., Jin, W., Zhang, L., Ren, Y., Zhou, J., Dai, C., Xu, J.,
645 Wang, J., Feng, Y., and Zhang, Y.: Effectiveness evaluation of temporary emission control action in 2016 in
646 winter in Shijiazhuang, China, Atmos. Chem. Phys., 18, 7019–7039, https://doi.org/10.5194/acp-18-7019-2018,
647 2018b.

648 Liu, J., Chu, B., Jia, Y., Cao, Q., Zhang, H., Chen, T., Ma, Q., Ma, J., Wang, Y., Zhang, P., and He, H.: Dramatic
649 decrease of secondary organic aerosol formation potential in Beijing: Important contribution from reduction of
650 coal combustion emission, Sci. Total Environ., 832, 155045, https://doi.org/10.1016/j.scitotenv.2022.155045,
651 2022.

652 Liu, Y., Zheng, M., Yu, M., Cai, X., Du, H., Li, J., Zhou, T., Yan, C., Wang, X., Shi, Z., Harrison, R. M., Zhang, Q.,
653 and He, K.: High-time-resolution source apportionment of $PM_{2.5}$ in Beijing with multiple models, Atmos. Chem.
654 Phys., 19, 6595–6609, https://doi.org/10.5194/acp-19-6595-2019, 2019.

655 Liu, Z., Wang, Y., Hu, B., Ji, D., Zhang, J., Wu, F., Wan, X., and Wang, Y.: Source appointment of fine particle number
656 and volume concentration during severe haze pollution in Beijing in January 2013, Environ. Sci. Pollut. Res.,
657 23, 6845–6860, https://doi.org/10.1007/s11356-015-5868-6, 2016.

658

659 Long, X., Li, N., Tie, X., Cao, J., Zhao, S., Huang, R., Zhao, M., Li, G., and Feng, T.: Urban dust in the Guanzhong
660 Basin of China, part I: A regional distribution of dust sources retrieved using satellite data, Sci. Total Environ.,
661 541, 1603–1613, https://doi.org/10.1016/j.scitotenv.2015.10.063, 2016.

662 Lu, J., Ge, P., Zhao, Y.: Recent development of effect mechanism of alloying elements in titanium alloy design, Rare
663 Metal Mat. Eng., 43, 775-779. https://doi.org/10.1016/S1875-5372(14)60082-5, 2014.

664 Lu, W., Tian, Q., Xu, R., Qiu, L., Fan, Z., Wang, S., Liu, T., Huang, J., Li, Y., Wang, Y., Shi, C., Liu, Y., and Zhou,
665 Y.: Ambient air pollution and hospitalization for chronic obstructive pulmonary disease: Benefits from Three-
666 Year Action Plan, Ecotoxicol. Environ. Saf., 228, 113034, https://doi.org/10.1016/j.ecoenv.2021.113034, 2021.

667 Lv, B., Zhang, B., and Bai, Y.: A systematic analysis of $PM_{2.5}$ in Beijing and its sources from 2000 to 2012, Atmos.
668 Environ., 124, 98–108, https://doi.org/10.1016/j.atmosenv.2015.09.031, 2016.

669 Lv, L., Chen, Y., Han, Y., Cui, M., Wei, P., Zheng, M., and Hu, J.: High-time-resolution $PM_{2.5}$ source apportionment
670 based on multi-model with organic tracers in Beijing during haze episodes, Sci. Total Environ., 772, 144766,
671 https://doi.org/10.1016/j.scitotenv.2020.144766, 2021.

672 Ma, Y., Huang, Y., Wu, J., E, J., Zhang, B., Han, D., and Ong, H. C.: A review of atmospheric fine particulate matters:
673 chemical composition, source identification and their variations in Beijing, Energ. Source. Part A, 44, 4783–
674 4807, https://doi.org/10.1080/15567036.2022.2075991, 2022.

Meng, H., Shen, Y., Fang, Y., and Zhu, Y.: Impact of the 'Coal-to-Natural Gas' Policy on Criteria Air Pollutants in Northern China, Atmosphere, 13, 945, https://doi.org/10.3390/atmos13060945, 2022.

Meng, J., Wang, G., Li, J., Cheng, C., Ren, Y., Huang, Y., Cheng, Y., Cao, J., and Zhang, T.: Seasonal characteristics of oxalic acid and related SOA in the free troposphere of Mt. Hua, central China: Implications for sources and formation mechanisms, Sci. Total Environ., 493, 1088–1097, https://doi.org/10.1016/j.scitotenv.2014.04.086, 2014.

Ng, N. L., Herndon, S. C., Trimborn, A., Canagaratna, M. R., Croteau, P. L., Onasch, T. B., Sueper, D., Worsnop, D. R., Zhang, Q., Sun, Y. L., and Jayne, J. T.: An Aerosol Chemical Speciation Monitor (ACSM) for Routine Monitoring of the Composition and Mass Concentrations of Ambient Aerosol, Aerosol Sci. Technol., 45, 780–794, https://doi.org/10.1080/02786826.2011.560211, 2011.

Ni, H., Tian, J., Wang, X., Wang, Q., Han, Y., Cao, J., Long, X., Chen, L.-W. A., Chow, J. C., Watson, J. G., Huang, R.-J., and Dusek, U.: $PM_{2.5}$ emissions and source profiles from open burning of crop residues, Atmos. Environ., 169, 229–237, https://doi.org/10.1016/j.atmosenv.2017.08.063, 2017.

Ouyang, J., Song, L.-J., Ma, L.-L., Luo, M., Dai, X.-X., Zhang, J.-T., and Xu, D.-D.: Quantification of secondary particle loading during a heavy air pollution event in Beijing: A simplified method based on coal emission indicators, Atmos. Environ., 215, 116896, https://doi.org/10.1016/j.atmosenv.2019.116896, 2019.

Pant, P. and Harrison, R.M.: Estimation of the contribution of road traffic emissions to particulate matter concentrations from field measurements: A review, Atmos. Environ., 77, 78-97. https://doi.org/10.1016/j.atmosenv.2013.04.028, 2013.

Pang, N., Gao, J., Zhu, G., Hui, L., Zhao, P., Xu, Z., Tang, W., and Chai, F.: Impact of clean air action on the $PM_{2.5}$ pollution in Beijing, China: Insights gained from two heating seasons measurements, Chemosphere, 263, 127991, https://doi.org/10.1016/j.chemosphere.2020.127991, 2021.

Pöschl, U.: Atmospheric Aerosols: Composition, Transformation, Climate and Health Effects, Angew. Chem. Int. Ed., 44, 7520–7540, https://doi.org/10.1002/anie.200501122, 2005.

Pui, D. Y. H., Chen, S.-C., and Zuo, Z.: $PM_{2.5}$ in China: Measurements, sources, visibility and health effects, and mitigation, Particuology, 13, 1–26, https://doi.org/10.1016/j.partic.2013.11.001, 2014.

Rai, P., Furger, M., Slowik, J. G., Canonaco, F., Fröhlich, R., Hüglin, C., Minguillón, M. C., Petterson, K., Baltensperger, U., and Prévôt, A. S. H.: Source apportionment of highly time-resolved elements during a firework episode from a rural freeway site in Switzerland, Atmos. Chem. Phys., 20, 1657–1674, https://doi.org/10.5194/acp-20-1657-2020, 2020.

Ren, Y.: Chemical components and source identification of $PM_{2.5}$ in non-heating season in Beijing: The influences of biomass burning and dust, Atmos. Res., 8, 2021.

Shen, G.: Changes from traditional solid fuels to clean household energies – Opportunities in emission reduction of primary $PM_{2.5}$ from residential cookstoves in China, Biomass Bioenerg., 86, 28–35, https://doi.org/10.1016/j.biombioe.2016.01.004, 2016.

Shen, W.-T., Yu, X., Zhong, S.-B., and Ge, H.-R.: Population Health Effects of Air Pollution: Fresh Evidence From China Health and Retirement Longitudinal Survey, Front. Public Health, 9, 779552, https://doi.org/10.3389/fpubh.2021.779552, 2021.

Shen, Z., Sun, J., Cao, J., Zhang, L., Zhang, Q., Lei, Y., Gao, J., Huang, R.-J., Liu, S., Huang, Y., Zhu, C., Xu, H., Zheng, C., Liu, P., and Xue, Z.: Chemical profiles of urban fugitive dust $PM_{2.5}$ samples in Northern Chinese cities, Sci. Total Environ., 569–570, 619–626, https://doi.org/10.1016/j.scitotenv.2016.06.156, 2016.

Simka, H., Shankar, S., Duran, C., and Haverty, M.: Fundamentals of Cu/Barrier-Layer Adhesion in Microelectronic Processing, MRS Proc., 863, B9.2, https://doi.org/10.1557/PROC-863-B9.2, 2005.

Tao, J., Zhang, L., Cao, J., and Zhang, R.: A review of current knowledge concerning $PM_{2.5}$ chemical composition, aerosol optical properties and their relationships across China, Atmos. Chem. Phys., 17, 9485–9518, https://doi.org/10.5194/acp-17-9485-2017, 2017.Tao, J., Zhang, L., Zhang, Z., Huang, R., Wu, Y., Zhang, R., Cao, J., and Zhang, Y.: Control of $PM_{2.5}$ in Guangzhou during the 16th Asian Games period: Implication for hazy weather prevention, Sci. Total Environ., 508, 57–66, https://doi.org/10.1016/j.scitotenv.2014.11.074, 2015.

Tao, Y., Ye, X., Ma, Z., Xie, Y., Wang, R., Chen, J., Yang, X., and Jiang, S.: Insights into different nitrate formation mechanisms from seasonal variations of secondary inorganic aerosols in Shanghai, Atmos. Environ., 145, 1–9, https://doi.org/10.1016/j.atmosenv.2016.09.012, 2016.

Thorpe, A. and Harrison, R. M.: Sources and properties of non-exhaust particulate matter from road traffic: A review, Sci. Total Environ., 400, 270–282, https://doi.org/10.1016/j.scitotenv.2008.06.007, 2008.

Tian, H. Z., Lu, L., Hao, J. M., Gao, J. J., Cheng, K., Liu, K. Y., Qiu, P. P., and Zhu, C. Y.: A Review of key hazardous trace elements in Chinese coals: Abundance, occurrence, behavior during coal combustion and their environmental impacts, Energ. Fuel., 27, 601–614, https://doi.org/10.1021/ef3017305, 2013.

Tian, J., Wang, Q., Zhang, Y., Yan, M., Liu, H., Zhang, N., Ran, W., and Cao, J.: Impacts of primary emissions and secondary aerosol formation on air pollution in an urban area of China during the COVID-19 lockdown, Environ. Int., 150, 106426, https://doi.org/10.1016/j.envint.2021.106426, 2021.

Tian, J., Wang, Q., Liu, H., Ma, Y., Liu, S., Zhang, Y., Ran, W., Han, Y., and Cao, J.: Measurement report: The importance of biomass burning in light extinction and direct radiative effect of urban aerosol during the COVID-19 lockdown in Xi'an, China, Atmos. Chem. Phys., 22, 8369–8384, https://doi.org/10.5194/acp-22-8369-2022, 2022.

Tian, Y. Z., Wang, J., Peng, X., Shi, G. L., and Feng, Y. C.: Estimation of the direct and indirect impacts of fireworks on the physicochemical characteristics of atmospheric PM_{10} and $PM_{2.5}$, Atmos. Chem. Phys., 14, 9469–9479, https://doi.org/10.5194/acp-14-9469-2014, 2014.

Vu, T. V., Shi, Z., Cheng, J., Zhang, Q., He, K., Wang, S., and Harrison, R. M.: Assessing the impact of clean air action on air quality trends in Beijing using a machine learning technique, Atmos. Chem. Phys., 19, 11303–11314, https://doi.org/10.5194/acp-19-11303-2019, 2019.

Wang, C., Li, X., Zhang, T., Tang, A., Cui, M., Liu, X., Ma, X., Zhang, Y., Liu, X., and Zheng, M.: Developing Nitrogen Isotopic Source Profiles of Atmospheric Ammonia for Source Apportionment of Ammonia in Urban

746   Beijing, Front. Environ. Sci., 10, 903013, https://doi.org/10.3389/fenvs.2022.903013, 2022a.

747 Wang, F., Yu, H., Wang, Z., Liang, W., Shi, G., Gao, J., Li, M., and Feng, Y.: Review of online source apportionment
748   research based on observation for ambient particulate matter, Sci. Total Environ., 762, 144095,
749   https://doi.org/10.1016/j.scitotenv.2020.144095, 2021a.

750 Wang, H. and Zhao, L.: A joint prevention and control mechanism for air pollution in the Beijing-Tianjin-Hebei
751   region in china based on long-term and massive data mining of pollutant concentration, Atmos. Environ., 174,
752   25–42, https://doi.org/10.1016/j.atmosenv.2017.11.027, 2018.

753 Wang, J., Zhao, B., Wang, S., Yang, F., Xing, J., Morawska, L., Ding, A., Kulmala, M., Kerminen, V.-M., Kujansuu,
754   J., Wang, Z., Ding, D., Zhang, X., Wang, H., Tian, M., Petäjä, T., Jiang, J., and Hao, J.: Particulate matter
755   pollution over China and the effects of control policies, Sci. Total Environ., 584–585, 426–447,
756   https://doi.org/10.1016/j.scitotenv.2017.01.027, 2017.

757 Wang, L., Wang, X., Gu, R., Wang, H., Yao, L., Wen, L., Zhu, F., Wang, W., Xue, L., Yang, L., Lu, K., Chen, J., Wang,
758   T., Zhang, Y., and Wang, W.: Observations of fine particulate nitrated phenols in four sites in northern China:
759   concentrations, source apportionment, and secondary formation, Atmos. Chem. Phys., 18, 4349–4359,
760   https://doi.org/10.5194/acp-18-4349-2018, 2018.

761 Wang, L. T., Wei, Z., Yang, J., Zhang, Y., Zhang, F. F., Su, J., Meng, C. C., and Zhang, Q.: The 2013 severe haze over
762   southern Hebei, China: model evaluation, source apportionment, and policy implications, Atmos. Chem. Phys.,
763   14, 3151–3173, https://doi.org/10.5194/acp-14-3151-2014, 2014.

764 Wang, M., Tian, P., Wang, L., Yu, Z., Du, T., Chen, Q., Guan, X., Guo, Y., Zhang, M., Tang, C., Chang, Y., Shi, J.,
765   Liang, J., Cao, X., and Zhang, L.: High contribution of vehicle emissions to fine particulate pollutions in
766   Lanzhou, Northwest China based on high-resolution online data source appointment, Sci. Total Environ., 798,
767   149310, https://doi.org/10.1016/j.scitotenv.2021.149310, 2021b.

768 Wang, P., Cao, J., Shen, Z., Han, Y., Lee, S., Huang, Y., Zhu, C., Wang, Q., Xu, H., and Huang, R.: Spatial and
769   seasonal variations of $PM_{2.5}$ mass and species during 2010 in Xi'an, China, Sci. Total Environ., 508, 477–487,
770   https://doi.org/10.1016/j.scitotenv.2014.11.007, 2015.

771 Wang, Q., Ye, J., Wang, Y., Zhang, T., Ran, W., Wu, Y., Tian, J., Li, L., Zhou, Y., Hang Ho, S. S., Dang, B., Zhang,
772   Q., Zhang, R., Chen, Y., Zhu, C., and Cao, J.: Wintertime Optical Properties of Primary and Secondary Brown
773   Carbon at a Regional Site in the North China Plain, Environ. Sci. Technol., 53, 12389–12397,
774   https://doi.org/10.1021/acs.est.9b03406, 2019.

775 Wang, Y., Wang, Q., Ye, J., Yan, M., Qin, Q., Prévôt, A. S. H., and Cao, J.: A Review of Aerosol Chemical
776   Composition and Sources in Representative Regions of China during Wintertime, Atmosphere, 10, 277,
777   https://doi.org/10.3390/atmos10050277, 2019.

778 Wang, Y., Zhang, Q. Q., He, K., Zhang, Q., and Chai, L.: Sulfate-nitrate-ammonium aerosols over China: response
779   to 2000–2015 emission changes of sulfur dioxide, nitrogen oxides, and ammonia, Atmos. Chem. Phys., 13,
780   2635–2652, https://doi.org/10.5194/acp-13-2635-2013, 2013.

781 Wang, Y., Yuan, Y., Wang, Q., Liu, C., Zhi, Q., and Cao, J.: Changes in air quality related to the control of coronavirus

in China: Implications for traffic and industrial emissions, Sci. Total Environ., 731, 139133, https://doi.org/10.1016/j.scitotenv.2020.139133, 2020a.

Wang, Y., Yu, M., Wang, Y., Tang, G., Song, T., Zhou, P., Liu, Z., Hu, B., Ji, D., Wang, L., Zhu, X., Yan, C., Ehn, M., Gao, W., Pan, Y., Xin, J., Sun, Y., Kerminen, V.-M., Kulmala, M., and Petäjä, T.: Rapid formation of intense haze episodes via aerosol–boundary layer feedback in Beijing, Atmos. Chem. Phys., 20, 45–53, https://doi.org/10.5194/acp-20-45-2020, 2020b.

Wang, Y., Liu, C., Wang, Q., Qin, Q., Ren, H., and Cao, J.: Impacts of natural and socioeconomic factors on $PM_{2.5}$ from 2014 to 2017, J. Environ. Manage., 284, 112071, https://doi.org/10.1016/j.jenvman.2021.112071, 2021c.

Wang, Z., Wang, R., Wang, J., Wang, Y., McPherson Donahue, N., Tang, R., Dong, Z., Li, X., Wang, L., Han, Y., and Cao, J.: The seasonal variation, characteristics and secondary generation of $PM_{2.5}$ in Xi'an, China, especially during pollution events, Environ. Res., 212, 113388, https://doi.org/10.1016/j.envres.2022.113388, 2022b.

Wei, F., Yang G., Jiang, D., Liu, Z., Sun, B.: Basic statistics and characteristics of background values of soil elements in China. Environ. Monit. in China (in Chinese) 7, 1–6. https://doi.org/10.19316/j.issn.1002-6002.1991.01.001, 1991.

Wood, E. C., Canagaratna, M. R., Herndon, S. C., Onasch, T. B., Kolb, C. E., Worsnop, D. R., Kroll, J. H., Knighton, W. B., Seila, R., Zavala, M., Molina, L. T., DeCarlo, P. F., Jimenez, J. L., Weinheimer, A. J., Knapp, D. J., Jobson, B. T., Stutz, J., Kuster, W. C., and Williams, E. J.: Investigation of the correlation between odd oxygen and secondary organic aerosol in Mexico City and Houston, Atmos. Chem. Phys., 10, 8947–8968, https://doi.org/10.5194/acp-10-8947-2010, 2010.

Xu, H. M., Cao, J. J., Ho, K. F., Ding, H., Han, Y. M., Wang, G. H., Chow, J. C., Watson, J. G., Khol, S. D., Qiang, J., and Li, W. T.: Lead concentrations in fine particulate matter after the phasing out of leaded gasoline in Xi'an, China, Atmos. Environ., 46, 217–224, https://doi.org/10.1016/j.atmosenv.2011.09.078, 2012.

Xu, J., Liu, D., Wu, X., Vu, T. V., Zhang, Y., Fu, P., Sun, Y., Xu, W., Zheng, B., Harrison, R. M., and Shi, Z.: Source apportionment of fine organic carbon at an urban site of Beijing using a chemical mass balance model, Atmos. Chem. Phys., 21, 2021.

Xu, P., Yang, Y., Zhang, J., Gao, W., Liu, Z., Hu, B., and Wang, Y.: Characterization and source identification of submicron aerosol during serious haze pollution periods in Beijing, J. of Environ. Sci., 112, 25–37, https://doi.org/10.1016/j.jes.2021.04.005, 2022.

Xu, W., Croteau, P., Williams, L., Canagaratna, M., Onasch, T., Cross, E., Zhang, X., Robinson, W., Worsnop, D., and Jayne, J.: Laboratory characterization of an aerosol chemical speciation monitor with $PM_{2.5}$ measurement capability, Aerosol Sci. Technol., 51, 69–83, https://doi.org/10.1080/02786826.2016.1241859, 2017.

Xue, J., Griffith, S. M., Yu, X., Lau, A. K. H., and Yu, J. Z.: Effect of nitrate and sulfate relative abundance in $PM_{2.5}$ on liquid water content explored through half-hourly observations of inorganic soluble aerosols at a polluted receptor site, Atmos. Environ., 99, 24–31, https://doi.org/10.1016/j.atmosenv.2014.09.049, 2014.

Yan, Y., Sun, Y. B., Weiss, D., Liang, L. J., and Chen, H. Y.: Polluted dust derived from long-range transport as a major end member of urban aerosols and its implication of non-point pollution in northern China, Sci. Total

818   Environ., 506–507, 538–545, https://doi.org/10.1016/j.scitotenv.2014.11.071, 2015.

819   Yang, D., Li, Z., Yue, Z., Liu, J. X., Zhai, Z., Li, Z., Gao, M., Hu, A. L., Zhu, W. J., Ding, N., Li, Z., Guo, S., Wang,
820   X., Wang, L., and Wei, J.: Variations in sources, composition, and exposure risks of $PM_{2.5}$ in both pre-heating
821   and heating seasons, Aerosol Air Qual. Res., 22, 14, https://doi.org/10.4209/aaqr.210333, 2022a.

822   Yang, S., Yuan, B., Peng, Y., Huang, S., Chen, W., Hu, W., Pei, C., Zhou, J., Parrish, D. D., Wang, W., He, X., Cheng,
823   C., Li, X.-B., Yang, X., Song, Y., Wang, H., Qi, J., Wang, B., Wang, C., Wang, C., Wang, Z., Li, T., Zheng, E.,
824   Wang, S., Wu, C., Cai, M., Ye, C., Song, W., Cheng, P., Chen, D., Wang, X., Zhang, Z., Wang, X., Zheng, J.,
825   and Shao, M.: The formation and mitigation of nitrate pollution: comparison between urban and suburban
826   environments, Atmos. Chem. Phys., 22, 4539–4556, https://doi.org/10.5194/acp-22-4539-2022, 2022b.

827   Yang, X. and Teng, F.: The air quality co-benefit of coal control strategy in China, Resour. Conserv. Recy., 129, 373–
828   382, https://doi.org/10.1016/j.resconrec.2016.08.011, 2018.

829   Yang, X., Zheng, M., Liu, Y., Yan, C., Liu, J., Liu, J., and Cheng, Y.: Exploring sources and health risks of metals in
830   Beijing $PM_{2.5}$: Insights from long-term online measurements, Sci. Total Environ., 814, 151954,
831   https://doi.org/10.1016/j.scitotenv.2021.151954, 2022c.

832   Zeng, J. and He, Q.: Does industrial air pollution drive health care expenditures? Spatial evidence from China, J.
833   Clean. Prod., 218, 400–408, https://doi.org/10.1016/j.jclepro.2019.01.288, 2019.

834   Zhang, Q., Zheng, Y., Tong, D., Shao, M., Wang, S., Zhang, Y., Xu, X., Wang, J., He, H., Liu, W., Ding, Y., Lei, Y.,
835   Li, J., Wang, Z., Zhang, X., Wang, Y., Cheng, J., Liu, Y., Shi, Q., Yan, L., Geng, G., Hong, C., Li, M., Liu, F.,
836   Zheng, B., Cao, J., Ding, A., Gao, J., Fu, Q., Huo, J., Liu, B., Liu, Z., Yang, F., He, K., and Hao, J.: Drivers of
837   improved $PM_{2.5}$ air quality in China from 2013 to 2017, Proc. Natl. Acad. Sci. U.S.A., 116, 24463–24469,
838   https://doi.org/10.1073/pnas.1907956116, 2019.

839   Zhang, Y., Vu, T. V., Sun, J., He, J., Shen, X., Lin, W., Zhang, X., Zhong, J., Gao, W., Wang, Y., Fu, T. M., Ma, Y., Li,
840   W., and Shi, Z.: Significant changes in chemistry of fine particles in wintertime Beijing from 2007 to 2017:
841   Impact of Clean Air Actions, Environ. Sci. Technol., 54, 1344–1352, https://doi.org/10.1021/acs.est.9b04678,
842   2020.

843   Zhang, Z., Gao, J., Zhang, L., Wang, H., Tao, J., Qiu, X., Chai, F., Li, Y., and Wang, S.: Observations of biomass
844   burning tracers in $PM_{2.5}$ at two megacities in North China during 2014 APEC summit, Atmos. Environ., 169,
845   54–64, https://doi.org/10.1016/j.atmosenv.2017.09.011, 2017.

846   Zhao, P., Feng, Y., Zhu, T., and Wu, J.: Characterizations of resuspended dust in six cities of North China, Atmos.
847   Environ., 40, 5807–5814, https://doi.org/10.1016/j.atmosenv.2006.05.026, 2006.

848   Zhao, S., Tian, H., Luo, L., Liu, H., Wu, B., Liu, S., Bai, X., Liu, W., Liu, X., Wu, Y., Lin, S., Guo, Z., Lv, Y., and
849   Xue, Y.: Temporal variation characteristics and source apportionment of metal elements in $PM_{2.5}$ in urban
850   Beijing during 2018–2019, Environ. Pollut., 268, 115856, https://doi.org/10.1016/j.envpol.2020.115856, 2021.

851   Zheng, G., Duan, F., Ma, Y., Zhang, Q., Huang, T., Kimoto, T., Cheng, Y., Su, H., and He, K.: Episode-Based
852   Evolution Pattern Analysis of Haze Pollution: Method Development and Results from Beijing, China, Environ.
853   Sci. Technol., 50, 4632–4641, https://doi.org/10.1021/acs.est.5b05593, 2016.

854   Zhang, R., Jing, J., Tao, J., Hsu, S.-C., Wang, G., Cao, J., Lee, C. S. L., Zhu, L., Chen, Z., Zhao, Y., and Shen, Z.:
855   Chemical characterization and source apportionment of $PM_{2.5}$ in Beijing: seasonal perspective, Atmos. Chem.
856   Phys., 13, 7053–7074, https://doi.org/10.5194/acp-13-7053-2013, 2013.

857   Zheng, M., Wang, Y., Yuan, L., Chen, N., and Kong, S.: Ambient observations indicating an increasing effectiveness
858   of ammonia control in wintertime $PM_{2.5}$ reduction in Central China, Sci. Total Environ., 824, 153708,
859   https://doi.org/10.1016/j.scitotenv.2022.153708, 2022.

860   Zhou, W., Lei, L., Du, A., Zhang, Z., Li, Y., Yang, Y., Tang, G., Chen, C., Xu, W., Sun, J., Li, Z., Fu, P., Wang, Z.,
861   and Sun, Y.: Unexpected increases of severe haze pollution during the post COVID‑19 Period: Effects of
862   emissions,   meteorology,   and   secondary   production,   J.   Geophy.   Res-Atmos.,   127,
863   https://doi.org/10.1029/2021JD035710, 2022.

864   Ziemann, P. J. and Atkinson, R.: Kinetics, products, and mechanisms of secondary organic aerosol formation, Chem.
865   Soc. Rev., 41, 6582, https://doi.org/10.1039/c2cs35122f, 2012.

866   _____

867

868

869

Table 1. Meteorological conditions, gas pollutants, chemical composition, and source contribution of $PM_{2.5}$ during pollution episodes in Xi'an, Shijiazhuang, and Beijing

Parameters	Xi'an		Shijiazhuang			Beijing		
	EP1	EP2	EP3	EP4	EP5	EP6	EP7	EP8
T (℃)	4.9 ± 2.6	1.5 ± 3.5	0.4 ± 3.4	-0.2 ± 3.3	-2.7 ± 3.3	0.3 ± 3.2	-1.6 ± 3.3	5.1 ± 3.6
RH (%)	52 ± 10	45 ± 10	61 ± 15	40 ± 13	75 ± 11	57 ± 19	45 ± 24	36 ± 10
WS (m s^{-1})	0.5 ± 0.2	0.7 ± 0.3	1.4 ± 0.6	1.9 ± 0.8	1.4 ± 0.7	1.0 ± 0.6	1.1 ± 0.6	1.0 ± 0.6
Dominant WD[a]	WSW, WNW	WSW	NNW	NNW	NNW	NNE	NNW, NNE	NNE, ENE
CO (mg m^{-3})	1.39 ± 0.40	1.15 ± 0.56	1.47 ± 0.62	0.60 ± 0.30	0.43 ± 0.33	1.04 ± 0.56	0.81 ± 0.32	1.00 ± 0.55
SO$_2$ (μg m^{-3})	15 ± 3	15 ± 5	9 ± 4	8 ± 4	3 ± 1	6 ± 5	4 ± 3	6 ± 4
NO$_2$ (μg m^{-3})	74 ± 22	63 ± 32	63 ± 14	47 ± 21	27 ± 11	54 ± 22	46 ± 17	42 ± 21
O$_x$ (ppm)	47 ± 8	42 ± 10	36 ± 7	32 ± 6	27 ± 3	36 ± 6	33 ± 4	43 ± 9
ALWC (μg m^{-3})	15 ± 11	8 ± 8	42 ± 37	12 ± 11	59 ± 448	28 ± 47	23 ± 8	11 ± 13
Dominant Chemical composition	OA (38%) NO$_3^-$ (24%)	OA (34%) NO$_3^-$ (24%)	NO$_3^-$ (27%) OA (26%)	OA (30%) NO$_3^-$ (23%)	NO$_3^-$ (32%) OA (26%)	OA (32%) NO$_3^-$ (26%)	OA (32%) NO$_3^-$ (26%)	OA (40%) NO$_3^-$ (23%)
Dominant source contribution[b]	BB (30%) SF (25%) CC (17%)	SF (34%) BB (24%) VE (16%)	SF (39%) BB (23%) CC (16%)	BB (40%) CC (16%) VE (16%)	SF (70%) BB (16%)	SF (62%) BB (13%)	SF (61%) BB (14%)	BB (38%) SF (27%) VE (15%)

[a] WSW : west-southwest; WNW : west-northwest; NNW : north-northwest; NNE : north-northeast; ENE : East-northeast

[b] BB: biomass burning; ~~SNpSSF~~: ~~secondary nitrate plus sulfate~~secondary formation source; CC: coal combustion; VE: vehicle emission

875

876 **Figure captions:**

877 **Figure 1.** Chemical composition and source apportionment results of $PM_{2.5}$ in three pilot cities of northern China
878 during the sampling period.

879 **Figure 2.** Mass fractions of chemical components (a-c) and sources contribution (d-f) with reconstructed $PM_{2.5}$
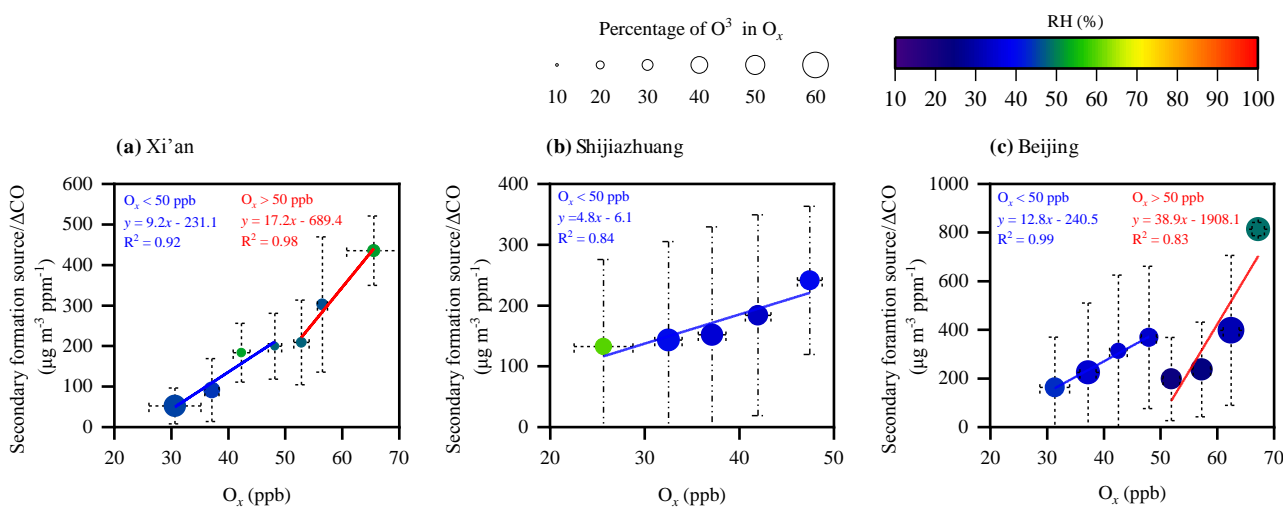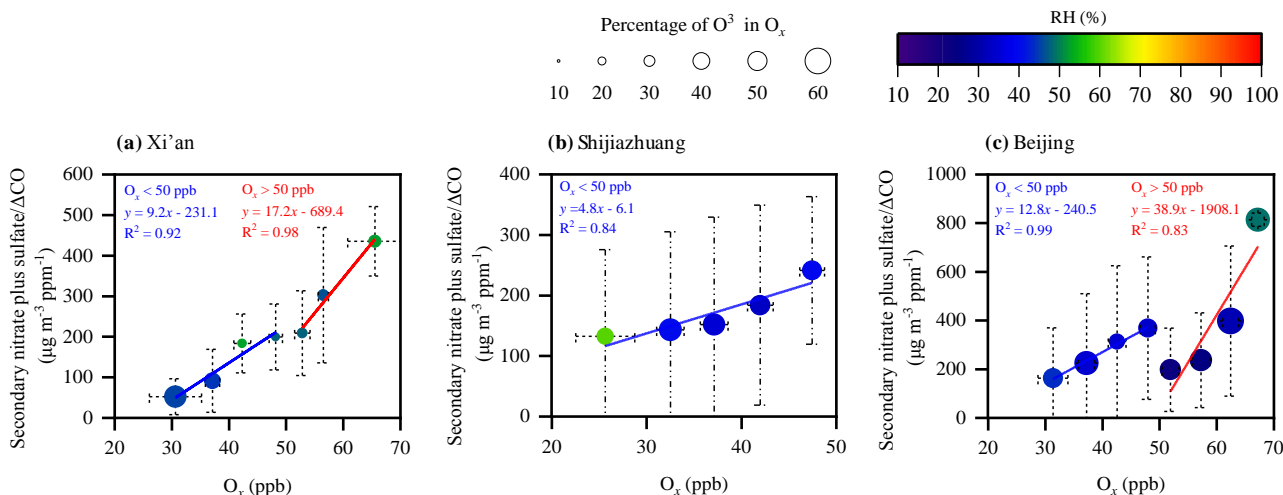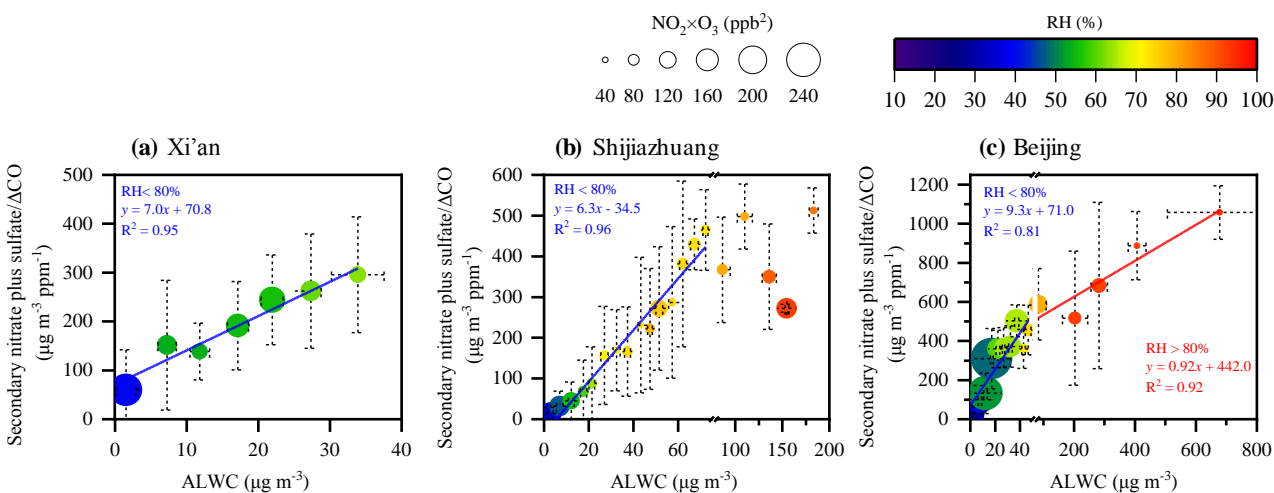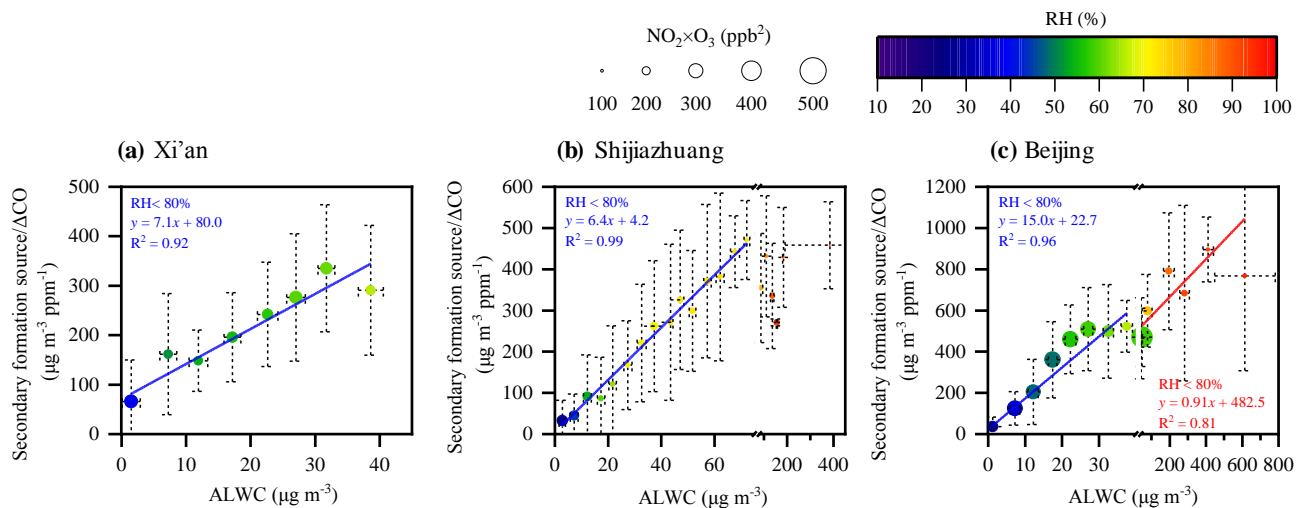880 concentration in Xi'an, Shijiazhuang, and Beijing.

881 **Figure 3.** Correlations of ~~secondary nitrate plus sulfate~~secondary formation source/ΔCO and O_x mixing ratio in (a)
882 Xi'an, (b) Shijiazhuang, and (c) Beijing. Each point and its error bar represent the mean and standard deviation in
883 each bin ($\Delta O_x = 5$ ppb).

884 **Figure 4.** Correlation of ~~secondary nitrate plus sulfate~~secondary formation source/ΔCO and ALWC during ~~winter~~
885 sampling periods in (a) Xi'an, (b) Shijiazhuang, and (c) Beijing, respectively. The points and error bar represent the
886 mean values and standard deviation values of ~~secondary nitrate plus sulfate~~secondary formation source/ΔCO and
887 ALWC~~O_x~~ in each bin. In Xi'an, each bin is 5 μg m^{-3} ($\Delta ALWC = 5$ μg m^{-3}). In Shijiazhuang, each bin is 5 μg m^{-3}
888 ($\Delta ALWC = 5$ μg m^{-3}) when ALWC ranged from 0 to 75μg m^{-3}, but 25 μg m^{-3} ($\Delta ALWC = 25$ μg m^{-3}) for ALWC
889 ranged from 75 to 200 μg m^{-3} due to limitations in data. In Beijing, each bin is 5 μg m^{-3} ($\Delta ALWC = 5$ μg m^{-3}) when
890 ALWC ranged from 0 to 50 μg m^{-3}, but 100 μg m^{-3} ($\Delta ALWC = 100$ μg m^{-3}) for ALWC ranged from 50 to 900 μg m^{-3}
891 $^{-3}$ due to limitations in data.

892 **Figure 5.** Summary of $PM_{2.5}$ and its composition (a, b, c) and source contribution (d, e, f) in Xi'an, Shijiazhuang,
893 and Beijing in winter in past decades. Where * represents the result of this study. The data and references used for
894 this figure are listed in Table S5 and S7.

895
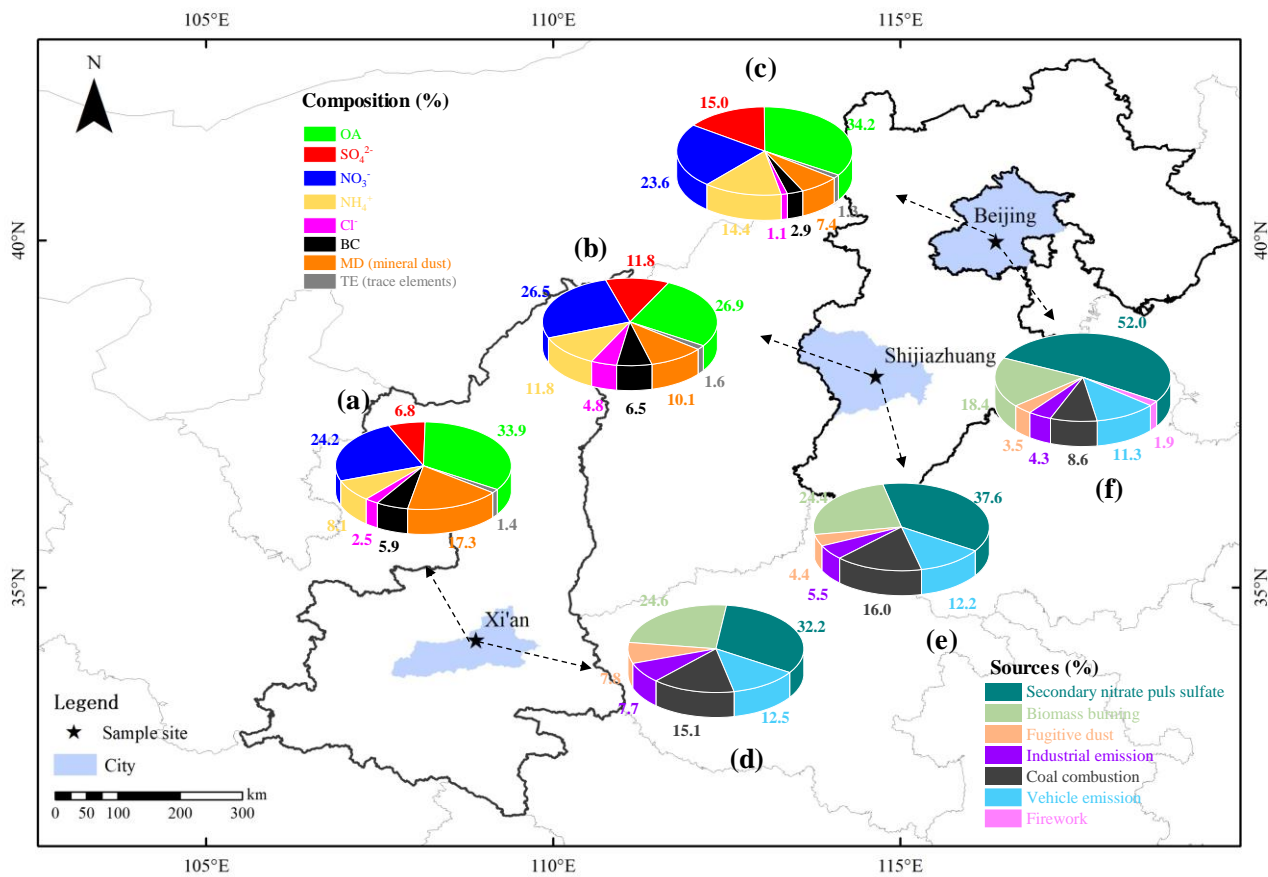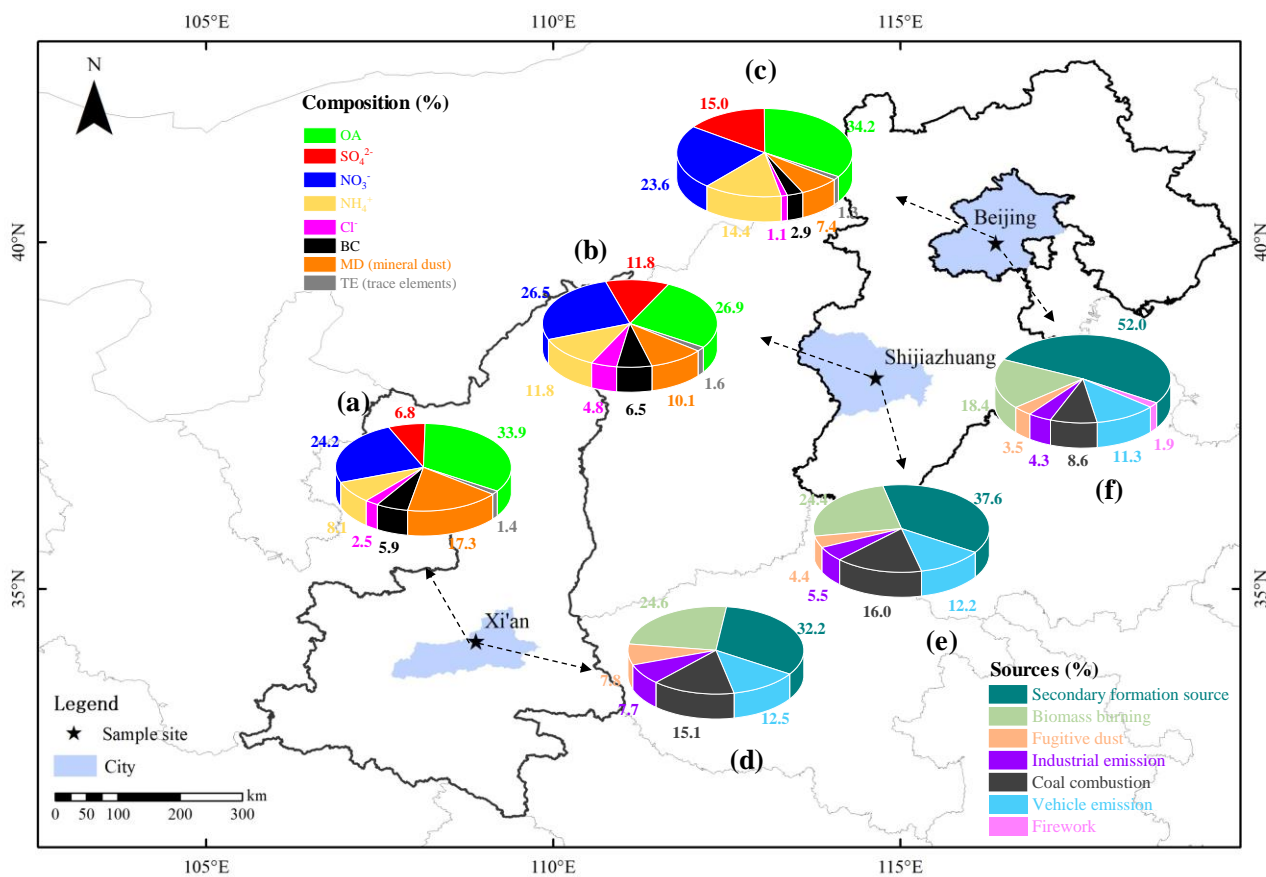
896

Figure 1. Chemical composition and source apportionment results of PM$_{2.5}$ in three pilot cities of northern China during the sampling period.
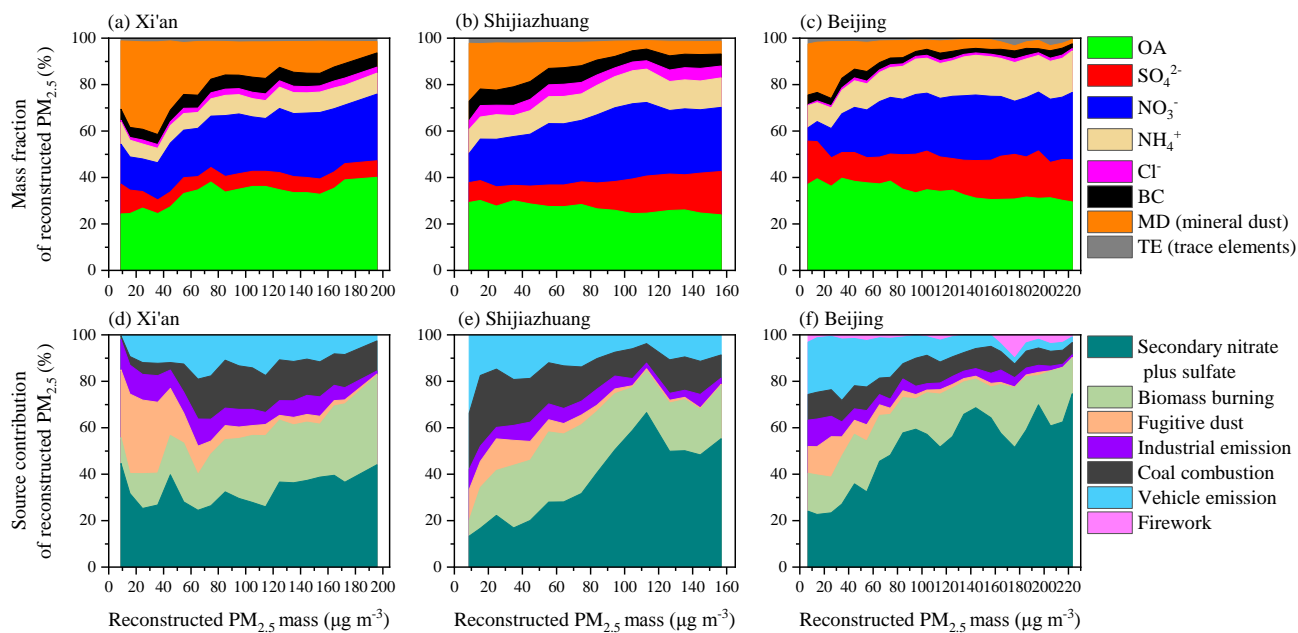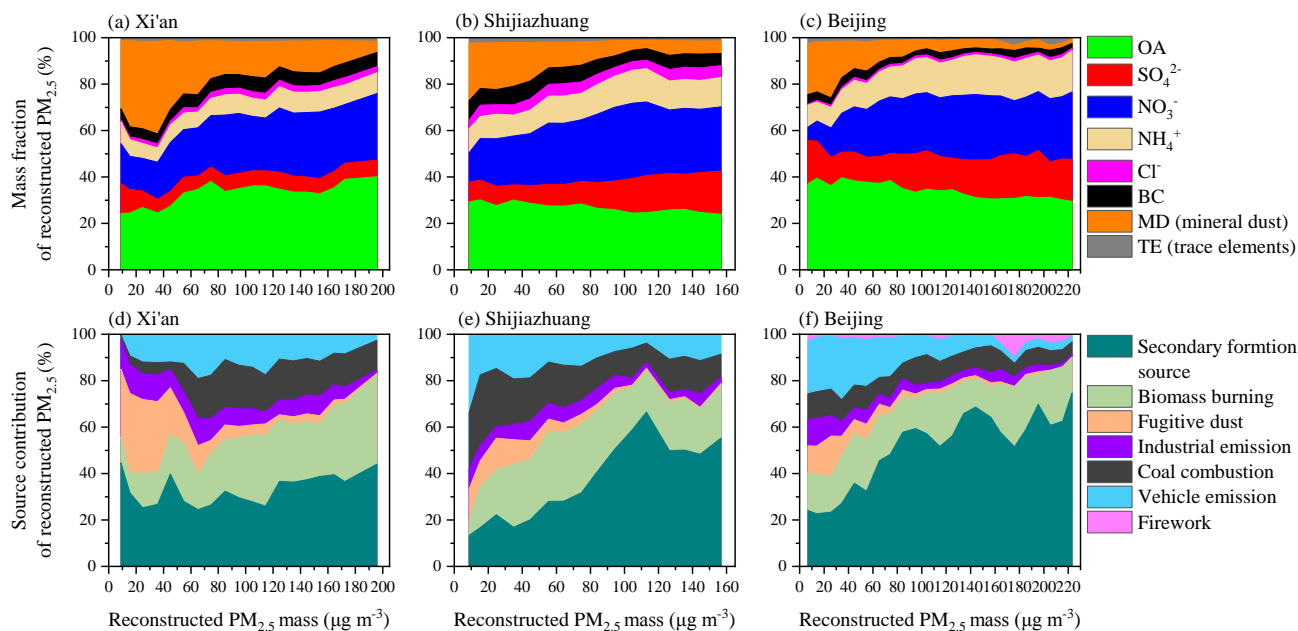
Figure 2. Mass fractions of chemical components (a-c) and sources contribution (d-f) with reconstructed PM$_{2.5}$ concentration in Xi'an, Shijiazhuang, and Beijing.

906

907

Figure 3. Correlations of ~~secondary nitrate plus sulfate~~secondary formation source/ΔCO and O_x mixing ratio in (a) Xi'an, (b) Shijiazhuang, and (c) Beijing. Each point and its error bar represent the mean and standard deviation in each bin ($\Delta O_x = 5$ ppb).

912

Figure 4. Correlation of ~~secondary nitrate plus sulfate~~secondary formation source/ΔCO and ALWC during ~~winter sampling periods~~ in (a) Xi'an, (b) Shijiazhuang, and (c) Beijing, respectively. The points and error bar represent the mean values and standard deviation values of ~~secondary nitrate plus sulfate~~secondary formation source/ΔCO and ALWC~~O*~~ in each bin. In Xi'an, each bin is 5 μg m^{-3} (ΔALWC = 5 μg m^{-3}). In Shijiazhuang, each bin is 5 μg m^{-3} (ΔALWC = 5 μg m^{-3}) when ALWC ranged from 0 to 75μg m^{-3}, but 25 μg m^{-3} (ΔALWC = 25 μg m^{-3}) for ALWC ranged from 75 to 200 μg m^{-3} due to limitations in data. In Beijing, each bin is 5 μg m^{-3} (ΔALWC = 5 μg m^{-3}) when ALWC ranged from 0 to 50 μg m^{-3}, but 100 μg m^{-3} (ΔALWC = 100 μg m^{-3}) for ALWC ranged from 50 to 900 μg m^{-3} due to limitations in data.

36

Figure 5. Summary of PM$_{2.5}$ and its composition (a, b, c) and source contribution (d, e, f) in Xi'an, Shijiazhuang, and Beijing in winter in past decades. Where * represents the result of this study, and the empty white area means no data. The data and references used for this figure are listed in Table S6 S7 and S7S8.

1   *Supplement of*

2   **High-time-resolution chemical composition and source apportionment of PM$_{2.5}$ in northern Chinese cities:**

3   **implications for policy**

4   Yong Zhang[1,2,3], Jie Tian[1,2,4], Qiyuan Wang[1,2,3,4*], Lu Qi[5], Manousos Ioannis Manousakas[5], Yuemei Han[1,4], Weikang

5   Ran[1,2], Yele Sun[6], Huikun Liu[1,2,4], Renjian Zhang[6], Yunfei Wu[6], Tianqu Cui[5], Kaspar Rudolf Daellenbach[5], Jay Gates

6   Slowik[5], André S. H. Prévôt[5], Junji Cao[6*]

7   [1] State Key Laboratory of Loess and Quaternary Geology, Institute of Earth Environment, Chinese Academy

8   of Sciences, Xi'an 710061, China

9   [2] National Observation and Research Station of Regional Ecological Environment Change and

10   Comprehensive Management in the Guanzhong Plain, Shaanxi, Xi'an 710061, China

11   [3] University of Chinese Academy of Sciences, Beijing 100049, China

12   [4] Center for Excellence in Quaternary Science and Global Change, Xi'an 710061, China

13   [5] Laboratory of Atmospheric Chemistry, Paul Scherrer Institute (PSI), Villigen 5232, Switzerland

14   [6] Institute of Atmospheric Physics, Chinese Academy of Sciences, Beijing 100029, China

15   *Correspondence:* wangqy@ieecas.cn (Qiyuan Wang), jjcao@mail.iap.ac.cn (Junji Cao).

Text S1. Selcation of inputted HERM chemical species and its uncertainty calculation

Considering the validity and credibility of monitoring data, chemical species including OA, NO_3^-, SO_4^{2-}, NH_4^+, Cl^-, and BC were all selected to input HERM model for three pilot cities. For inorganic elements, Si, K, Ca, Cr, Mn, Fe, Ni, Cu, Zn, As, Se, Ba, and Pb in Xi'an and Beijing, and Si, K, Ca, Ti, Cr, Mn, Fe, Ni, Cu, Zn, As, Se, Ba, and Pb in Shijiazhuang were selected for source apportionment, respectively.

The uncertainty data of chemical species inputting HERM was calculated according to the recommendation in the PMF5.0 user guideline. If the measured chemical species concentration is greater than the minimum detection limit (MDL) provided, the uncertainty (Unc) calculation is based following equation:

$$Unc_i = \sqrt{(C_i \times E_i)^2 + (0.5 \times MDL_i)^2} \qquad (1)$$

where C_i represents measured concertation for species i, E_i represents error fraction of species i. For online measured data, the error fraction was recommended to use 10% (Rai et al., 2020). If the measured concentration is less than or equal to the MDL provided, the Unc is calculated as the following equation:

$$Unc = \frac{5}{6} \times MDL \qquad (2)$$

Text S2 Diagnostics of HERM solutions

In this study, factors numbering from two to ten were selected and run in the HERM software. Each factor solution was run thirty times with completely unconstrained profiles to explore the possible sources. The optimal factor number solution was determined by examining the ratio of Q and expected Q (Q_{exp}). The Q_{exp} in HERM was equal to (samples ×species – factors × (samples + species) + the number of constrained source profiles). As shown in Fig. S5, the value of Q/Q_{exp} decreased with the increase of the factor number, which suggests increasing the factor number could lead to a better explanation of the variance by HERM. However, the utility of increasing factors declined with the number of factors. Too many factors could cause splitting profiles, although the Q/Q_{exp} may be desirable (Liu et al., 2021; Salameh et al., 2018, 2016). Thus, the drops of Q/Q_{exp} ($\Delta Q/Q_{exp}$) were subsequently evaluated to choose the optimal solution factor number. As shown in Table S2, when the number of factors increases to more than six in Xi'an, the value of $\Delta Q/Q_{exp}$ shows a relatively stable change trend. A six-factor solution is preferable because $\Delta Q/Q_{exp}$ between the five-solution and six-solution is smaller than that between the six-solution and seven-solution (Liu et al., 2021). In addition, secondary ~~nitrate plus sulfate~~formation source and biomass burning were mixed when the factor number was five, and vehicle emission was split into two profiles when the factor number

44   was seven (Table S3). Therefore, the six-factor solution was determined as the optimal HERM solution for Xi'an.

45   Similar criterias were used for Shijiazhuang and Beijing, six-factor and eight-factor solutions were determined as

46   optimal HERM solutions, respectively.

47

48   **Text S3 Estimation of secondary organic aerosol (SOA).**

49   Due to lack of critical tracers of SOA, the sources of SOA cannot be individually resolved by receptor model.

50   In this study, In this study, the secondary sources were mainly characterized by high EV values for inorganic

51   aerosols such as SO_4^{2-}, NO_3^-, NH_4^+, but the medium EV values for OA (16~29%) were also presented on

52   secondary sources in three pilot cities. This means that the SOA maybe mixed in with the factors of secondary

53   sources. To verify this, the SOA concentrations we estimated by using a BC-tracer method (Wang et al., 2019)

54   and then compared the results with those based on source apportionment. The SOA calculation by BC-tracer

55   method was calculated as follow:

56       $[SOA]_{\text{BC-tracer}} = [OA] - (OA/BC)_{pri} \times [BC]$ (S-1)

57   where [ ] means mass concentration, $(OA/BC)_{pri}$ is the ratio of [OA] to [BC] in primary emission. The

58   $(OA/BC)_{pri}$ ratios vary among sources, therefore, a minimum R squired (MRS) method was used to derive

59   appropriate $(OA/BC)_{pri}$ values for three pilot cities. In previous studies (Srivastava et al., 2018; Wang et al.,

60   2019), MRS method has been used to calculated the concertation of secondary organic carbon and brown carbon.

61   More detailed information on the method and a validation of this approach can be found in Wang et al. (2019).

62   In addition, according to results of receptor model, SOA concentration can also be estimated as follow

63   based on EV values of OA from secondary source factors.

64       $[SOA]_{\text{source apportionment}} = [OA] \times EV\_{OA}$ (S-2)

65   where EV_OA represents the EV values of OA in secondary sources factors resolved by HERM model.

66   As shown in Fig. S9, the $(OA/BC)_{pri}$ ratios were determined as 4.73 for Xi'an, 3.12 for Shijiazhuang and

67   7.6 for Beijing, respectively. Furthermore, the concentrations of SOA from three pilot cities were shown in

68   Table R1 based two different methods. As we can see, the SOA concentrations estimated by EV values of OA

69   are close to that by BC-tracer method for three pilot cities. This indicated SOA was mixed in secondary sources

70   factors.

71
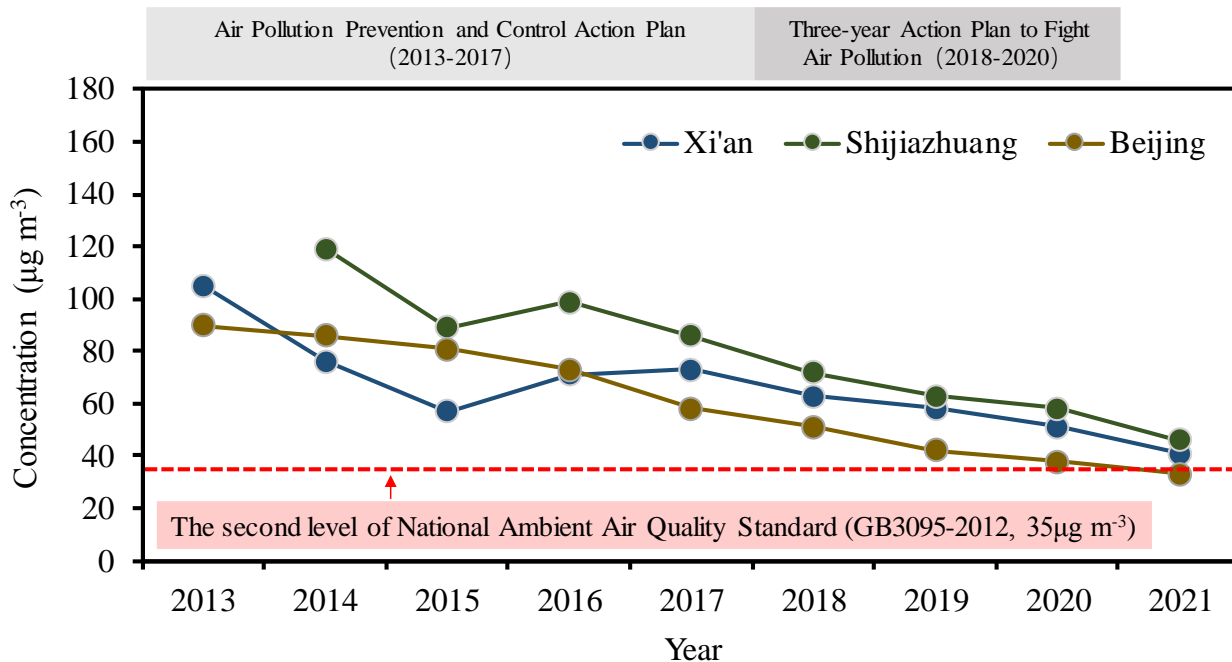
Figure S1. Annual average concentration of PM$_{2.5}$ from 2013 to 2021 in Xi'an, Shijiazhuang, and Beijing. (The data are from the website of the local Ecological Environment Bureau, Xi'an: http://xaepb.xa.gov.cn/, Shijiazhuang: https://sthjj.sjz.gov.cn/, Beijing: http://sthjj.beijing.gov.cn/). The red dotted line represents the second level of the National Ambient Air Quality Standard (GB3095-2012, 35 µg m^{-3})
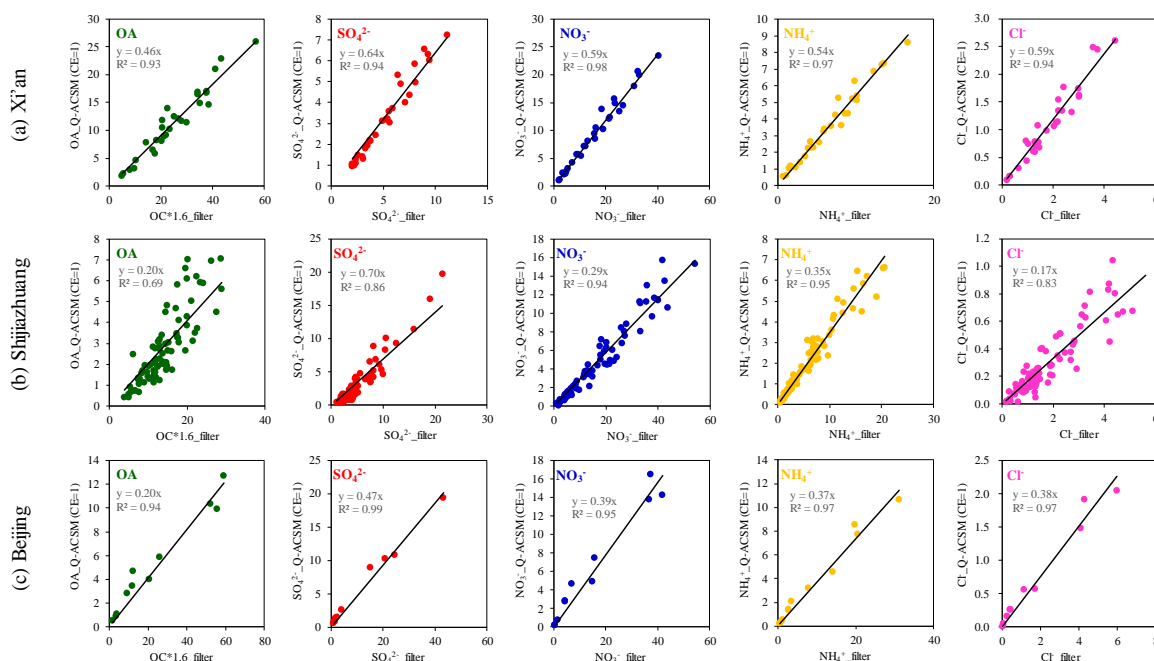

Figure S2. Correction of chemical components measured by Q-ACSM in different cities. During the campaigns, offline filter samples were simultaneously sampled for the correction. In summary, 29 offline samples in Xi'an, 83 offline samples in Shijiazhuang, and 10 offline samples in Beijing were sampled respectively.

82
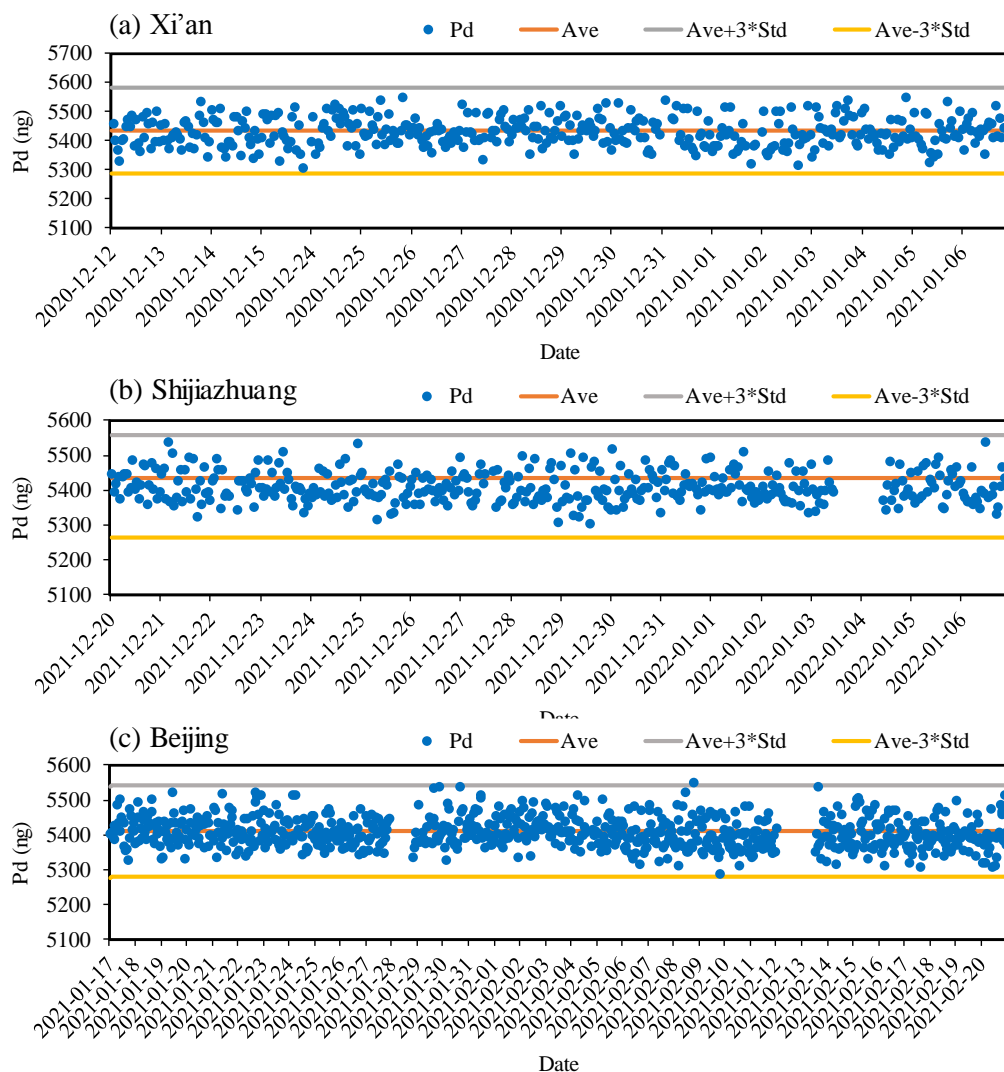
Figure S3. Concentration of the internal standard element (Pd) of Xact625 during sampling periods in (a) Xi'an,
(b) Shijiazhuang, and (c) Beijing.

85
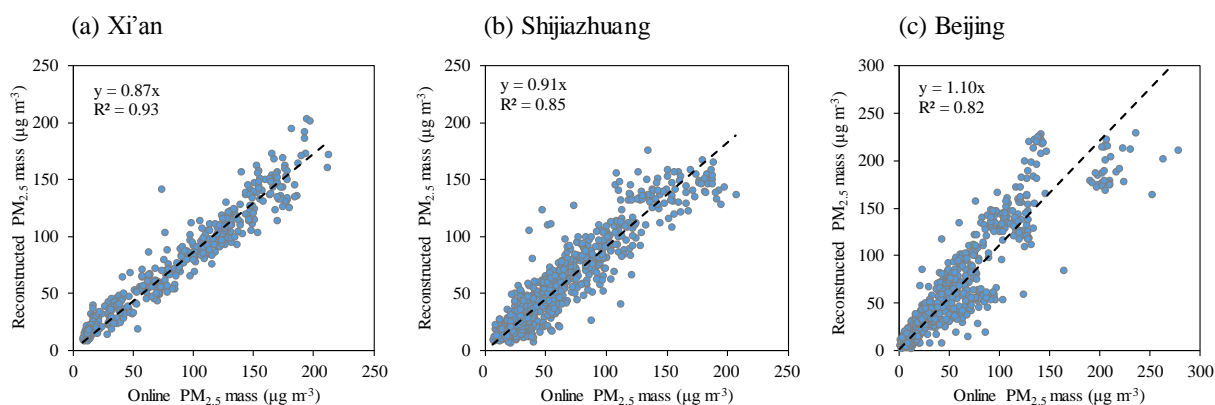
Figure S4. Correlation of online and reconstructed $PM_{2.5}$ concentration in (a) Xi'an, (b) Shijiazhuang, and (c) Beijing
during the campaigns. The online $PM_{2.5}$ mass data in the X axis from national monitor stations near sampling sites.

88
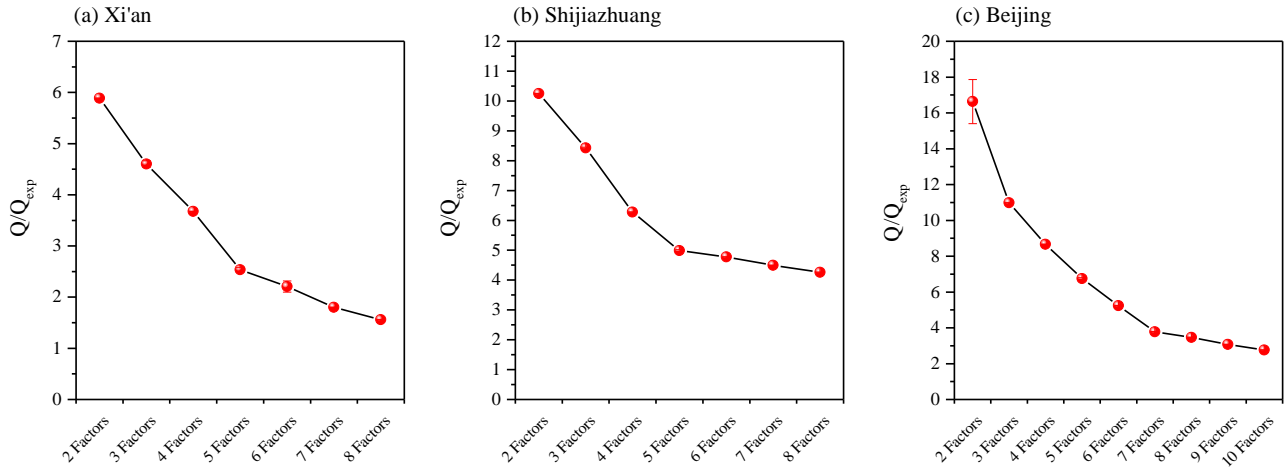
Figure S5. Values of Q/Q_{exp} for the unconstrained profile solutions with two to ten factors based on thirty runs in (a) Xi'an, (b) Shijiazhuang, and (c) Beijing, respectively.
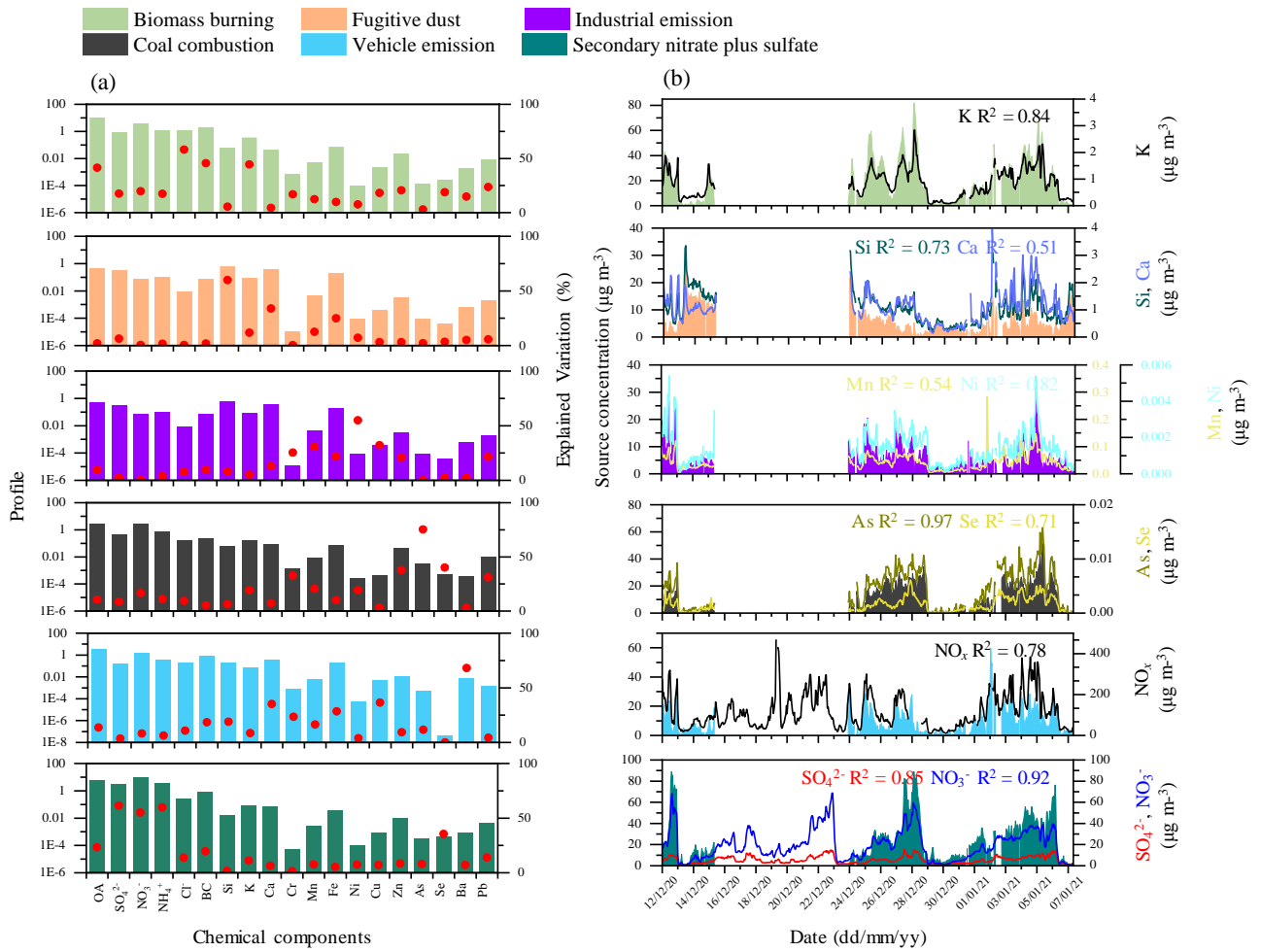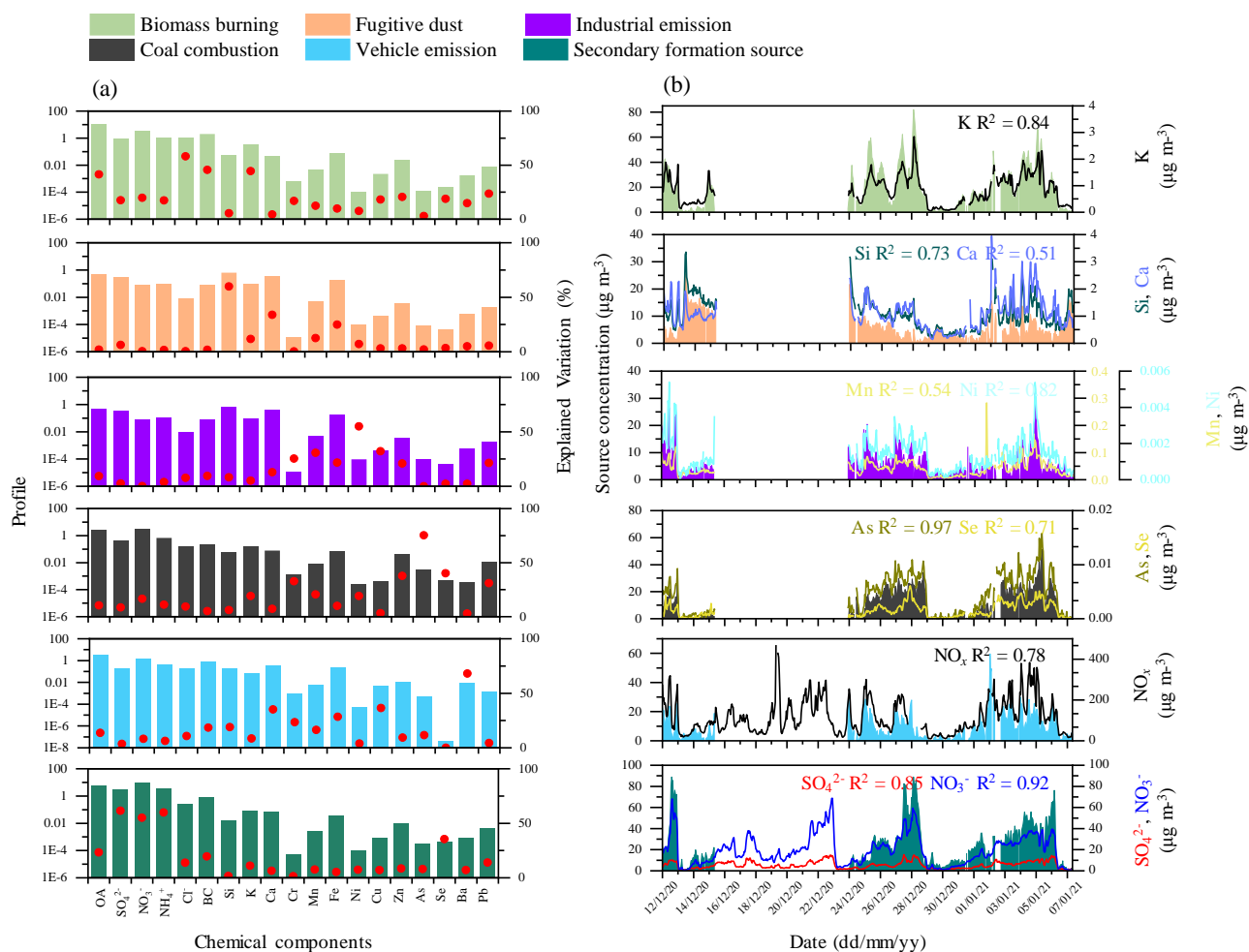
Figure S6. (a) Sources profiles obtained from HERM with a six-factor solution in Xi'an, the columns in each factor are the profile that displays the relative relation of the absolute values of variables. The red dot represents the explained variation (EV) in species for different factors. (b) Time series plots of sources concentration, including biomass burning, fugitive dust, industrial emission, coal combustion, vehicle emission, and secondary ~~nitrate plus sulfate~~formation source. The corresponding time trends of chemical tracers are also shown.

8
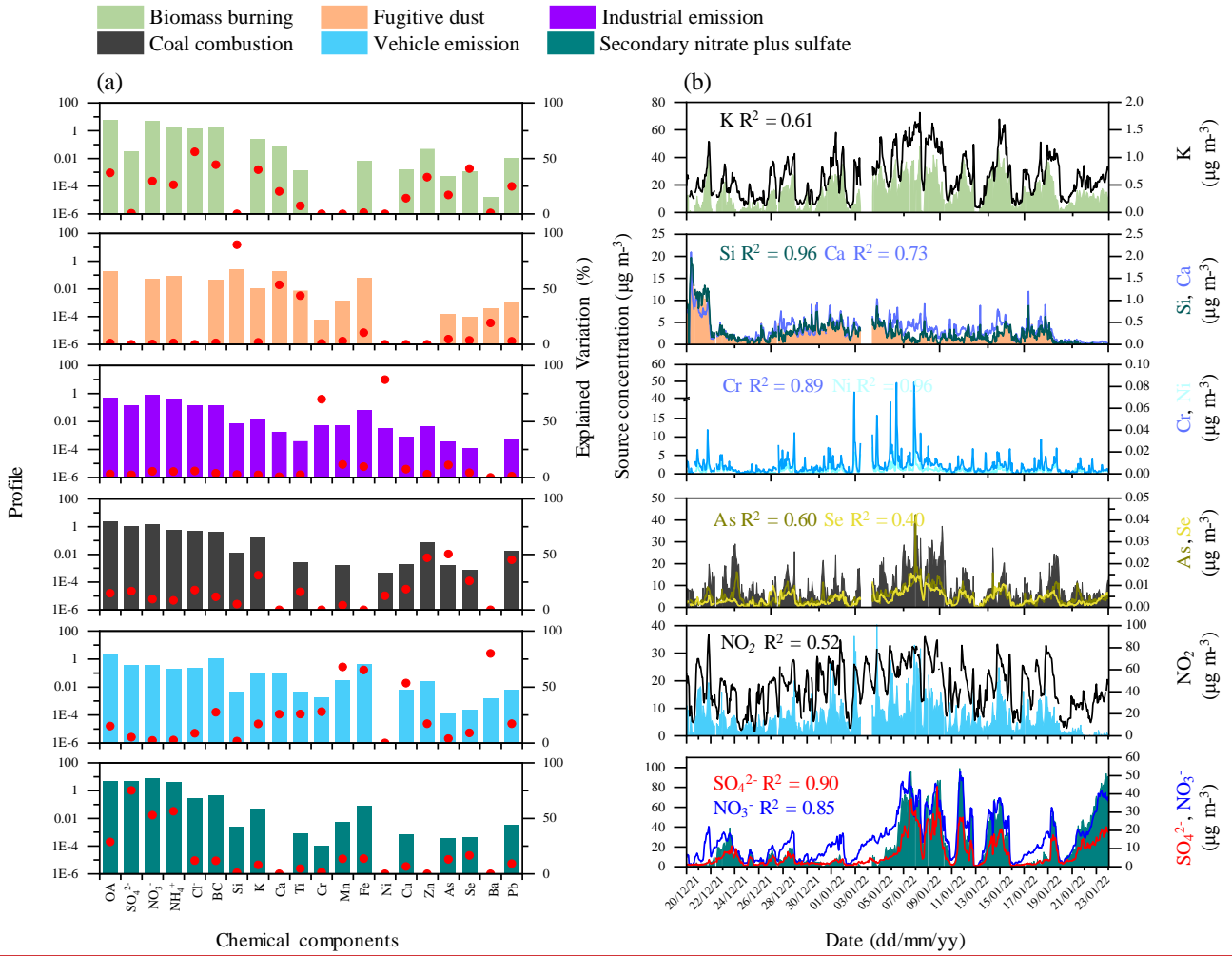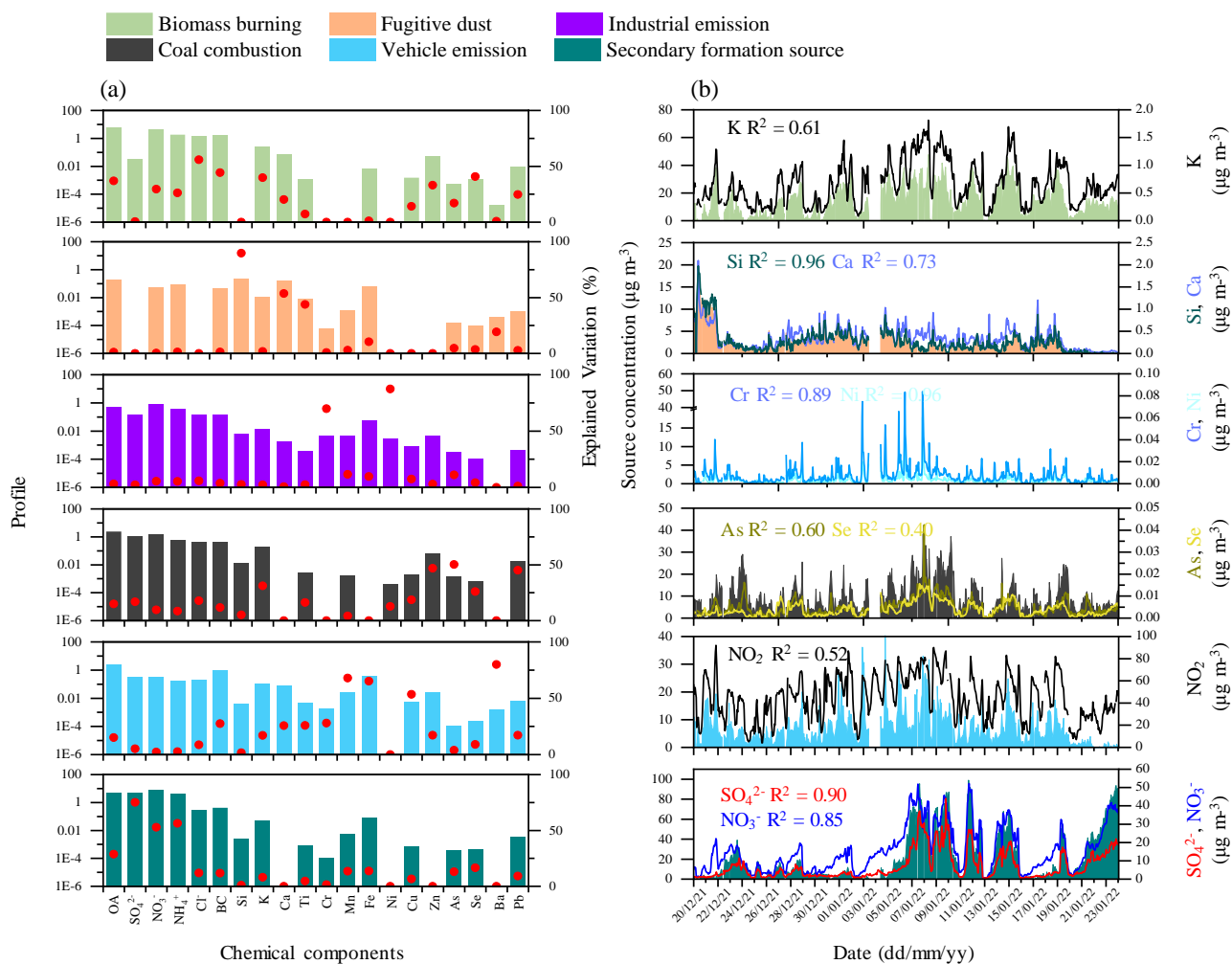
Figure S7. (a) Sources profiles obtained from HERM with a six-factor solution in Shijiazhuang, the columns in each factor are the profile that displays the relative relation of the absolute values of variables. The red dot represents the explained variation (EV) in species for different factors. (b) Time series plots of sources concentration, including biomass burning, fugitive dust, industrial emission, coal combustion, vehicle emission, and secondary ~~nitrate plus sulfate~~formation source. The corresponding time trends of chemical tracers are also shown.
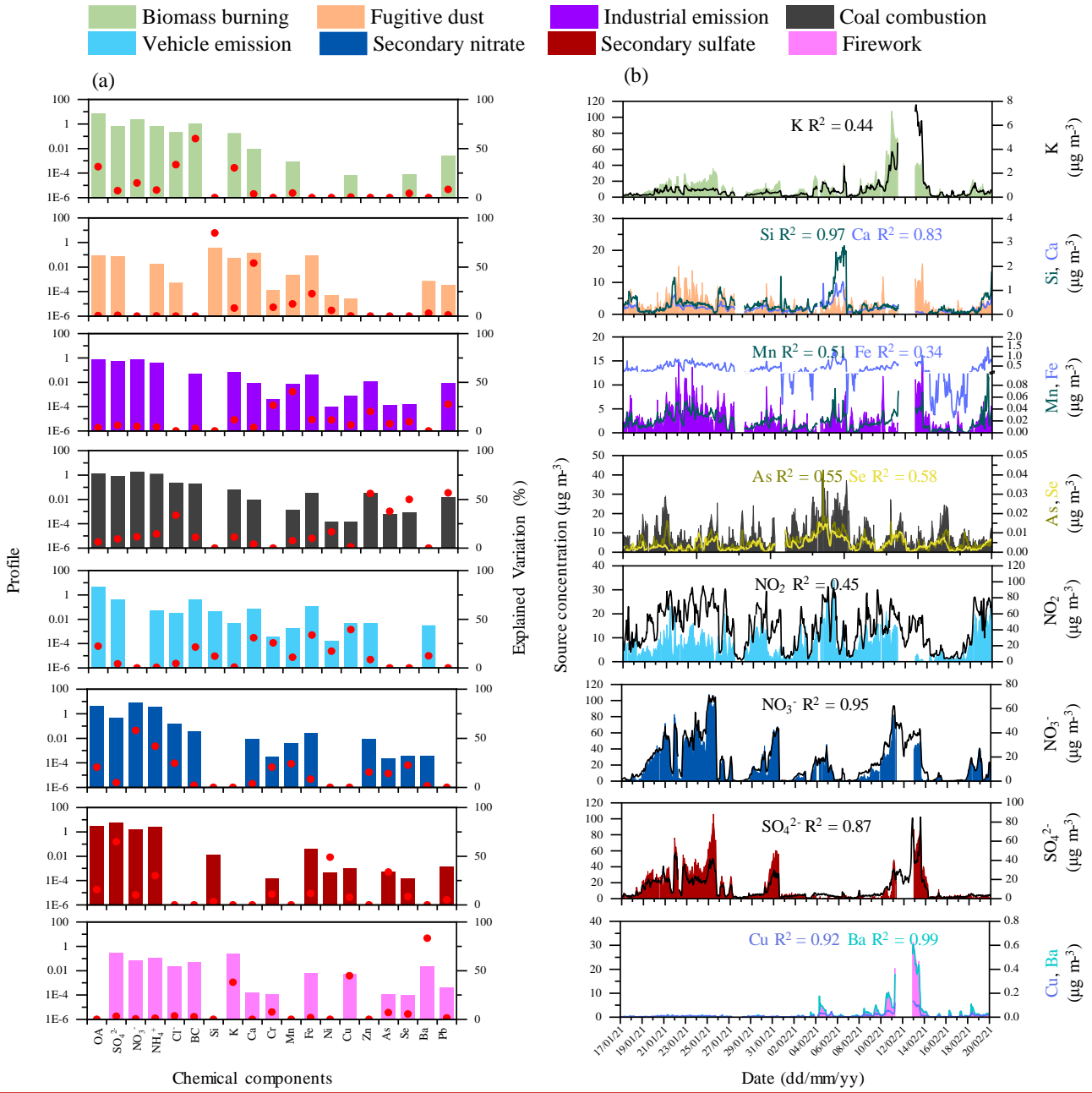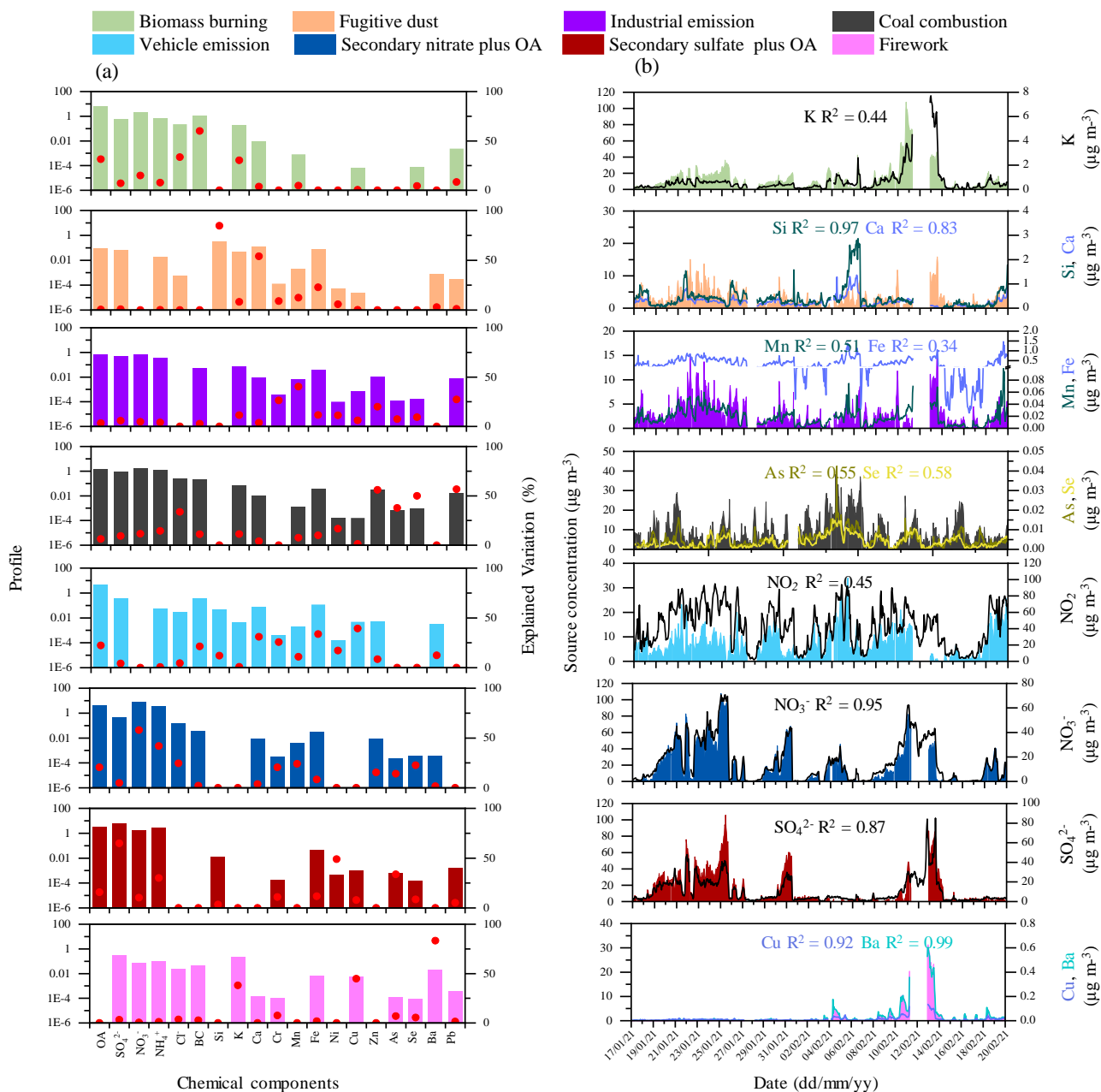
Figure S8. (a) Sources profiles obtained from HERM with an eight-factor solution in Beijing, the columns in each factor are the profile that displays the relative relation of the absolute values of variables. The red dot represents the explained variation (EV) in species for different factors. (b) Time series plots of sources concentration, including biomass burning, fugitive dust, industrial emission, coal combustion, vehicle emission, secondary nitrate plus OA, secondary sulfate plus OA, and firework. The corresponding time trends of chemical tracers are also shown.
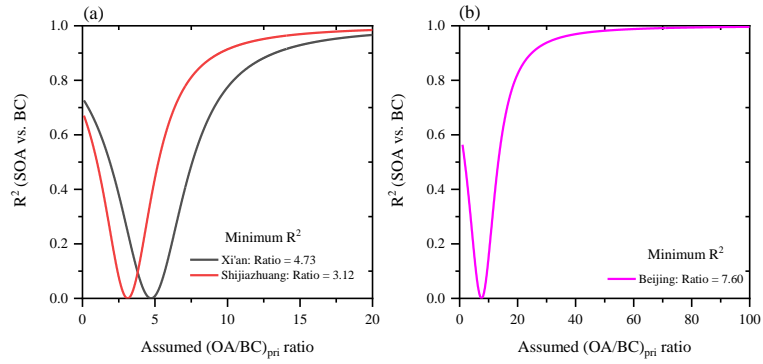
Figure S9. Coefficients of determination (R^2) for SOA versus BC mass concentration plotted against assumed ratios for OA to BC in primary emissions (($OA/BC)_{pri}$) in Xi'an, Shijiazhuang and Beijing.
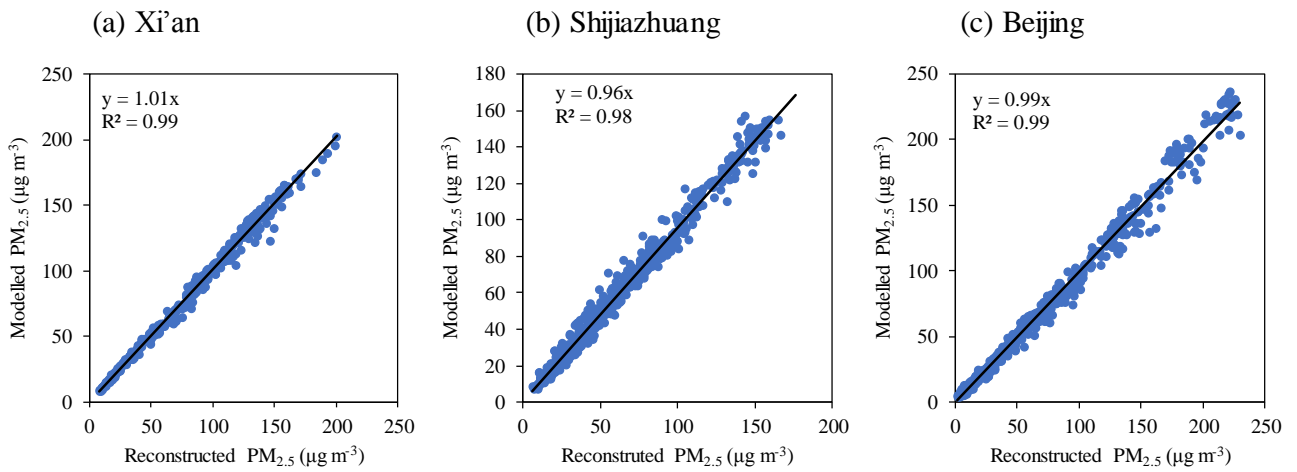
Figure S9S10. Correlation between reconstructed $PM_{2.5}$ and modeled $PM_{2.5}$ mass concentrations derived by HERM in Xi'an, Shijiahuznag, and Beijing with optimal solutions
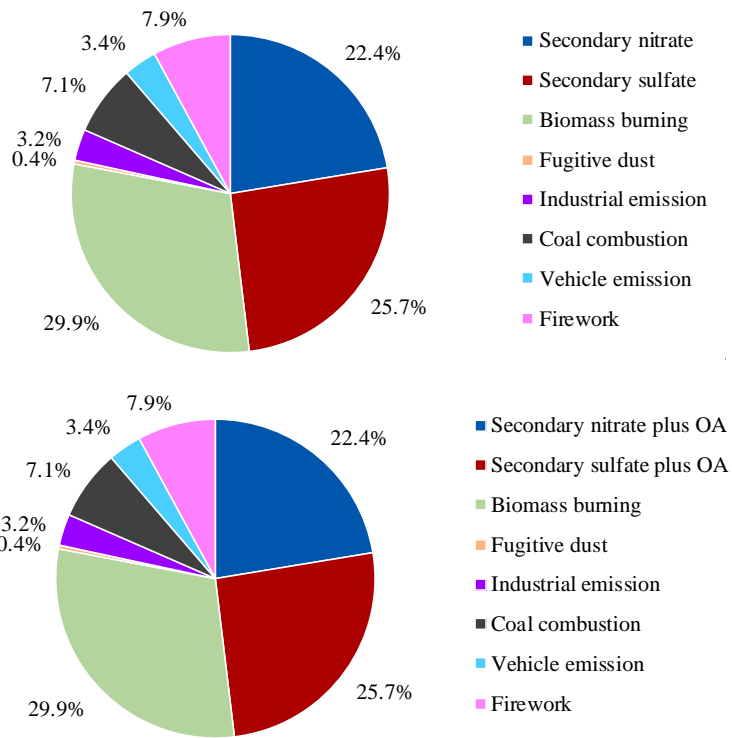
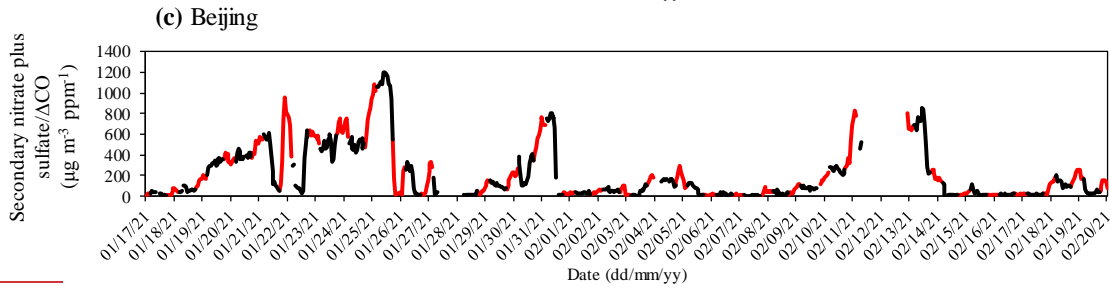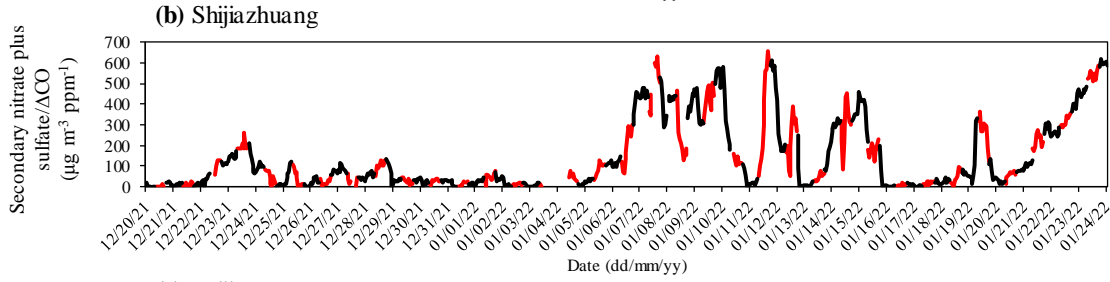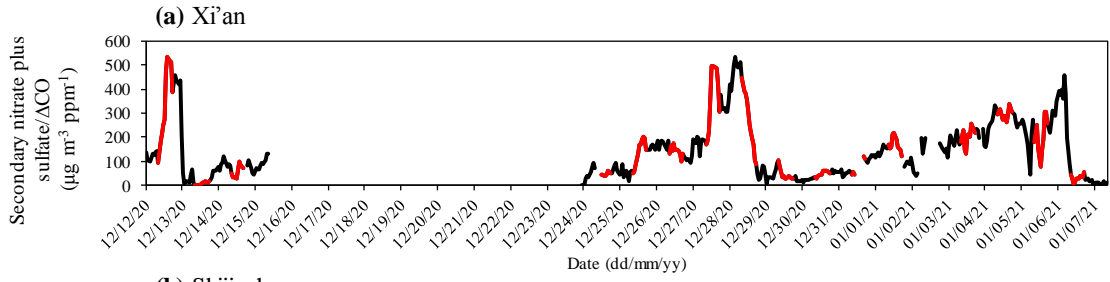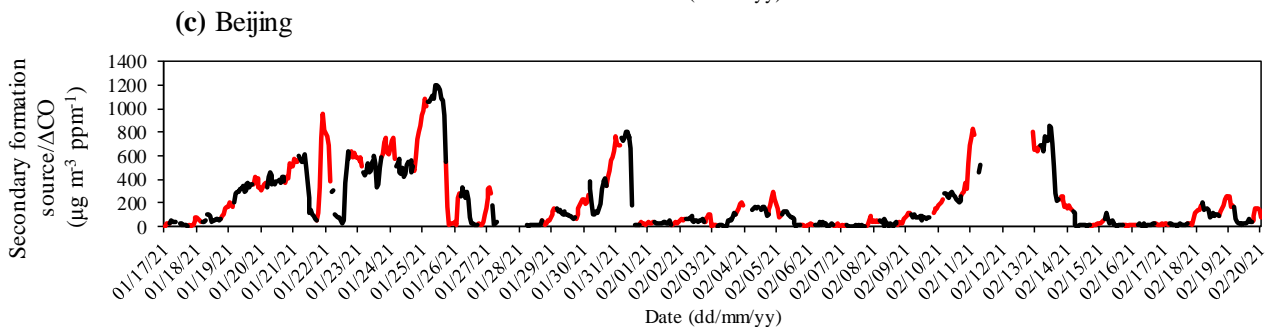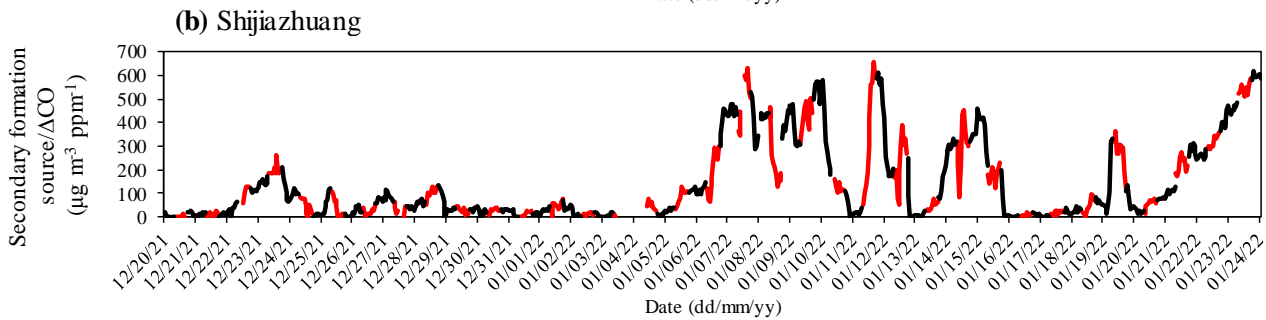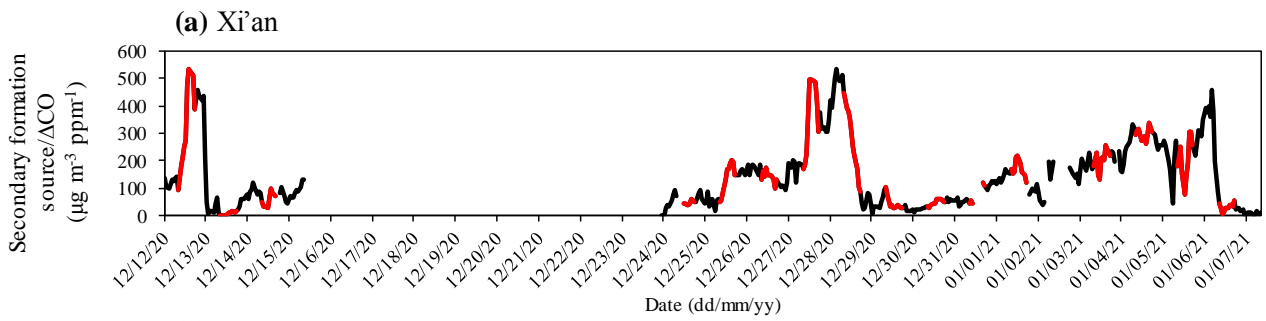**Figure** ~~S10~~<u>S11</u>. Source contribution of $PM_{2.5}$ during Chinese Spring Festival (from New Year's Eve to January 3rd of the Lunar Calendar) in Beijing
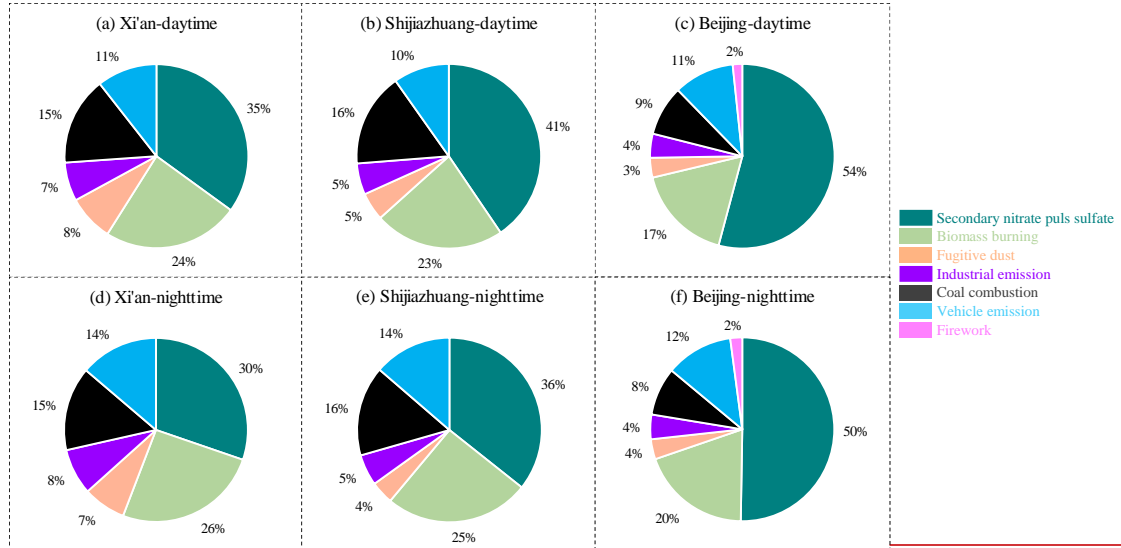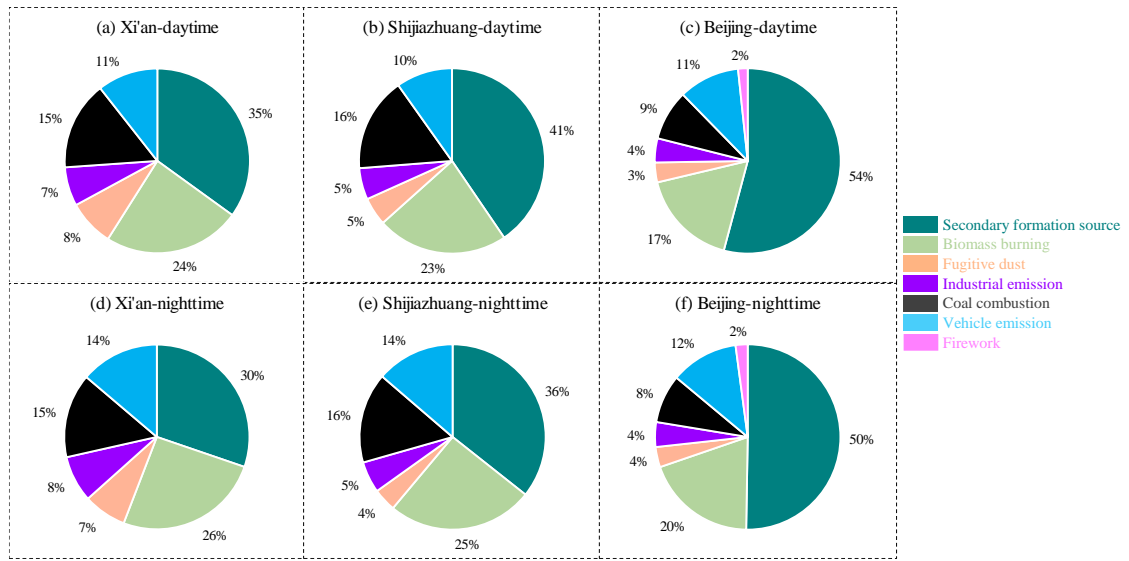
(a) Xi'an

(b) Shijiazhuang

(c) Beijing

125

(a) Xi'an

(b) Shijiazhuang

(c) Beijing

126

15

127   **Figure** ~~S11~~S12. Time series plots of secondary ~~nitrate plus sulfate~~formation source/ΔCO in (a) Xi'an, (b)
128   Shijiazhuang, and (c) Beijing. The red and black lines represent daytime (08:00-17:00 LST) and nighttime
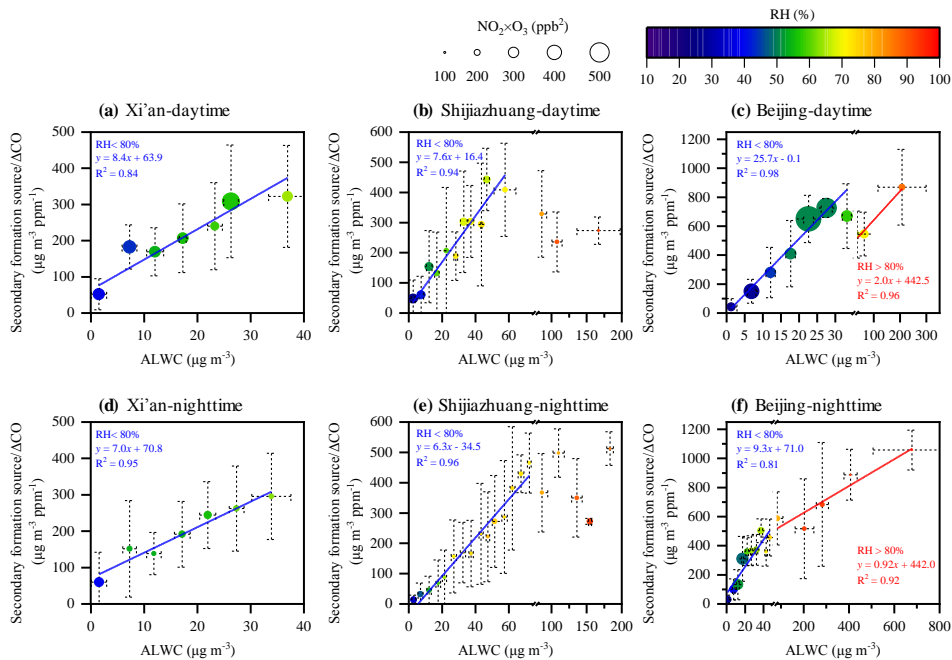129   (18:00 - 07:00 the next day LST), respectively.

130

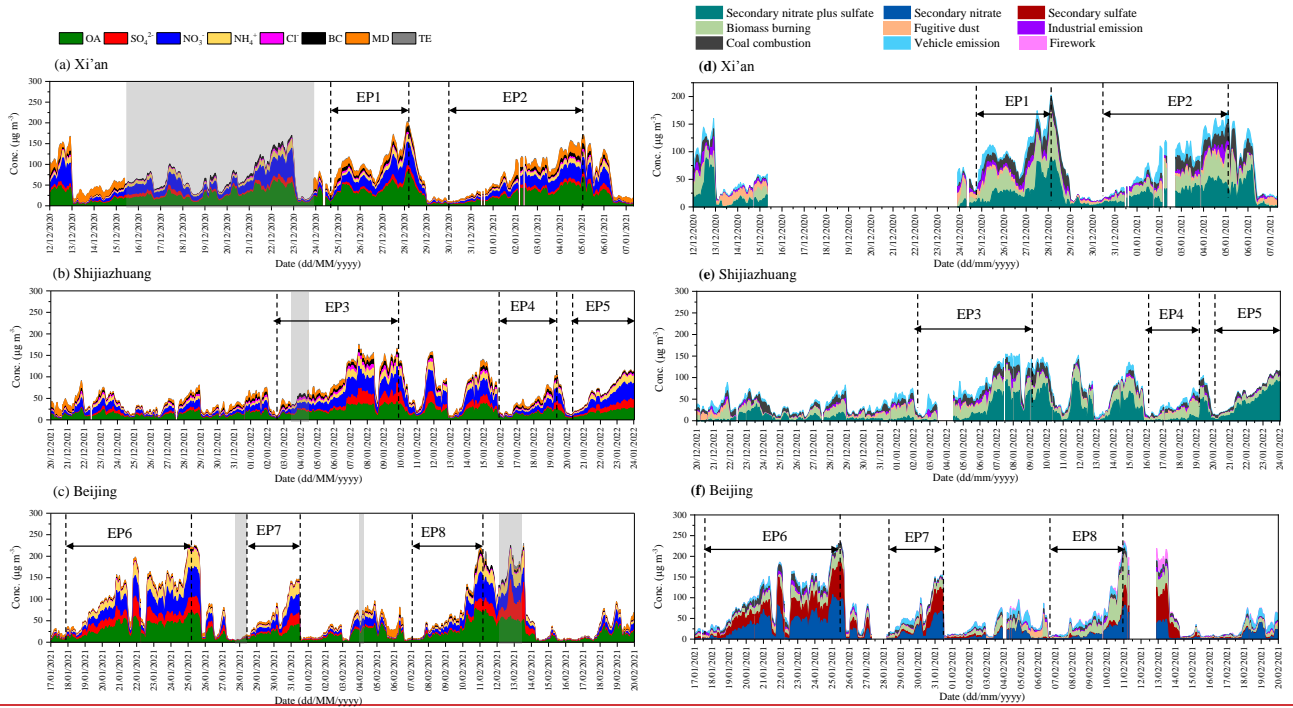133   **Figure** ~~S12~~S13. Source contribution of PM$_{2.5}$ in three pilot cities during daytime and nighttime, respectively.
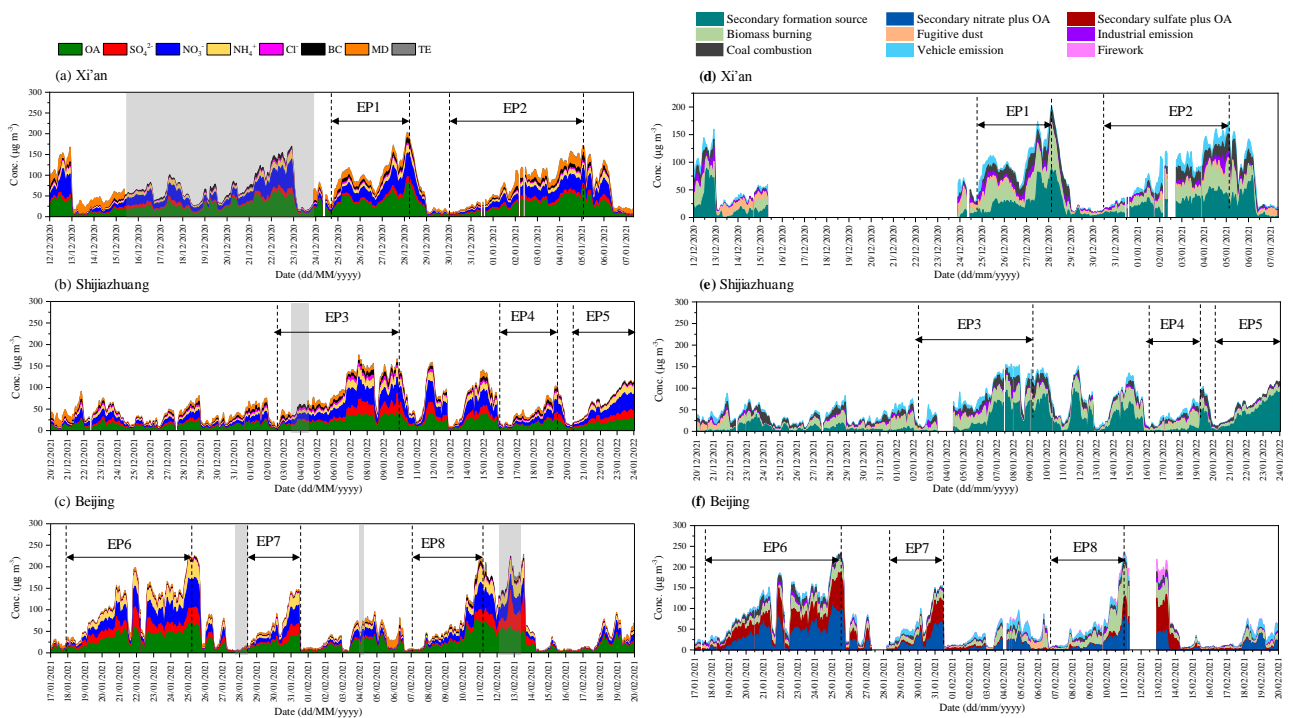
16

Figure S14. Correlation of secondary formation source/ΔCO and ALWC during daytime (08:00–17:00 LST, a–c) and nighttime (18:00–7:00 the next day LST, d–f) in Xi'an, Shijiazhuang, and Beijing, respectively. The points and error bar represent the mean values and standard deviation values of secondary formation source /ΔCO and ALWC in each bin. In Xi'an, each bin is 5 µg m^{-3} (ΔALWC = 5 µg m^{-3}). In Shijiazhuang, each bin is 5 µg m^{-3} (ΔALWC = 5 µg m^{-3}) when ALWC ranged from 0 to 75µg m^{-3}, but 25 µg m^{-3} (ΔALWC = 25 µg m^{-3}) for ALWC ranged from 75 to 200 µg m^{-3} due to limitations in data. In Beijing, during daytime, each bin is 5 µg m^{-3} (ΔALWC = 5 µg m^{-3}) when ALWC ranged from 0 to 40 µg m^{-3}, but 100 µg m^{-3} (ΔALWC = 100 µg m^{-3}) for ALWC ranged from 40 to 450 µg m^{-3} due to limitations in data. During nighttime, each bin is 5 µg m^{-3} (ΔALWC = 5 µg m^{-3}) when ALWC ranged from 0 to 50 µg m^{-3}, but 100 µg m^{-3} (ΔALWC = 100 µg m^{-3}) for ALWC ranged from 50 to 900 µg m^{-3} due to limitations in data.

Figure ~~S13~~S15. The pollution episodes selection according to temporal variation of PM$_{2.5}$ chemical components (a-c) and source contribution (d-f) during the campaigns in Xi'an, Shijiazhuang, and Beijing, respectively. The gray shape parts were lack of MD values due to the out-of-order Xact625, and missing values in the time series owing to the out-of-order ACSM, AE33, and Xact625 at the same time.

153
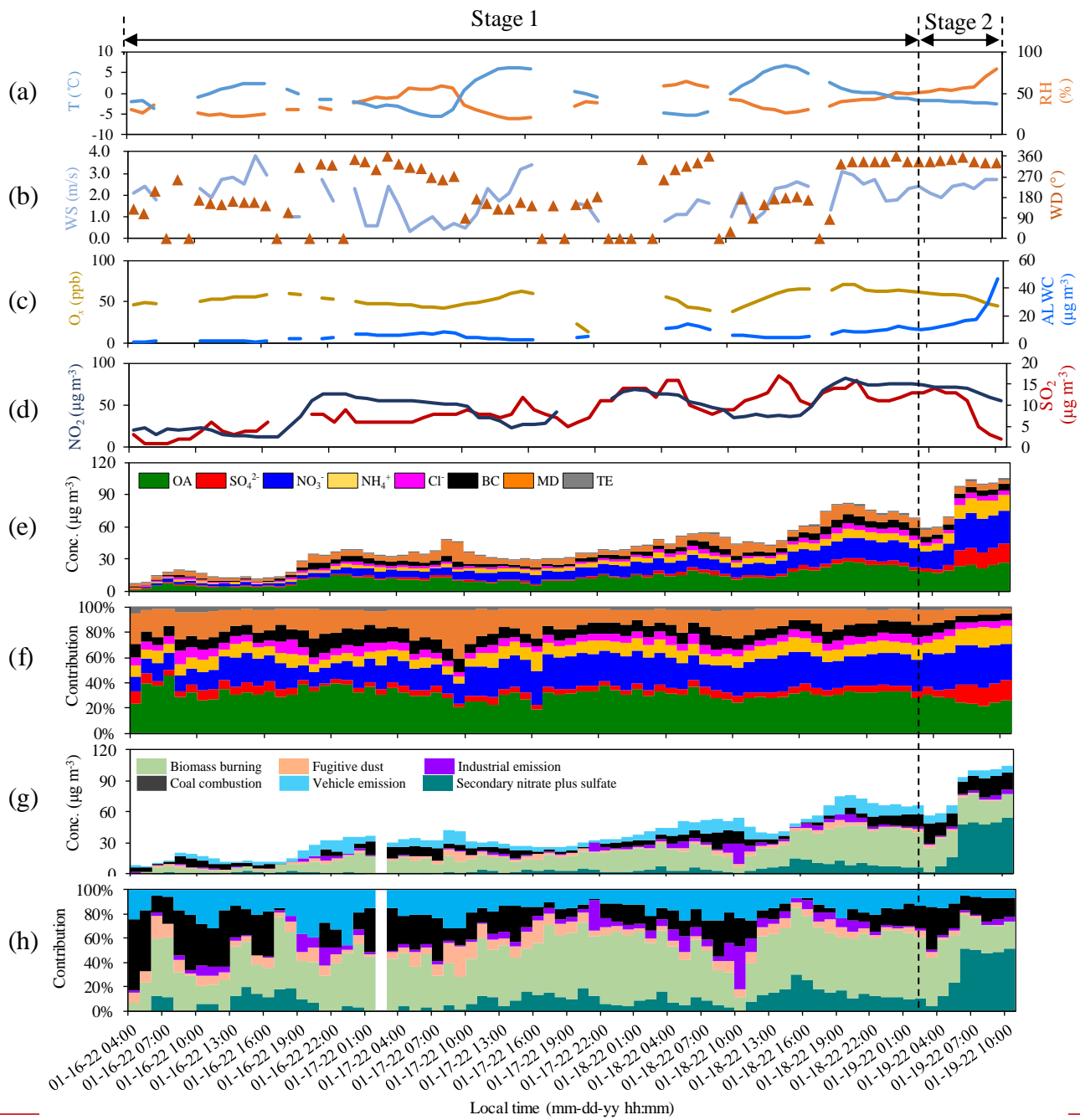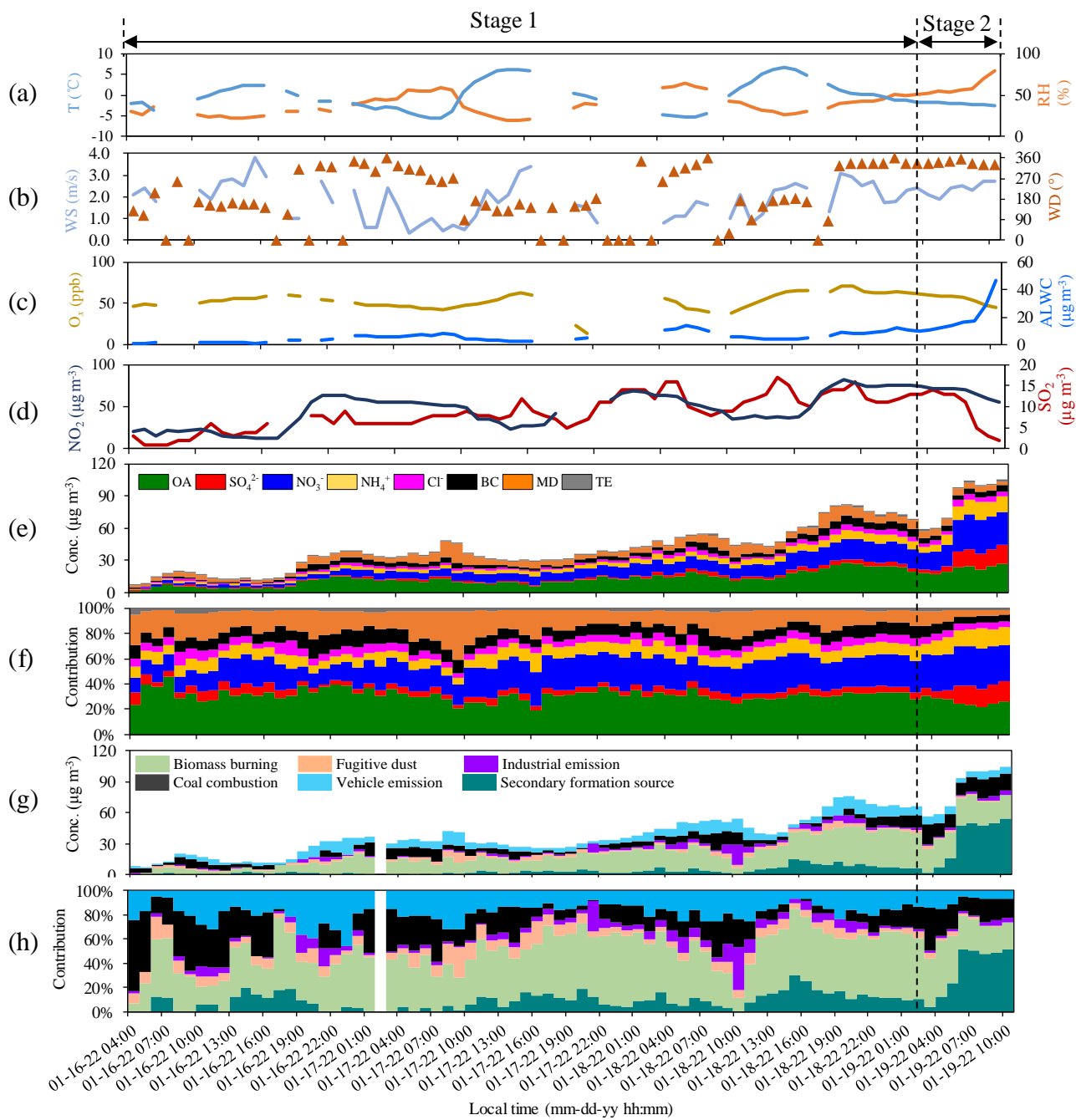
Figure S14.6 Time series of T and RH (a), WS and WD (b), O_x and ALWC (c), NO_2 and SO_2 (d), chemical components (e,f), and source contribution (g, h) of $PM_{2.5}$ during EP4 in Shijiazhuang.
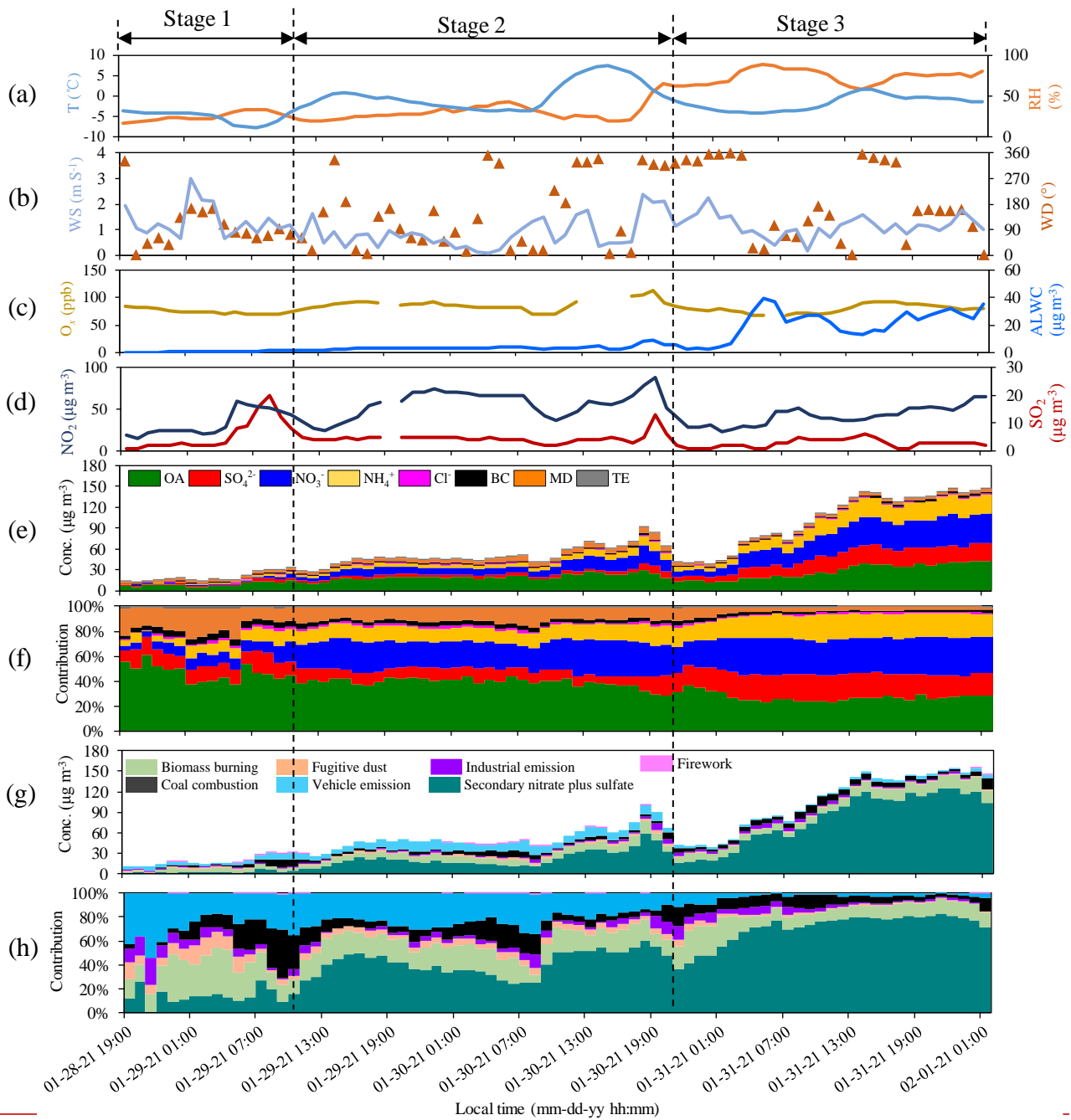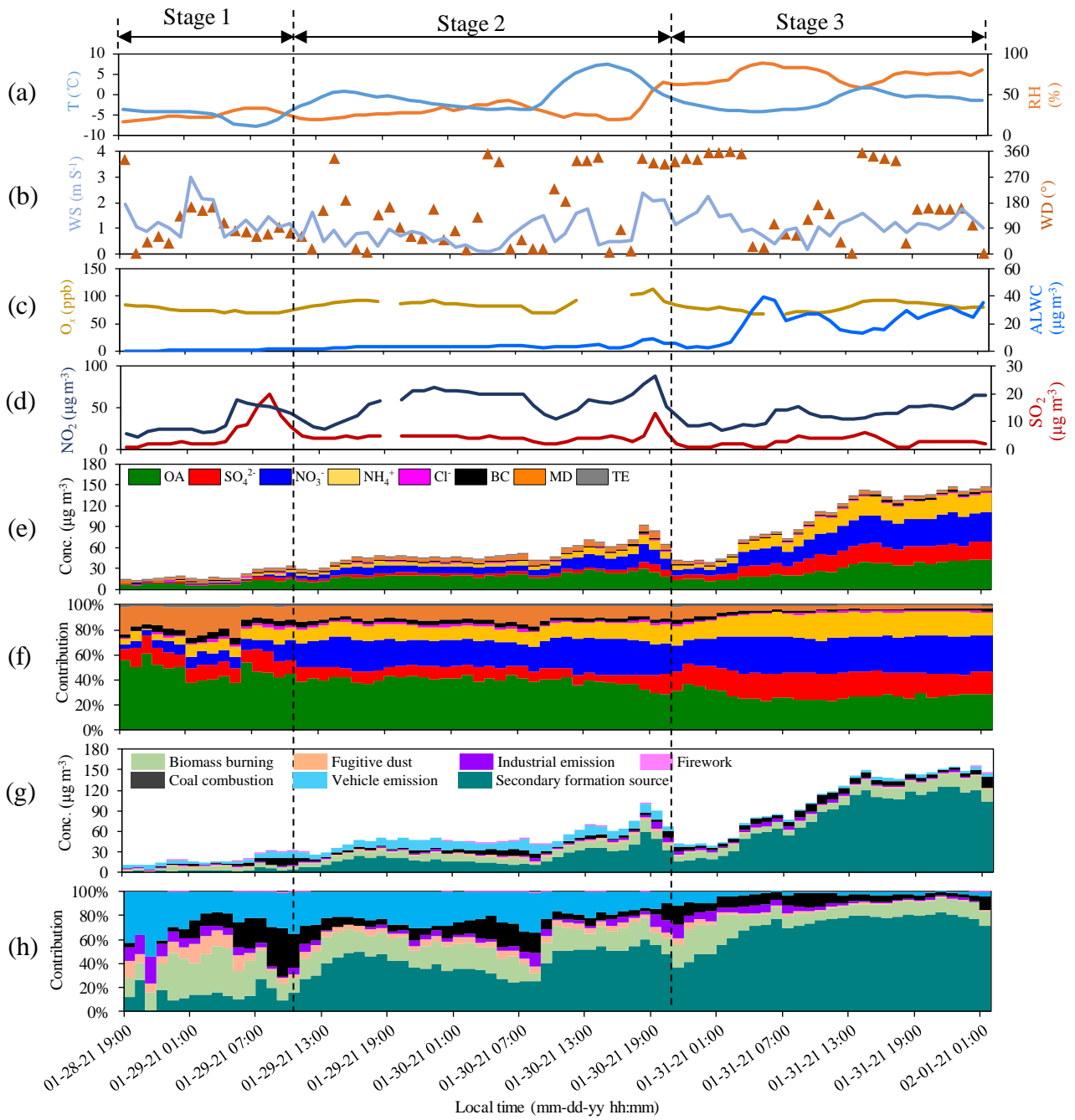
Figure ~~S15~~S17. Time series of T and RH (a), WS and WD (b), O_x and ALWC (c), NO_2 and SO_2 (d), chemical components (e, f), and source contribution (g, h) of $PM_{2.5}$ during EP7 in Beijing
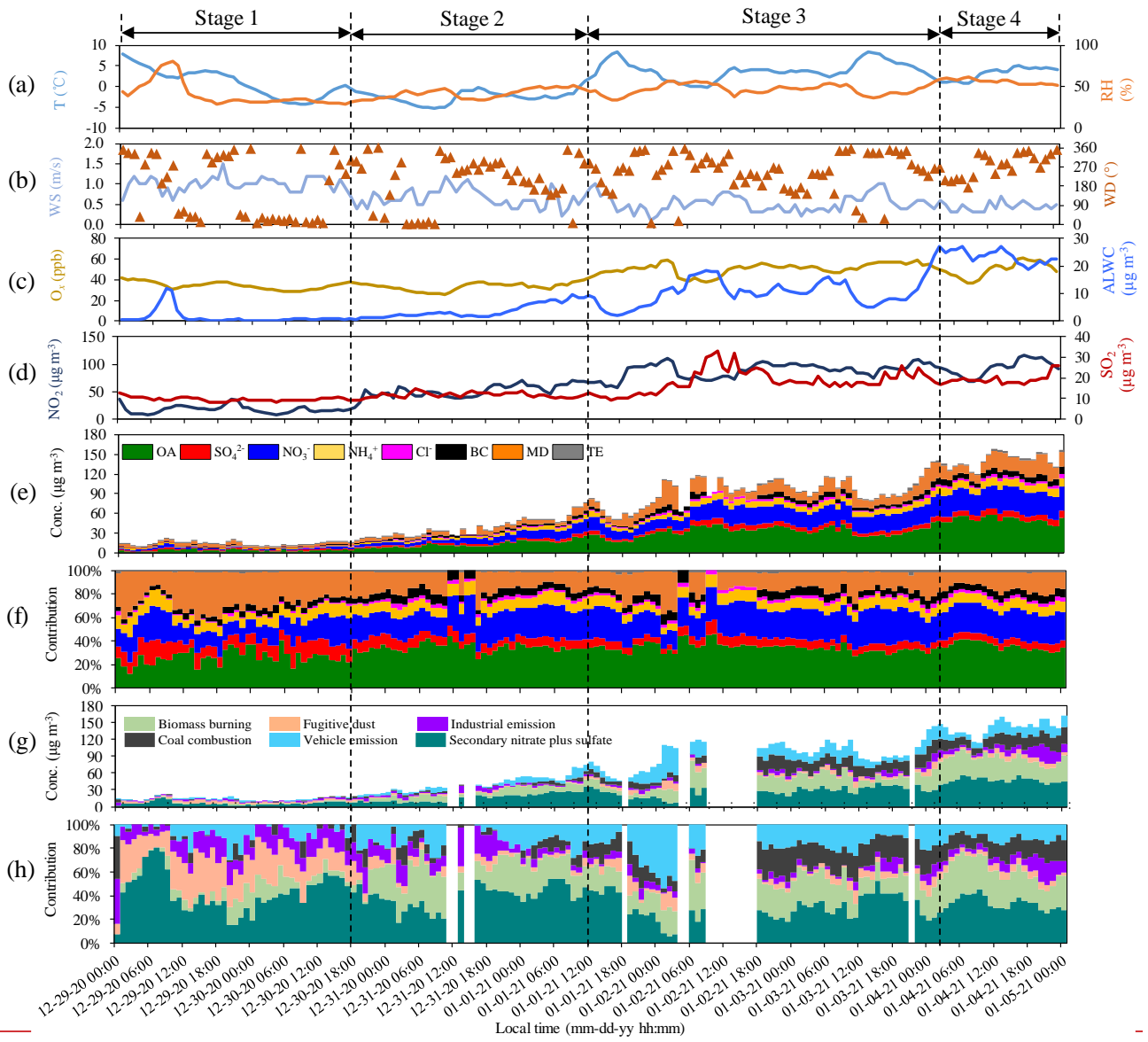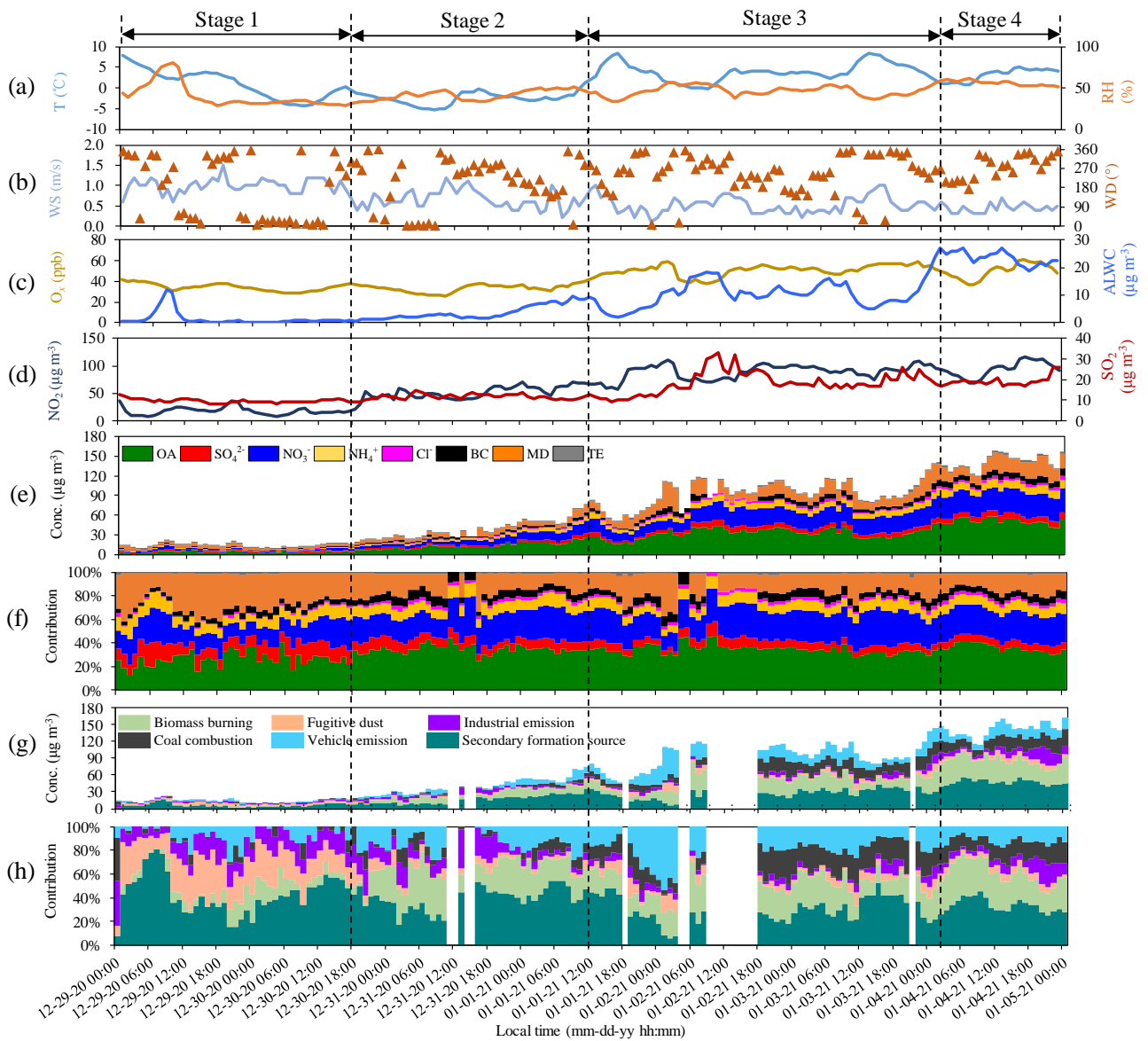
Figure S16S18. Time series of T and RH (a), WS and WD (b), O_x and ALWC (c), NO_2 and SO_2 (d), chemical components (e, f), and source contribution (g, h) of $PM_{2.5}$ during EP2 in Xi'an.

(a) The first round
Period: 2012/6-2013/12
PM$_{2.5}$: 90 µg cm^{-3}
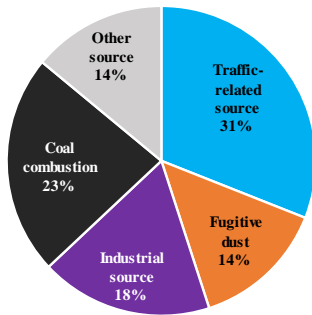
(b) The second round
Period: 2017/1-2018/5
PM$_{2.5}$: 58 µg cm^{-3}
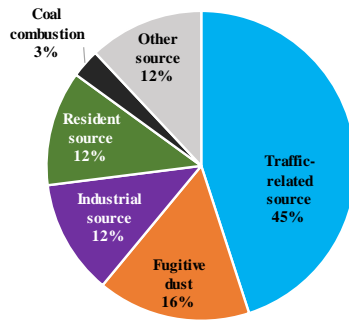
(c) The third round
Period: 2020/1-2021/6
PM$_{2.5}$: 38 µg cm^{-3}
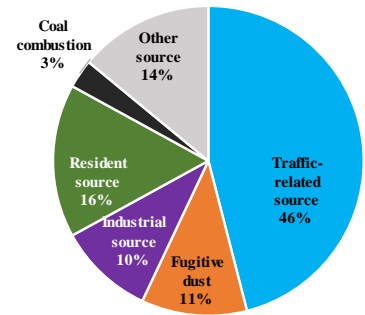
Figure S19. PM$_{2.5}$ sources apportionment in Beijing released by Beijing Municipal Ecology and Environment Bureau in the last decade (http://sthjj.beijing.gov.cn/so/s?tab=all&sourceCode=1100000122, in Chinese).

169 **Table S1.** Detailed information on complementary data for sampling sites

Sampling site	National Air Quality Monitoring Station	National Meteorological Station	complementary data
Xi'an	Gaoxinxiqu station, 1.1km from the sampling site	Haidian station, 7.6 km from the sampling site	hourly $PM_{2.5}$, NO_x, NO_2, CO, SO_2, O_3, WS, WD, T, RH
Shijiazhuang	Gaoxinqu station, 4.2 km from the sampling site	Shijiazhuang station, 23.8 km from the sampling site	hourly $PM_{2.5}$, NO_2, CO, SO_2, O_3, WS, WD, T, RH
Beijing	ChaoyangAotizhongxin station, 1.2 km from the sampling site	Jinghe station, 21.2 km from the sampling site	hourly $PM_{2.5}$, NO_2, CO, SO_2, O_3, WS, WD, T, RH

170 Note: WS: wind speed, WD: wind direction, T: temperature, RH: relative humidity.

171

172 **Table S2.** The $\Delta Q/Q_{exp}$[a] value with increasing factor number from two to ten of the runs in Xi'an, Shijiazhuang, and
173 Beijing.

Parameter[b]	$\Delta Q/Q_{exp}$		
	Xi'an	Shijiazhuang	Beijing
F2-F3	1.3	1.8	5.7
F3-F4	0.9	2.2	2.3
F4-F5	1.1	1.2	1.9
F5-F6	0.4	0.3	1.5
F6-F7	0.3	0.3	1.5
F7-F8	0.2	0.2	0.3
F8-F9			0.4
F9-F10			0.3

174 [a] $\Delta Q/Q_{exp}$ means the difference of Q/Q_{exp} of two sequent factor numbers.

175 [b] Parameters represent the factor numbers (F) – (F+1).

176

177 **Table S3.** Sources diagnostics with increasing factor numbers from four to ten of the runs in Xi'an, Shijiazhuang,
178 and Beijing.

Factor number	Sources identification		
	Xi'an	**Shijiazhuang**	**Beijing**
4	Secondary ~~nitrate plus sulfate~~formnation source mixed with biomass burning and coal burning mixed with industrial emission	i) Secondary ~~nitrate plus sulfate~~formation source mixed with primary sources including biomass burning and coal combustion ii) Biomass burning, coal combustion, and vehicle emission was also mixed	i) Secondary sources mixed with primary sources including biomass burning, coal combustion, and vehicle emission ii) Biomass burning and coal combustion was mixed
5	Secondary ~~nitrate plus sulfate~~foramtion source mixed with biomass burning	Biomass burning, coal combustion, and vehicle emissions were mixed	Secondary sulfate plus OA mixed with coal combustion and industrial emission; secondary nitrate plus OA mixed with biomass burning
6	Six individual sources were identified	Six individual sources were identified	Secondary sulfate plus OA mixed with coal combustion and secondary nitrate plus OA mixed with industrial emission
7	Vehicle emission was split into two profiles	Coal combustion was split into two profiles	Secondary sulfate plus OA mixed with coal combustion
8	Vehicle emission and industrial emission was split into two profiles, respectively.	Vehicle emission and coal combustion were split into two profiles, respectively.	Eight individual sources were identified
9			Coal combustion was split into two profiles
10			Coal combustion and biomass burning were split into two profiles, respectively.

179

180   **Table S4.** Average concentrations of reconstructed PM$_{2.5}$ and its chemical species in Xi'an, Shijiazhuang, and Beijing

181   during the campaign* (μg m^{-3})

Chemical Species	Xi'an	Shijiazhuang	Beijing
Reconstructed PM$_{2.5}$	77 ± 47	60 ± 39	64 ± 57
OA	25.9 ± 18.0	16.0 ± 9.7	22.1 ± 18.1
SO$_4^{2-}$	5.2 ± 3.4	7.0 ± 7.6	9.6 ± 11.3
NO$_3^-$	18.5 ± 14.5	15.8 ± 12.5	15.2 ± 16.7
NH$_4^+$	6.2 ± 4.5	7.0 ± 5.5	9.2 ± 10.3
Cl$^-$	1.9 ± 1.5	2.8 ± 2.2	0.7 ± 0.8
BC	4.5 ± 3.2	3.9 ± 2.5	1.9 ± 1.8
MD[a]	13.2 ± 7.0	6.0 ± 4.0	4.8 ± 3.8
TE[b]	1.1 ± 0.7	1.0 ± 0.6	0.9 ± 1.5

182   * Data during Xact625 failure shown in Figure S2 was excluded to calculate average concentration of campaign

183   [a] MD means mineral dust, which is equal to 2.20Al + 2.49Si + 1.63Ca + 2.42Fe + 1.94Ti

184   [b] TE means trace elements which is equal to K + Cr + Mn + Ni + Cu + Zn + As +Se + Ba + Pb

185

186   **Table S5.** The nitrogen oxidation ratio (NOR) and sulfur oxidation ratio (SOR) in Xi'an, Beijing, and Shijiazhuang

187   during the campaigns[a]

Parameters	Xi'an	Shijiazhuang	Beijing
NOR	0.15 ± 0.08	0.20 ± 0.11	0.16 ± 0.12
SOR	0.18 ± 0.08	0.36 ± 0.25	0.48 ± 0.23

188   [a] NOR = n(NO$_3^-$)/(n(NO$_3^-$) + n(NO$_2$)); SOR = n(SO$_4^{2-}$)/(n(SO$_4^{2-}$) + n(SO$_2$)). where n(NO$_3^-$), n(NO$_2$), n(SO$_4^{2-}$), and n(SO$_2$) are the molar

189   concentrations of NO$_3^-$, NO$_2$, SO$_4^{2-}$, and SO$_2$, respectively.

190

191   **Table S6.** Average concentrations of SOA in Xi'an, Shijiazhuang, and Beijing during sampling periods estimated by BC-

192   tracer method and source apportionment results (μg m^{-3})

SOA	Xi'an	Shijiazhuang	Beijing
SOA $_{BC\text{-}tracer}$	5.1 ± 5.8	4.2 ± 4.4	8.0 ± 9.0
SOA $_{source\ apportionment}$	6.0 ± 4.1	4.6 ± 2.8	8.2 ± 6.7

193

194

195 **Table** ~~S6~~**S7.** The concentration of PM$_{2.5}$ and its main chemical components during wintertime in Xi'an,

196 Shijiazhuang, and Beijing in the last decades.

City	Year	PM$_{2.5}$	OA[a]	EC	SO$_4^{2-}$	NO$_3^-$	NH$_4^+$	Others	References
		µg m^{-3}	µg m^{-3}	µg m^{-3}	µg m^{-3}	µg m^{-3}	µg m^{-3}	µg m^{-3}	
Xi'an	2003	356	153.3	21.5	53.8	29.2	29.6	68.9	Cao et al., 2012
	2006	230	57.4	11.4	45.9	20.6	14.2	80.0	Xu et al., 2016
	2008	199	48.3	9.9	42.5	20.8	11.0	66.9	Xu et al., 2016
	2010	233	60.0	14.7	30.6	22.9	12.3	92.8	Xu et al., 2016
	2012	196	56.3	8.2	27.0	19.2	13.3	71.9	Zhang et al., 2015
	2013	263	45.8	7.1	31.7	29.2	17.1	132.5	Niu et al., 2016
	2014	156	57.4	2.5	16.2	20.6	9.4	49.7	Dai et al., 2018
	2018	189	42.1	4.9	9.7	14.5	6.6	111.0	Wang et al., 2022
	2020*	77	25.9	4.5	5.2	18.5	6.2	16.2	This study
Shijiazhuang	2010	227	75.6	12.2	33.2	25.3	10.5	70.2	Zhao et al., 2013
	2015	232	82.0	16.3	26.6	27.4	19.8	59.7	Huang et al., 2017
	2016	193	63.2	13.5	29.5	24.0	17.0	45.8	Liu et al., 2019
	2017	97	31.2	6.5	12.5	16.5	12.5	17.8	Liu et al., 2019
	2018	96	35.8	10.1	10.5	15.3	6.3	18.0	Zhang et al., 2020
	2022*	60	16.0	3.9	7.0	15.8	7.0	9.8	This study
Beijing	2001	122	51.5	11.3	9.9	10.7	7.1	31.5	Duan et al., 2006
	2003	116	38.2	6.2	20.0	13.1	9.4	29.1	Cao et al., 2012
	2004	107	53.8	8.3	12.7	8.3	6.0	17.9	Song et al., 2007
	2010	127	42.9	7.1	14.2	17.1	5.2	40.5	Zhao et al., 2013
	2013	132	38.5	6.4	21.9	18.5	15.1	31.6	Tao et al., 2015
	2014	138	46.4	5.2	21.0	26.0	14.1	25.3	Ma et al., 2017
	2016	130	75.7	20.2	12.3	5.5	10.5	5.3	Xu et al., 2018
	2021*	64	22.1	1.9	9.6	15.2	9.2	6.4	This study

197 * study was conducted on online monitoring equipment, and the rest studies were researched on filter sampling experiments.

198 [a] Assumption of OA = 1.6 × OC for the filter-based sampling experiments

29

Table S7S8. The concentration of PM$_{2.5}$ and its source contribution during wintertime in Xi'an, Shijiazhuang, and Beijing in the last decades.

City	Year	PM$_{2.5}$	Vehicle emission	Coal combustion	Secondary formation source	Fugitive dust	Industrial emission	Biomass burning	Others	References
		μg m^{-3}	μg m^{-3}	μg m^{-3}	μg m^{-3}	μg m^{-3}	μg m^{-3}	μg m^{-3}	μg m^{-3}	
Xi'an	2006	392	74.5	121.5	82.3	51.0	39.2	23.5		Xu et al., 2016
	2008	199	41.8	55.7	45.8	23.9	21.9	10.0		Xu et al., 2016
	2010	233	48.9	55.9	41.9	44.3	30.3	11.7		Xu et al., 2016
	2014	169	20.3	47.3	71.0	8.5	6.8	15.2		Dai et al., 2020
	2018	189	26.5	28.4		15.1	22.7	58.6	37.8	Wang et al., 2022
	2020*	77	10.0	11.6	24.6	6.2	6.2	19.3		This study
Shijiazhuang	2015	232	46.4	62.6	30.2	20.9	16.2	7.0	48.7	Huang et al., 2017
	2016	181	23.5	54.3	54.3	30.8	9.1		7.2	Liu et al., 2018
	2019	119	21.4	21.4	42.8	21.4	6.0	6.0		Diao et al., 2021
	2022*	60	7.2	9.6	22.8	2.4	3.0	14.4		This study
Beijing	2004	107	8.6	40.7	19.3	7.5		16.1	15.0	Song et al., 2007
	2010	139		79.2	8.3	22.2	16.7	9.7	2.8	Zhang et al., 2013
	2013	159	9.5	41.3	79.5	15.9		9.5	3.2	Huang et al., 2014
	2015	125	48.8	15.0	23.8	8.8	2.5	6.3	18.8	Huang et al., 2017
	2021*	64	7.0	5.8	33.3	2.6	2.6	11.5	1.3	This study

* study was conducted on online monitoring equipment, and the rest studies were researched on filter sampling experiments.

References:

Cao, J.-J., Shen, Z.-X., Chow, J. C., Watson, J. G., Lee, S.-C., Tie, X.-X., Ho, K.-F., Wang, G.-H., and Han, Y.-M.: Winter and summer $PM_{2.5}$ chemical compositions in fourteen Chinese cities, J. Air Waste Manage., 62, 1214–1226, https://doi.org/10.1080/10962247.2012.701193, 2012.

Chen, L., Lowenthal, D., Watson, J., Koracin, D., Kumar, N., Knipping, E., Wheeler, N., Craig, K., Reid, S.: Toward effective source apportionment using positive matrix factorization: experiments with simulated $PM_{2.5}$ data. J. Air Waste Manage., 60(1), 43–54, https://doi.org/10.3155/1047-3289.60.1.43, 2010.

Dai, Q., Bi, X., Liu, B., Li, L., Ding, J., Song, W., Bi, S., Schulze, B. C., Song, C., Wu, J., Zhang, Y., Feng, Y., and Hopke, P. K.: Chemical nature of $PM_{2.5}$ and PM_{10} in Xi'an, China: Insights into primary emissions and secondary particle formation, Environ. Pollut., 240, 155–166, https://doi.org/10.1016/j.envpol.2018.04.111, 2018.

Dai, Q., Hopke, P. K., Bi, X., and Feng, Y.: Improving apportionment of $PM_{2.5}$ using multisite PMF by constraining G-values with a prioriinformation, Sci. Total Environ., 736, 139657, https://doi.org/10.1016/j.scitotenv.2020.139657, 2020.

Diao, L., Zhang, H., Liu, B., Dai, C., Zhang, Y., Dai, Q., Bi, X., Zhang, L., Song, C., and Feng, Y.: Health risks of inhaled selected toxic elements during the haze episodes in Shijiazhuang, China: Insight into critical risk sources, Environ. Pollut., 276, 116664, https://doi.org/10.1016/j.envpol.2021.116664, 2021.

Duan, F., He, K., Ma, Y., Yang, F., Yu, X., Cadle, S., Chan, T., and Mulawa, P.: Concentration and chemical characteristics of $PM_{2.5}$ in Beijing, China: 2001–2002, Sci. Total Environ., 355, 264–275, https://doi.org/10.1016/j.scitotenv.2005.03.001, 2006.

Huang, R.-J., Zhang, Y., Bozzetti, C., Ho, K.-F., Cao, J.-J., Han, Y., Daellenbach, K. R., Slowik, J. G., Platt, S. M., Canonaco, F., Zotter, P., Wolf, R., Pieber, S. M., Bruns, E. A., Crippa, M., Ciarelli, G., Piazzalunga, A., Schwikowski, M., Abbaszade, G., Schnelle-Kreis, J., Zimmermann, R., An, Z., Szidat, S., Baltensperger, U., Haddad, I. E., and Prévôt, A. S. H.: High secondary aerosol contribution to particulate pollution during haze events in China, Nature, 514, 218–222, https://doi.org/10.1038/nature13774, 2014.

Huang, X., Liu, Z., Liu, J., Hu, B., Wen, T., Tang, G., Zhang, J., Wu, F., Ji, D., Wang, L., and Wang, Y.: Chemical characterization and source identification of $PM_{2.5}$ at multiple sites in the Beijing–Tianjin–Hebei region, China, Atmos. Chem. Phys., 17, 12941–12962, https://doi.org/10.5194/acp-17-12941-2017, 2017.

Liu, B., Cheng, Y., Zhou, M., Liang, D., Dai, Q., Wang, L., Jin, W., Zhang, L., Ren, Y., Zhou, J., Dai, C., Xu, J., Wang, J., Feng, Y., and Zhang, Y.: Effectiveness evaluation of temporary emission control action in 2016 in winter in Shijiazhuang, China, Atmos. Chem. Phys., 18, 7019–7039, https://doi.org/10.5194/acp-18-7019-2018, 2018.

Liu, G., Xin, J., Wang, X., Si, R., Ma, Y., Wen, T., Zhao, L., Zhao, D., Wang, Y., and Gao, W.: Impact of the coal banning zone on visibility in the Beijing-Tianjin-Hebei region, Sci. Total Environ., 692, 402–410, https://doi.org/10.1016/j.scitotenv.2019.07.006, 2019.

236 Liu, H., Wang, Q., Ye, J., Su, X. li, Zhang, T., Zhang, Y., Tian, J., Dong, Y., Chen, Y., Zhu, C., Han, Y., and Cao, J.: Changes
237   in Source‑Specific Black Carbon Aerosol and the Induced Radiative Effects Due to the COVID‑19 Lockdown,
238   Geophys. Res. Lett., 48, https://doi.org/10.1029/2021GL092987, 2021.

239 Ma, Q., Wu, Y., Tao, J., Xia, Y., Liu, X., Zhang, D., Han, Z., Zhang, X., and Zhang, R.: Variations of Chemical Composition
240   and Source Apportionment of $PM_{2.5}$ during Winter Haze Episodes in Beijing, Aerosol Air Qual. Res., 17, 2791–2803,
241   https://doi.org/10.4209/aaqr.2017.10.0366, 2017.

242 Niu, X., Cao, J., Shen, Z., Ho, S. S. H., Tie, X., Zhao, S., Xu, H., Zhang, T., and Huang, R.: $PM_{2.5}$ from the Guanzhong
243   Plain: Chemical composition and implications for emission reductions, Atmos. Environ., 147, 458–469,
244   https://doi.org/10.1016/j.atmosenv.2016.10.029, 2016.

245 Rai, P., Furger, M., Slowik, J. G., Canonaco, F., Fröhlich, R., Hüglin, C., Minguillón, M. C., Petterson, K., Baltensperger,
246   U., and Prévôt, A. S. H.: Source apportionment of highly time-resolved elements during a firework episode from a
247   rural freeway site in Switzerland, Atmos. Chem. Phys., 20, 1657–1674, https://doi.org/10.5194/acp-20-1657-2020,
248   2020.

249 Salameh, D., Pey, J., Bozzetti, C., El Haddad, I., Detournay, A., Sylvestre, A., Canonaco, F., Armengaud, A., Piga, D.,
250   Robin, D., Prevot, A. S. H., Jaffrezo, J.-L., Wortham, H., and Marchand, N.: Sources of $PM_{2.5}$ at an urban-industrial
251   Mediterranean city, Marseille (France): Application of the ME-2 solver to inorganic and organic markers, Atmos. Res.,
252   214, 263–274, https://doi.org/10.1016/j.atmosres.2018.08.005, 2018.

253 Salameh, T., Sauvage, S., Afif, C., Borbon, A., and Locoge, N.: Source apportionment vs. emission inventories of non-
254   methane hydrocarbons (NMHC) in an urban area of the Middle East: local and global perspectives, Atmos. Chem.
255   Phys., 16, 3595–3607, https://doi.org/10.5194/acp-16-3595-2016, 2016.

256 Shrivastava, M., Cappa, C., Fan, J., Goldstein, A., Guenther, A., Jimenez, J., Kuang, C., Laskin, A., Martin S., Ng, N.,
257   Petaja, T., Pierce, J., Rasch, P., Roldin, P., Senfeld, J., Shiling, J., Smith, J., Thornton, J., Volkamer, R., Wang, J.,
258   Worsnop, D., Zaveri, R., Zelenyuk, A., Zhang, Q.: secondary organic aerosol: Implications for global climate forcing.
259   Rev. Geophys., 55, 509–559. https://doi.org/10.1002/2016RG000540, 2017.

260 Song, Y., Tang, X., Xie, S., Zhang, Y., Wei, Y., Zhang, M., Zeng, L., and Lu, S.: Source apportionment of $PM_{2.5}$ in Beijing
261   in 2004, J. Hazard. Mater., 146, 124–130, https://doi.org/10.1016/j.jhazmat.2006.11.058, 2007.

262 Tao, J., Zhang, L., Gao, J., Wang, H., Chai, F., and Wang, S.: Aerosol chemical composition and light scattering during a
263   winter season in Beijing, Atmos. Environ., 110, 36–44, https://doi.org/10.1016/j.atmosenv.2015.03.037, 2015.

264 Wang, Q.; Han, Y.; Ye, J.; Liu, S.; Pongpiachan, S.; Zhang, N.; Han, Y.; Tian, J.; Wu, C.; Long, X.; Zhang, Q.; Zhang, W.;
265   Zhao, Z.; Cao, J.: High Contribution of secondary brown carbon to aerosol light absorption in the southeastern margin
266   of Tibetan Plateau. Geophys. Res. Lett. 46, 4962−4970, https://doi.org/10.1029/2019GL082731, 2019.

267 Wang, Z., Wang, R., Wang, J., Wang, Y., McPherson Donahue, N., Tang, R., Dong, Z., Li, X., Wang, L., Han, Y., and Cao,
268   J.: The seasonal variation, characteristics and secondary generation of $PM_{2.5}$ in Xi'an, China, especially during
269   pollution events, Environ. Res., 212, 113388, https://doi.org/10.1016/j.envres.2022.113388, 2022.

270   Xu, H., Cao, J., Chow, J. C., Huang, R.-J., Shen, Z., Chen, L. W. A., Ho, K. F., and Watson, J. G.: Inter-annual variability
271   of wintertime $PM_{2.5}$ chemical composition in Xi'an, China: Evidences of changing source emissions, Sci. Total
272   Environ., 545–546, 546–555, https://doi.org/10.1016/j.scitotenv.2015.12.070, 2016.

273   Xu, X., Zhang, H., Chen, J., Li, Q., Wang, X., Wang, W., Zhang, Q., Xue, L., Ding, A., and Mellouki, A.: Six sources
274   mainly contributing to the haze episodes and health risk assessment of $PM_{2.5}$ at Beijing suburb in winter 2016,
275   Ecotoxicol. Environ. Saf., 166, 146–156, https://doi.org/10.1016/j.ecoenv.2018.09.069, 2018.

276   Zhang, Q., Shen, Z., Cao, J., Zhang, R., Zhang, L., Huang, R.-J., Zheng, C., Wang, L., Liu, S., Xu, H., Zheng, C., and Liu,
277   P.: Variations in $PM_{2.5}$, TSP, BC, and trace gases (NO_2, SO_2, and O_3) between haze and non-haze episodes in winter
278   over Xi'an, China, Atmos. Environ., 112, 64–71, https://doi.org/10.1016/j.atmosenv.2015.04.033, 2015.

279   Zhang, R., Jing, J., Tao, J., Hsu, S.-C., Wang, G., Cao, J., Lee, C. S. L., Zhu, L., Chen, Z., Zhao, Y., and Shen, Z.: Chemical
280   characterization and source apportionment of $PM_{2.5}$ in Beijing: seasonal perspective, Atmos. Chem. Phys., 13, 7053–
281   7074, https://doi.org/10.5194/acp-13-7053-2013, 2013.

282   Zhang, W., Liu, B., Zhang, Y., Li, Y., Sun, X., Gu, Y., Dai, C., Li, N., Song, C., Dai, Q., Han, Y., and Feng, Y.: A refined
283   source apportionment study of atmospheric $PM_{2.5}$ during winter heating period in Shijiazhuang, China, using a
284   receptor model coupled with a source-oriented model, Atmos. Environ., 222, 117157,
285   https://doi.org/10.1016/j.atmosenv.2019.117157, 2020.

286   Zhao, P. S., Dong, F., He, D., Zhao, X. J., Zhang, X. L., Zhang, W. Z., Yao, Q., and Liu, H. Y.: Characteristics of
287   concentrations and chemical compositions for $PM_{2.5}$ in the region of Beijing, Tianjin, and Hebei, China, Atmos. Chem.
288   Phys., 13, 4631–4644, https://doi.org/10.5194/acp-13-4631-2013, 2013.